The use of settling velocity to predict the potential fate of aggregated sediment and associated SOC

Inauguraldissertation

zur

Erlangung der Würde eines Doktors der Philosophie

vorgelegt der

Philosophisch-Naturwissenschaftlichen Fakultät

der Universität Basel

von

Liangang Xiao

China

Basel, 2016

Genehmigt von der Philosophisch-Naturwissenschaftlichen Fakultät
auf Antrag von

Prof. Dr. Nikolaus J. Kuhn
University of Basel
Faculty representative / dissertation supervisor

_____

Dr. Thomas Iserloh
Trier University
Co-examiner

Basel, June 21, 2016

_____

Prof. Dr. Jörg Schibler
The Dean of Faculty of Science

ABSTRACT

The impacts of lateral movement of soil organic carbon (SOC) by soil erosion on global carbon (C) cycling and climate change have been the subject of a controversial debate for decades. Because of the limited availability of data on SOC erosion history, the effects of erosion on CO_2 emissions have mostly been calculated by determining SOC inventories at sites of erosion and comparing against depositional sites. The use of SOC inventories to calculate C fluxes relies on the assumption that sediment properties are temporally and spatially stable during erosion events. However, on eroded lands, it always involves a temporal-dynamic pattern of SOC content, as well as a spatial enrichment and/or depletion of SOC in sediment that differs from original soils. Therefore, the approach of using SOC inventories at the slope-scale to back-calculate C fluxes caused by erosion would result in a biased assessment. Improving our assessment of soil erosion and its impact on C cycling thus requires a better understanding of the behavior of eroded SOC during transport and deposition across agricultural landscapes.

In a given water layer, the transport distance of eroded sediment is mainly determined by particle settling velocity. Settling velocity distribution, calculated based on the diameter of dispersed mineral grains, has been used in some erosion models to predict the redistribution of sediment and associated SOC across landscapes. However, most eroded particles are transported in the form of aggregates rather than individual mineral grains. Aggregation dramatically increases the settling velocity of individual mineral grains that are incorporated into aggregates, as well as the transport distance of associated SOC. Consequently, the uncertainties of calculating the lateral redistribution of sediment and associated SOC may further lead to a biased estimate of the vertical C released from eroded SOC during redistribution. Therefore, identifying the settling velocity of natural aggregated-sediment represents an essential step if the redistribution of eroded SOC, as well as further assessing the potential CO_2 mineralization, is to be more accurately modeled.

Several laboratory-based studies conducted on dry-sieved aggregates have examined the transport fate of aggregated sediment and associated SOC based on settling velocity. However, the erodibility of the soil in the field is more temporally and spatially variable due to the impacts of tillage, rainfall, wetting-drying cycles, freezing, and biological effects. For example, rainfall kinetic energy will affect the breakdown of aggregates and the development of crust. It is not entirely clear whether changes in natural surface conditions could impact on the characteristics of sediment and thereby diminish the effect of aggregation on the fate of eroded SOC. Moreover, from the perspective of parametrizing erosion models, it would require a large amount of accurate settling velocity data from a wide range of soils in order to cover the broad spatial heterogeneity that is inherent during soil development. Identifying the settling velocity distribution based on laboratory or field tests with flumes, even if well-designed, are both far too much work to test all soils over a sufficiently wide range of rainfall conditions. Therefore, it is vital to develop a simple proxy to generate quasi-natural sediment in a time and labor-saving manner, and to further identify accurate settling information of sediment that could be incorporated into erosion models.

To address the above knowledge gaps, four objectives were identified in this study. They are: 1) to quantitatively identify the potential fate of SOC eroded from a natural crusted soil surface and further compare the observations with that based on dry-sieved aggregates in the laboratory; 2) to investigate the sensitivity of the sediment settling behavior to increased kinetic energy during a series of rainfall events and thereafter examine the effect of aggregation on the quality of eroded SOC; 3) to develop a simple but efficient proxy method to generate natural or quasi-natural sediment; and 4) to evaluate the feasibility and sensitivity of such a proxy method. In this study, a series of experiments were conducted to attain those four objectives: ***Field Experiments 1&2*** involved investigating the effect of a natural crusted

soil surface on SOC transport and mineralization; ***Laboratory Experiments 1&2*** involved developing an approach to identify the settling velocity of quasi-natural sediment.

In ***Field Experiments 1&2,*** short term wind driven storms simulated with a modified portable wind and rainfall simulator (PWRS) were conducted on a natural crusted soil surface after harvesting in the village of Witterswil, in northwest Switzerland. The collected sediment was fractionated with a settling tube according to their respective settling velocities. The sediment mass, SOC concentration and cumulative CO_2 emission of each fraction were measured. The results show: 1) 53% of eroded sediment and 62% of eroded SOC would potentially deposit across landscapes. This is six times and three times higher compared to that implied by mineral grains, respectively; 2) the underestimation of eroded SOC deposited across landscapes can mainly be attributed to underestimating mineral-associated organic carbon (MOC); 3) the preferential deposition of SOC-rich fast-settling sediment leads to a higher SOC stock than that at a comparable depth of non-eroded original soil. This would potentially release approximately 50% more CO_2 than the same layer of the non-eroded original soil; 4) about 15% of SOC could be mineralized during the redistribution process of sediment, especially from the silt and clay fractions; 5) the settling velocity distributions of eroded sediment, as well as the SOC concentration and cumulative mineralization of each fraction, did not change during a series of rainfall events, suggesting settling velocity distribution of eroded SOC could be regarded as a stable parameter during redistribution. The results obtained from ***Field Experiments 1&2*** confirm in general the conclusions drawn from the laboratory-based work and thus demonstrate that aggregation can affect the redistribution of sediment associated SOC under field conditions, including an increase in CO_2 emissions compared to bulk soil. This illustrates the need to integrate the effect of aggregation on SOC redistribution into soil erosion models, which could help precisely distinguish SOC potentially re-deposited across landscapes from that possibly transported to aquatic systems, and further assess the impacts on global C cycling. In order to capture the effect of aggregation on settling behavior and thus the redistribution of eroded sediment, in ***Laboratory Experiments 1&2,*** a combined Raindrop Aggregate Destruction Device-Settling Tube (RADD-ST) proxy was developed to effectively simulate aggregate breakdown under raindrop impact, and further identify the settling velocity of aggregated sediment and associated SOC. The results show: 1) for an aggregated soil, applying dispersed mineral grain size distribution, rather than actual aggregate distribution, to soil erosion models would lead to an underestimate of deposition of eroded sediment and SOC across landscapes; 2) the RADD-ST designed in this study effectively captures the effects of raindrop impact on aggregate destruction and is thus able to simulate the quasi-natural sediment spatial redistribution; 3) the combined RADD-ST approach is adequately sensitive to measure actual settling velocities of differently aggregated soils; 4) this combined RADD-ST approach provides an effective tool to improve the parameterization of settling velocity input for erosion models.

Overall, the results observed from this study confirm that aggregation effects, even on crusted soil surfaces, considerably reduce the likely transport distance of eroded SOC. It thus potentially skews the re-deposition of SOC-rich coarse sediment fractions towards terrestrial systems and contributes additional CO_2 to the atmosphere. Therefore, current erosion models urgently need to be optimized by the development of a computable parameter integrating aggregated sediment settling velocity and the associated SOC distribution. The RADD-ST approach developed in this study has the potential to provide actual settling information generated under relatively simple simulated rainfall conditions to optimize the parametrization of sediment behavior and quality in erosion models. If further extrapolated appropriately to a specific erosion scenario, the RADD-ST derived sediment quality parameters can also help improve our understanding of sediment movement through watersheds and thus contribute to reaching consensus on the role of erosion on C cycling.

ACKNOWLEDGEMENT

I would like to extend thanks to numerous people, who kindly helped me in the last five years and generously contributed to my work presented in the PhD thesis.

First, I am extremely grateful to my supervisor, Prof. Nikolaus J. Kuhn. My PhD has been an amazing experience and I thank Prof. Nikolaus J. Kuhn wholeheartedly, not only for giving me the wonderful opportunity to conduct a PhD study at the University of Basel, but also for the patient guidance and tremendous academic support in the last five years.

I also would like to thank Dr. Yaxian Hu, who generously helped me with my research from the first day that I came to Basel; Dr. Phil Greenwood, who has been a truly dedicated advisor to my study; and Dr. Wolfgang Fister, who guided me through my experiment work in the field.

I also would like to give my thanks to other colleagues in the research group of Physical Geography and Environmental Change: Ms. Marianne Caroni and Ms. Ruth Strunk for their assistance in the laboratory; our secretary Ms. Rosmarie Gisin for her kind help in the office; Mr. Hans-Rudolf Rüegg for his technical support in my experiments.

I am also very grateful to other colleagues in our research group: Matthias Hunziker, Chatrina Caviezel, Mathias Würsch, Miriam Widmer, Sarah Strähl, Vladimir Wingate, Brice Prudat, Juliane Krenz, who either assisted my work in the lab, or kindly discussed the PhD work with me.

Particular thanks go to Jedsada Kerdsrilek, Mohammadali Saremi Naeini, and Ali Mohammadian Behbahani, who share the happiest research time with me in Basel during the past five years.

I am especially grateful to China Scholarship Council for sponsoring my expenses to conduct this study at the University of Basel.

Finally, sincere thanks go to my parents and Shengye Zhang for the unbelievable support. They are the most important people to me in the world and I dedicate this thesis to them.

TABLE OF CONTENTS

Chapter 1

Introduction 1

1.1 Soil erosion and global carbon (C) cycling 1

1.1.1 Climate change and global C cycling 1

1.1.2 Soil erosion 2

1.1.3 The C dynamics during erosion process 2

1.1.4 Controversy of C sink vs. C source 3

1.2 Knowledge gaps in studies of C dynamics on eroded lands 4

1.2.1 Uncertainties of using C inventories to calculate C fluxes 4

1.2.2 Erosion modeling and settling velocity based on mineral grains 6

1.2.3 Settling velocity based on wet-sieved aggregates 7

1.2.4 Mineralization of eroded SOC during transport 8

1.2.5 Previous investigations regarding settling behavior 8

1.3 Objectives of this study 10

1.4 Experiment rationale 11

1.4.1 Overview on the experimental design 11

1.4.2 Field experiments 11

1.4.3 Laboratory experiment 12

1.5 Thesis structure 13

Chapter 2

Potential fate of SOC eroded from natural crusted soil surface under wind-driven rainfall..... 15

2.1 Introduction 17

2.1.1 C dynamics and sediment redistribution 17

2.1.2 Erodibility changes and field conditions 18

2.1.3 Aim of this study 19

2.2 Materials and methods 19

2.2.1 Study site description 19

2.2.2 Field rainfall simulation with a portable wind and rainfall simulator (PWRS) 21
2.2.3 Settling tube test 22
2.2.4 Sediment respiration measurements 23
2.2.5 Mineral particle size distribution 23
2.2.6 Soil and sediment analysis 24
2.3 Results 24
2.4 Discussion 28
2.4.1 Aggregation-induced skew of SOC deposition on crusted soil 28
2.4.2 Potential mineralization from slow-settling sediment 29
2.5 Conclusion 31
Chapter 3
Effect of aggregation on transport of eroded sediment and SOC under wind-driven rainfall 33
3.1 Introduction 35
3.1.1 C dynamics and sediment redistribution 35
3.1.2 The effects of aggregation on sediment redistribution 35
3.1.3 Knowledge gaps 36
3.1.4 Aim of this study 37
3.2 Materials and methods 37
3.2.1 Study site description 37
3.2.2 Rainfall simulation 38
3.2.3 Settling tube test 40
3.2.4 Mineral particle size distribution 42
3.2.5 Soil and sediment analysis 42
3.2.6 Sediment respiration measurements 42
3.3 Results 43
3.3.1. Erosional response during rainfall 43
3.3.2 EQS distribution of eroded sediment 45
3.3.3 SOC distribution and quality of eroded sediment 45
3.3.4 SOC mineralization during long-term incubation 46
3.4 Discussion 49

3.4.1 Overall dynamics of runoff, erosion and sediment properties. 49
3.4.2 Skewing effect of aggregation on sediment and SOC redistribution 50
3.4.3 Effect of aggregation on SOC quality and mineralization 50
3.5 Conclusion 51
Chapter 4
The use of a raindrop aggregate destruction device (RADD) to evaluate sediment and SOC transport 53
4.1 Introduction 55
4.2 Materials and methods 56
4.2.1. Soil samples and preparations 56
4.2.2. Raindrop aggregate destruction device and rainfall simulation 57
4.2.3. Settling tube and settling velocity measurement 58
4.2.4 Mineral grain size distribution 58
4.2.5 Laboratory measurements 59
4.3 Results and discussion 59
4.3.1 Aggregation effects 59
4.3.2 Sensitivity to accumulative kinetic energy 60
4.3.3 Effectiveness of the RADD 60
4.4 Conclusion 61
Chapter 5
A combined Raindrop Aggregate Destruction Device -Settling Device (RADD-ST) approach to identify the settling velocity of sediment 63
5.1 Introduction 66
5.1.1 Soil erosion and sediment settling velocity 66
5.1.2 Parametrization of settling velocity 67
5.2 The design of RADD-ST method 68
5.2.1 Experimental rationale 68
5.2.2 Raindrop Aggregate Destruction Device (RADD) 69
5.2.3 Settling Tube (ST) 69
5.2.4 Mean Weight Settling Velocity (MWSV) 70

5.3 The application of the RADD-ST method 71
5.3.1 Soil samples and preparations 71
5.3.2 RADD-ST test procedure and rainfall simulation 71
5.3.3 Mineral grain size distribution 72
5.4 Results and discussion 73
5.5 Conclusion 77
Chapter 6
Summary and Conclusions 83
6.1. Summary of primary results from each experiment 83
6.2. General conclusions 85
6.3. Potential research in the future 87
References 89

Chapter 1

Introduction

1.1 Soil erosion and global carbon (C) cycling

1.1.1 Climate change and global C cycling

In recent decades, climate changes have caused profound impacts all around the world, such as temperature increase, modification of wind and precipitation patterns, sea level rise, snow and ice cover (IPCC, 2014). The long-lasting changes to the climate system will increase the likelihood of severe, pervasive, and irreversible impacts for people and ecosystems (Parmesan and Yohe, 2003). It is well documented that continued emission of greenhouse gases such as CO_2 is one of the main factors that lead to global warming and consequently climate change (Lal, 2004; IPCC, 2014). Globally, soil as the third largest reservoir stores 2500 petagrams of carbon (Pg C), which is over 3.3 times the amount that is present in the atmosphere (760 Pg), and 4.5 times the size of the biotic pool (560 Pg) (Lal, 2004). Because of the extent of the C pool and the active interconnections with other C pools (e.g. atmosphere, biosphere), any changes in pool size and flux rates of soil C can have significant implications on global C cycling and ultimately climate change (Lal, 2004; Berhe et al., 2007; Van Oost et al., 2007). In agriculture ecosystems, extensive tillage has induced severe soil degradation and thus has profoundly contributed to a decline in the soil C pool (Van Oost et al., 2012). Soil C thus has to be regarded as a very dynamic pool that is closely related to human activities (Kuhn et al., 2009).

Soil erosion, as one of the most widespread forms of soil degradation, can redistribute a large amount of C across landscapes, ranging from 0.4 Pg C yr^{-1} estimated by Doetterl et al. (2012) to 4-6 Pg C yr^{-1} reported by Lal (2004). Despite the different magnitudes, one consensus among soil scientists is that lateral C movement in terrestrial ecosystems by soil erosion does not only affect C lateral redistribution across landscapes, but also has an important impact on the vertical C exchange between the soil and the atmosphere (e.g. Stallard, 1998; Harden et al., 1999; Berhe et al., 2007; Van Oost et al., 2007; Quinton et al., 2010; Kuhn et al., 2009; Van Oost et al., 2012; Kuhn, 2013). For example, Lal (2004) estimated that erosion leads to a net CO_2 emission of about 1 Pg C yr^{-1} from the soil to the atmosphere due to accelerated mineralization. In contrast, Van Oost et al. (2007) reported that 0.12 Pg C yr^{-1} is fixed from the atmosphere into the soil by a process known as ‘dynamic replacement’, i.e. fresh C input to subsoil at eroding sites. The effects of soil erosion on global C cycling, especially as a source or sink for greenhouse gases has been subject to a controversial debate for decades (Stallard, 1998; Harden et al., 1999; Berhe et al., 2007; Van Oost et al., 2007; Quinton et al., 2010; Kuhn et al.,

2009; van Hemelryck et al., 2010a). Irrespective of the controversy surrounding the vertical direction of C transfers, either of the two estimates strongly indicates that any changes in soil erosion processes are predicted to have a profound impact on global C cycling.

1.1.2 Soil erosion

The process of soil erosion by water flowing over the soil surface involves three distinct stages: (i) detachment; (ii) transport; and (iii) deposition (Lal 2005, Legout et al., 2005). Raindrops impacting onto the soil surface can detach and disintegrate soil material. The shearing forces of surface runoff can cause further detachment by mechanical breakdown when eroded material is transported through a catchment (Le Bissonnais, 1996). The detached material can further be transported by both splash erosion and overland flow (Kuhn et al., 2003), which always involves preferential deposition and selective transport. Deposition occurs when hydraulic conditions provide lower transport capacity (Savat and DePloey, 1982), leading to a selective redistribution of eroded material across a landscape according to their settling velocity (Kuhn, 2013). The fast-settling fractions deposit on depositional sites, such as foot slopes and floodplains, whereas the slow-settling fractions are transported further into aquatic ecosystems (Lal, 2005). This overall process is conceptualized in Figure 1.1.

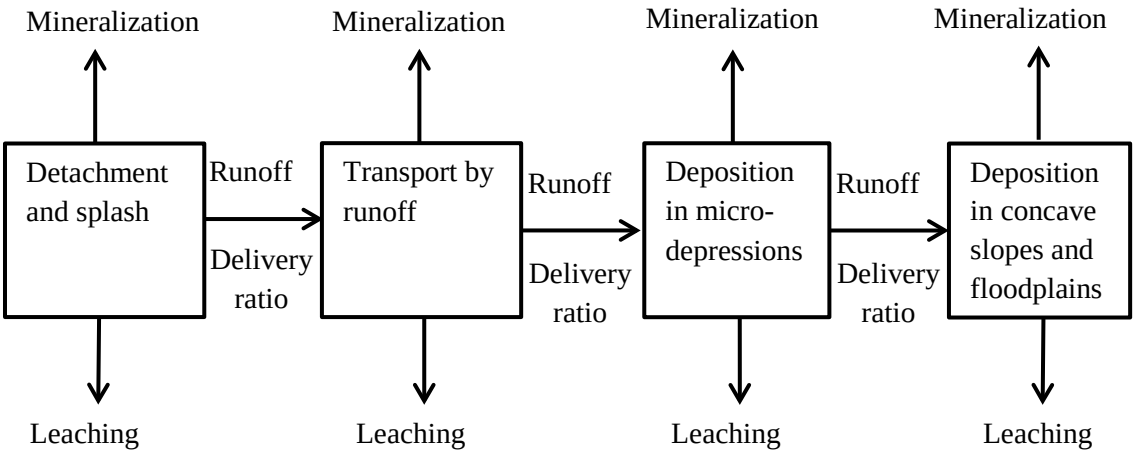

Figure 1.1 Erosion processes on landscapes (adapted from Lal, 2005). Delivery ratio changes depend on erosion event when sediment moves through landscapes.

1.1.3 The C dynamics during erosion, transport and deposition

Erosion processes do not only move and transport sediment across landscapes (Figure 1.1), but also affect SOC dynamics temporally and spatially (Van Oost et al., 2007). The impact of erosion on SOC dynamics differs for sites of erosion, deposition and during transport (Kirkels et al., 2014). The detailed effects of soil erosion on SOC dynamics are listed in Table 1.1. According to the erosion process, the main domains can be summarized into:

1) Potential changes of net primary productivity (NPP), mineralization (Lal, 2004; Jacinthe et al, 2004), as well as dynamic replacement at eroding sites (Stallard, 1998; Harden et al., 1999);

2) Exposure of SOC due to aggregate breakdown and preferential deposition of sediment and associated SOC, resulting in changes of mineralization during transport (Lal and Pimentel, 2008);

3) The mineralization changes because of deep burial of eroded SOC at depositional sites (Berhe et al., 2007; Van Oost et al., 2007).

Table 1.1 Summary of the C dynamics on eroded lands.

Erosion processes	Locations	C dynamics	Sink / source	References
Detachment	Eroding site (convex)	Exposure of previously protected SOC to microbes and thus accelerating mineralization due to detachment of aggregates	Vertical source	Lal, 2004
		Partial replacement of lost SOC by newly decomposed plants	Vertical sink	Stallard, 1998
Transport	Transport pathway (slope)	Preferential removal of light carbon in runoff	Lateral source	Polyakov et al., 2008
		Redistribution of eroded SOC including deposition on landscapes and transfer to aquatic systems	Lateral sink	Starr et al. 2000
		Mineralization of SOC on eroding sites, depositional sites and during transport	Vertical source	Jacinthe et al., 2004
Deposition	Depositional site (concave, floodplains, rivers and oceans)	Increased mineralization due to anthropogenic and climatic perturbations on the surface layer	Vertical source	Lal, 2005
		Protection of deposited SOC by re-aggregation of eroded particles	Vertical sink	Berhe, 2011
		Deep burial of C-enriched sediment in depositional sites	Lateral sink	Van Oost et al., 2012

1.1.4 Controversy of C sink vs. C source

Substantial studies have contributed to investigate the C dynamics at different steps of erosion, i.e. eroding sites, transport, depositional sites (e.g. Stallard, 1998; Harden et al., 1999; Lal, 2003; Starr et al., 2000; Kuhn et al., 2009; van Hemelryck et al., 2010b; Van Oost et al., 2012; Hoffmann et al., 2013; X. Wang et al., 2014; Hu and Kuhn, 2014). However, the exact magnitude and dominance of these processes is still being debated, which has resulted in an on-going controversy over whether the redistribution of C across landscapes, and the associated impact on agro-ecosystems productivity, leads to a C sink from the atmosphere to the soil (e.g. Lal, 2003; Lal, 2004; Jacinthe et al., 2004; Polyakov and Lal, 2008), or a C source from the soil to the atmosphere (e.g. Stallard, 1998; Harden et al., 1999; Berhe et al., 2007; Van Oost et al., 2007).

The C source asserters argue that erosion promotes CO_2 emissions from agricultural land to the atmosphere, because:

1) Reduced NPP on eroded lands causes decrease of C input (Lal, 2003; Lal; 2004; Lal, 2005);

2) Aggregate detachment under raindrop impact and further breakdown during transport leads to increased mineralization (Polyakov and Lal, 2004; Jacinthe et al. 2002 & 2004);

3) Decomposition of SOC in the top soil layer of depositional sites results in high CO_2 emission (Schlesinger, 1990; Jacinthe and Lal, 2001; Lal and Pimentel, 2008).

Other scientists argue the opposite: soil erosion increases C sequestration and reduces CO_2 emission, finally generating a C sink on arable lands. Their evidences are:

1) Erosion causes exposure of C-depleted subsoil to store more SOC through dynamic replacement (Six et al., 2004; Van Oost et al., 2007);

2) The mineralization during transport is limited, especially for rill and gully erosion (Stallard, 1998; Harden et al., 1999; Liu et al., 2003; Van Oost et al., 2007&2012);

3) The SOC buried in depositional site is largely protected and not readily mineralized (Berhe et al., 2007).

The controversy highlights the large amount of uncertainties in C dynamics due to the lack of spatial data and models to completely simulate C dynamics (Kuhn, 2013). Therefore, gaining more insight into the fate of SOC in erosion and depositional processes across agricultural landscapes is still urgently required in order to understand the role of lateral soil movement for regional and global biogeochemical cycles and hence, climate change, and ultimately finally resolve this current controversy (Kirkels et al., 2014).

1.2 Knowledge gaps in studies of C dynamics on eroded lands

1.2.1 Uncertainties of using C inventories to calculate C fluxes

Because of limited availability of data on SOC stocks and their history, many investigations regarding C dynamics on eroded lands are based on extrapolation of slope-scale SOC inventories to a global scale by coupling erosion models with observed SOC inventories (e.g. Van Oost et al., 2007; Quinton et al., 2010; Van Oost et al., 2012). The calculations using SOC inventories of slope-scale to back-calculate C fluxes caused by erosion has been questioned, because they are based on the assumption that soil conditions and dynamic replacement of SOC in source areas is stationary (e.g. Van Oost et al., 2007). However, Kuhn et al (2009) showed that SOC erosion rates do not have the same pattern as soil erosion rates over long term (e.g. the Holocene period), because erosion affects the soil C content

profile and thus the C content of the sediment over time. This illustrates that SOC erosion is dynamic rather than stationary in a changing environment.

Moreover, the use of SOC inventories to calculate C fluxes also relies on the assumption that sediment properties during transport and after deposition are unchanged, i.e. non-selective transport and deposition. In fact, within the transport pathways that link eroding sites to depositional sites, entrainment and transportation processes nearly always involve selective removal of fine and light sediment, as well as preferential deposition of coarse and heavy sediment (Kuhn et al., 2009; Kuhn, 2013). It is well documented that the selective transport of SOC-rich material during interrill erosion events leads to a higher enrichment ratio of sediment-associated SOC compared to the bulk soil (e.g. Polyakov and Lal, 2004; Kuhn, 2007; Schiettecatte et al., 2008; Hu et al., 2013a). For rill erosion, although the transport of sediment is not selective, the eroded sediment and sediment-associated SOC are gradually re-settled across landscapes when hydraulic conditions change (Nearing et al., 1989). During this process, some of the coarse sediment and associated SOC is deposited in depressions, whereas some light fractions, including fine silts, clays and labile SOC, are preferentially transported further into aquatic ecosystems (Lal, 2004). Because of the different C concentrations in coarse and fine sediment, it leads to non-uniform distribution of C across landscapes. (Kuhn et al., 2009; Z. Wang et al., 2010). Therefore, without considering the differentiation of sediment associated C during redistribution, the approach of using SOC inventories to back-calculate C fluxes caused by erosion can lead to biased estimate (Kuhn, 2013). Improving the assessment the impact of soil erosion on C cycling thus requires a better understanding of the movement of eroded sediment and associated SOC across agricultural landscapes (Kuhn, 2013; Kirkels et al., 2014). Therefore, out of the numerous uncertainties in the studies of SOC dynamics on eroded lands, one key issue to be addressed is to correctly assess the potential impact of redistribution of sediment on the subsequent fate of eroded SOC. This process is conceptualized in Figure 1.2.

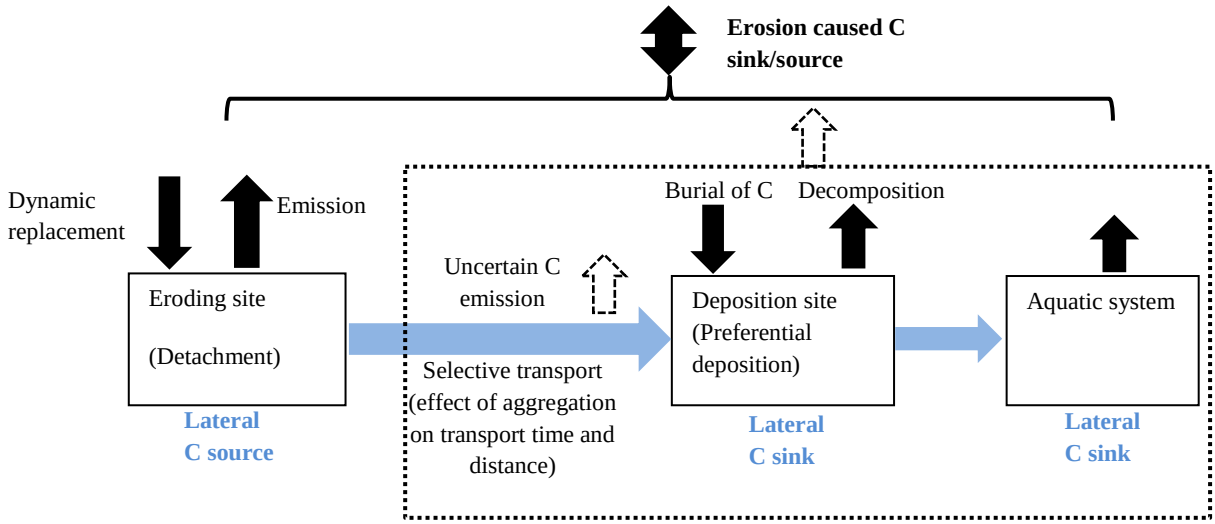

Figure 1.2 C flux budget and study target of this study (dashed box). Blue arrows indicate the redistribution of C. Black arrows represent C fluxes. Blue arrows represent water flow.

1.2.2 Erosion modeling and settling velocity based on mineral grains

The redistribution of sediment and associated SOC across landscapes is determined by the transport distances of differently-sized sediment fractions (Kinnell, 2001; Kinnell, 2005; Kuhn and Armstrong, 2012). Hence, erosion models describing sediment transport would be an effective approach to gain a deeper understanding of sediment redistribution and the emerging spatial patterns of SOC depletion and deposition across landscapes (Kuhn, 2013). Such improved modeling would also contribute to understanding the effects of sediment associated SOC on land degradation, river ecology, regional and global biogeochemical cycles, climate change and environmental health (Loch, 2001; Van Oost, et al. 2005; Kuhn, 2013; Hu and Kuhn, 2014; Hu and Kuhn, 2016).

Despite the promising application of erosion models in investigating the redistribution of sediment and associated SOC across landscapes, the quality of the output depends highly on the quality of input parameters, i.e. the "gigo" principle ("gigo" refers to "**g**arbage **i**n = **g**arbage **o**ut"). Traditionally, size and density distributions of eroded sediment have been applied to erosion models to predict selective transport and deposition (Loch, 2001), such as the Chemicals, Run-off, and Erosion from Agricultural Management Systems (CREAMS) erosion model (Knisel, 1980). However, the density of each fraction of eroded sediment is difficult to determine, especially for the wet-density when sediment is saturated during erosion events. In response to this limitation, Foster et al. (1985) developed an algorithm to estimate sediment size and density distributions according to the mineral particle size distribution. However, the poor performance of the algorithm for many soils has limited its application (Loch, 2001).

Apart from the sediment discharge and hydraulic conditions such as flow velocity, flow depth, and flow turbulence, the transport distance of eroded sediment is closely related to settling velocity, which integrates the effects of size, shape and density of eroded sediment into one single parameter (Gibbs et al., 1971; Hallermeier, 1981; Dietrich, 1982; Cheng, 1997; Ferguson and Church, 2004). Settling velocity has already been applied in some erosion models to predict the redistribution of sediment. For example, Hairsine et al. (2002) developed a model for the description of processes and sediment fluxes through landscapes, in which settling velocity is a key parameter input. Based on the model of Hairsine et al. (2002), Van Oost et al. (2004) presented a model named Multi-class Sediment Transport and Deposition (MSTD) to describe sediment fluxes and depositional processes in a two-dimensional spatial context. In these models, settling velocity was calculated from the mineral particle size distribution and an assumed density equivalent to 2.65 g cm^{-3}, according to an equation proposed by Dietrich (1982). However, soil is not often eroded as individual mineral grains, but is mostly eroded in the form of aggregates (Walling, 1988; Nadeu et al., 2011). Aggregation can considerably increase the size of eroded sediment by combining mineral grains into aggregates, and thus increasing the settling velocity (Hu et al., 2013b, Hu and Kuhn, 2014). Therefore, the upper limits of mineral grain size classes used in current erosion models are often smaller than actual aggregate size. In

addition, for the same sized mineral particles and/or aggregates, their settling velocities are also distinct due to the different densities and shapes (Dietrich, 1982; Loch, 2001). Using settling velocities based on mineral grain size distribution in erosion models therefore carries the risk of generating erroneous transport distance data.

1.2.3 Settling velocity based on wet-sieved aggregates

In order to overcome the disadvantages of using settling velocities based on mineral grain size distribution, aggregate destruction, based on the actual aggregate breakdown mechanism, represents a more reasonable way to determine the settling velocity of sediment in erosion events. According to Le Bissonnais (1996), four basic mechanisms are involved in aggregate breakdown. These are: (i) slaking caused by the compression of entrapped air during wetting; (ii) microcracking caused by and due to partial slaking; (iii) mechanical breakdown due to raindrop impact; and (iv) physico-chemical dispersion due to osmotic stress. Le Bissonnais (1996) further developed a unified methodological framework for distinguishing elementary mechanisms of aggregate breakdown and further measuring their stability. Generally, the framework identifies three different aggregate breakdown mechanisms, which include (i) fast-wetting; (ii) slow-wetting; and (iii) stirring of pre-wetted aggregates artificially with a stick. Fast-wetting is used to simulate aggregate breakdown during the initial period of heavy rain storms. Slow-wetting, which is less destructive compared to fast-wetting, is used to simulate aggregate breakdown during the initial period under gentle rain. The stirring method is expected to simulate the aggregate breakdown caused by raindrop impact as rainfall accumulated.

The wet-sieving methods, such as that proposed by Le Bissonnais (1996), separate the aggregate breakdown processes into different sub-processes according to the different physical mechanisms listed above. It has been widely used in measuring aggregate stability for various soils (e.g. Legout et al., 2005; J. Wang et al., 2014). Some researchers have also used size distribution of wet-sieved aggregates to calculate settling velocity for inclusion in erosion models (e.g. Angima et al., 2003). Apart from the successful application in measuring aggregate stability, it should be noted that the aggregate breakdown is a complicated process under impacting raindrops. The effects of different mechanisms on aggregate breakdown vary depending on the rainfall scenario as well as rainfall process. For example, microcracking plays a key role at the beginning of rainfall, while mechanical breakdown becomes dominant as rainfall accumulates (Legout et al., 2005). Directly copying the wet-sieving method may not properly simulate all the mechanisms involved during a rainfall event (Le Bissonnais, 1996). Moreover, aggregate size distribution derived from wet-sieving fractionation ignores the potential influence of porosity, irregular shape, and the involvement of organic matter, and thus cannot accurately reflect the settling behavior of aggregates (Loch, 2001). Therefore, a proxy that can simulate the natural breakdown process of aggregate and generate natural or quasi-natural sediment is urgently needed.

1.2.4 Mineralization of eroded SOC during transport

Apart from the knowledge gaps in terms of estimating the redistribution of sediment and associated SOC, the mineralization of eroded SOC also represents a large source of uncertainty. Many studies have reported that erosion accelerates mineralization during detachment and transport, because aggregate breakdown exposes previously incorporated, and hence, protected SOC within the aggregates themselves (e.g. Polyakov and Lal, 2004; Jacinthe et al., 2004). Lal et al. (2004) conclude that more than 20% of eroded SOC would be mineralized during transport. They therefore proposed that SOC mineralization during transport should be taken into account within the overall C budget. However, other studies have argued that the SOC mineralization is negligible due to the rapid transport of sediment (e.g. Van Oost et al., 2007 & 2012). To resolve the discrepancies of potential mineralization of eroded SOC, it needs to investigate the potential transport distance of eroded SOC after erosion. However, current studies, with respect to the fate of eroded SOC across landscapes, are either based on SOC inventory of eroding and depositional sites, or deduced based on an arbitrary transport distance. For example, Jacinthe et al. (2004) only identified respiration rates of SOC collected from outlets of watersheds, ignoring potential effects of various transport processes on accelerating SOC mineralization. It is therefore unable to reflect the actual SOC mineralization potential during transport as well as to predict the fate of eroded SOC during natural erosion events (Hu and Kuhn, 2014). An approach to efficiently fractionate eroded SOC, according to respective transport distance, to determine the potential mineralization of each SOC fraction is urgently needed. As discussed in section **1.2.2** above, apart from the sediment discharge and hydraulic conditions such as flow velocity, flow depth, and flow turbulence, the transport distance of eroded sediment is closely related to settling velocity (Loch, 2001). Therefore, the potential transport distance of eroded SOC can be identified by fractionating sediment according to settling velocity. The mineralization potential of each fractionated SOC fraction can thus be further determined and related to potential transport distance.

1.2.5 Previous investigations and questions to be addressed in this study

Recent studies have reported that settling velocity represents a promising parameter for modeling the redistribution of eroded sediment as well as for assessing the potential CO_2 mineralization based on transport distances of the sediment associated SOC (e.g. Hu et al., 2013b; Hu and Kuhn, 2014). Most notably, Hu et al. (2013b) developed a settling tube apparatus based on the “Griffith”-tube described by Hairsine and McTainsh (1986) and Loch (2001). The settling tube apparatus was first acknowledged as an efficient tool for determining the actual settling velocity of aggregates destroyed by fast-wetting (Hu et al., 2013b). Since the aggregates destroyed by fast-wetting cannot represent the natural sediment, Hu and Kuhn (2014) further used the settling tube apparatus to fractionate an aggregated silty loam eroded from a 150 × 80 cm flume after a number of simulated rainfall events. According to the settling behavior of the eroded soil fractions, the transport distance of eroded sediment was predicted. Based on the fractionation, the mineralization potential of the sediment with

different transport fates was further identified. By taking account of the potential effects of various transport processes on accelerating SOC mineralization, this method is much improved compared to the prediction of mineralization potential based on arbitrary transport distance (e.g. Jacinthe et al., 2004, see above in 1.2.4). While the observations highlight the necessity to account for the effect of aggregation on the redistribution of sediment associated SOC and C dynamics, there are still several open questions to be addressed:

Question 1: Effect of aggregation still maters on crusted soil?

Previous investigations were conducted under ideal conditions in the laboratory: soils sampled from the field were artificially dry-sieved to aggregates of small size (e.g. < 8 mm), leading to a uniform and smooth soil surface. However, the artificial plot surface prepared in the laboratory is much different from natural soil surfaces exposed to rainfall under field scenarios. The natural soil surface development always involves more complex factors than the artificial soil surface, such as tillage practices, wetting and drying cycles, vegetation cover, and animal activities (Freebairn et al., 1991; Le Bissonnais et al., 1996; Fox et al., 1998), resulting in much different and variable soil conditions (Kuhn et al., 2003). Overall, the artificial plot developed in the laboratory offers a convenient approach to investigate the erosion processes. However, the preferential study of a flat surface with uniform aggregates would overlook the important spatial and temporal variability of soil conditions found in the field (Freebairn et al., 1991; Le Bissonnais et al., 1995; Fox et al., 1998). It thus bears the risk of leading to a biased estimate of sediment detachment and movement. Therefore, it is necessary to conduct an investigation in the field to take into account the importance of natural soil conditions on the redistribution and fate of eroded sediment and SOC.

Question 2: How does aggregation affect SOC quality?

Despite recent studies (e.g. Hu et al., 2013b; Hu and Kuhn, 2014) have illustrated that aggregation can profoundly facilitate the settling velocities of individual mineral particles, and thus skew the redistribution and subsequent fate of eroded SOC, little is known about potential effect of aggregation on the quality of the redistributed SOC. Generally, two types of SOC can be distinguished in soils, i.e. mineral-associated organic carbon (MOC) and particulate organic carbon (POC) (Tisdall and Oades, 1982, Elliott, 1986), with the former being more recalcitrant with respect to mineralization than the latter (Z. Wang et al., 2010). Aggregation potentially reduces the settling velocity, and therefore the potential transport distance of both MOC and POC, that are incorporated into aggregates. The combination of MOC and POC with different respiration activities in aggregates may thus lead to contrasting mineralization potential during redistribution, as compared to that indicated by mineral grain distribution.

Question 3: How sensitive is sediment to repeated rainfalls?

Increased rainfall kinetic energy would lead to the breakdown of aggregates and the development of crusts. It is not entirely clear whether the changes of surface conditions could impact on the characteristics of sediment and thereby diminish the effects of aggregate on the fate of eroded SOC. Therefore, the significance of the greater kinetic energy on soil surface changes as well as on the sediment properties in soil erosion experiments, particularly on SOC erosion, need to be systematically investigated. This is not only important in terms of gaining a better understanding of the redistribution of eroded SOC, but also critical to the parameterization of erosion models. For instance, if sediment properties are dynamic as cumulative rainfall increases, all factors related to erosion process must be properly accounted for in order to avoid a large amount of uncertainty in the further application of modeling. Alternatively, if sediment properties are stable during a given rainfall event, they could be regarded as stable parameters, which will significantly simplify the parameterization process.

Question 4: Can we develop a simple proxy to capture the effect of aggregation?

From the perspective of parametrizing erosion models, such a task requires a large amount of accurate settling velocity data from a wide range of soils in order to cover the broad spatial heterogeneity that is involved in soil development. Identifying the settling velocity distribution based on laboratory or field tests with flumes, even if well-designed, is still far too much work for testing all soils over a sufficiently wide range of rainfall conditions. Therefore, it is also crucial to develop a simple but efficient proxy method to effectively capture the potential influence of raindrop impact induced aggregate breakdown on the transport distance of sediment and eroded SOC.

1.3 Objectives of this study

Based on the knowledge gaps identified above, the two aims of this study are:

1) To evaluate the potential effects of natural aggregated soil surface on settling velocity distributions and thus the potential fate of eroded sediment as well as associated SOC;

2) To develop a simple but efficient proxy method that provides accurate settling velocity information of various soil types for erosion models.

Four objectives were further identified in order to address those two aims. They are:

1) To investigate the potential fate of SOC eroded from natural crusted soil surface;

2) To identify the effect of aggregation on the quality of eroded SOC and examine the sensitivity of the sediment settling behavior to increased kinetic energy;

3) To develop a simple but efficient proxy method to generate natural or quasi-natural sediment; and

4) To evaluate the feasibility and sensitivity of such a proxy method.

1.4 Experiment rationale

1.4.1 Overview on the experimental design

The objectives mentioned above were investigated by performing a series of experiments conducted in the field and in the laboratory (Table 1.2). All four objectives involved undertaking a series of rainfall simulations in order to generate sufficient sediment, as well as settling-tube tests to identify the settling velocity of the generated material. Such design would allow capturing the effects of natural aggregation on settling velocity and thus the potential fate of eroded sediment during transport and deposition.

1.4.2 Field experiments

The first two objectives of this study, i.e. effect of aggregation on the redistribution of eroded sediment and SOC in a quasi-natural erosion event, as well as the mineralization potential of eroded SOC during transport, were investigated by a field experiment conducted on a crusted soil surface after harvest near the village of Witterswil, in northwestern Switzerland. In ***Field Experiments***, a modified portable wind and rainfall simulator (PWRS) (Fister et al., 2012) was used to generate wind-driven rainfall on a crusted agricultural land to mimic natural rainfall conditions. In ***Field Experiment 1***, one run of wind-driven rainfall (10 minutes) was conducted to generate natural sediment and investigate the settling velocity distribution of the eroded sediment. The distributions of SOC by aggregate size and by mineral grain size were compared in order to illustrate the effect of aggregation on the potential transport distance of sediment associated SOC. The potential mineralization of eroded SOC during transportation was determined by measuring the long-term mineralization of each settling fraction. During the same field campaign on the same plot, two more runs of wind-driven rainfall and one run of windless rainfall (10 minutes for each) were further conducted to identify the effect of aggregation on the quality of sediment associated SOC and investigate the sediment sensitivity to accumulated rainfall. This part hereafter refers to ***Field Experiment 2.*** Furthermore, the natural settling information of sediment obtained in ***Field Experiment 1&2*** would also provide a baseline of settling velocity distribution for developing a proxy method for generating quasi-natural sediment in ***Laboratory Experiment 1&2***.

Table 1.2 An overview of the experiment design of this study.

Aim	Experiment	Objective	Chapter
Effect of aggregation on the potential fate of eroded SOC	***Field Experiment 1***	To investigate the potential fate of SOC eroded from natural crusted soil surface	2
	Field Experiment 2	To identify the effect of aggregation on the quality of eroded SOC and examine the sensitivity of the sediment settling behavior to increased kinetic energy	3
Develop proxy method to identify settling velocity of aggregated soil	***Laboratory Experiment 1***	To develop a simple but efficient proxy method to generate natural or quasi-natural sediment	4
	Laboratory Experiment 2	To evaluate the feasibility and sensitivity of such a proxy method	5

1.4.3 Laboratory experiment

The third and fourth objectives, to develop a simple and efficient proxy to generate quasi-natural sediment, and to evaluate the feasibility and sensitivity of this proxy method, were conducted under controlled rainfall simulations in the laboratory. ***Laboratory Experiment 1*** therefore aimed to identify accurate settling velocity information for erosion models. An ideal settling velocity measurement of eroded sediment should involve quasi-natural destruction of aggregates followed by a settling velocity measurement, but avoiding any modifications in sediment size distribution by selective deposition. To generate such sediment, a Raindrop Aggregate Destruction Device (RADD) was devised to simulate the physical processes when aggregates are subjected to direct raindrop impact under simulated rainfall events. Those raindrop-impacted aggregates could then be fractionated by a settling tube apparatus according to their respective settling velocities. The combined Raindrop Aggregate Destruction Device- Settling Tube method (RADD-ST) was designed to capture the destructive effects of raindrop impact onto the aggregates, on the one hand, as well determine the actual settling behaviors of destroyed aggregates on the other hand. The efficiency of the combined RADD-ST method to reflect the actual settling behavior of those raindrop destroyed aggregates could be evaluated by comparing their settling velocity distributions with the settling velocity distribution calculated from mineral grain size distributions and that of sediment eroded from a plot (e.g. the flume in Hu and Kuhn (2014)). Based on the findings from ***Laboratory Experiment 1***, ***Laboratory Experiment 2*** extended the combined RADD-ST approach to various soils with similar texture but with different aggregation degrees. The feasibility and sensitivity of this method could be further verified by the settling behaviors of soils with different degrees of aggregation in response to increasing cumulative raindrop kinetic energy.

1.5 Thesis structure

There are five chapters in the remaining part of this thesis, which are outlined as follows:

Chapter 2 reports the results from ***Field Experiment 1***: Erosion of aggregated sediment and associated SOC under simulated wind-driven rainfall. It mainly discusses the effect of aggregation to reduce the likely transport distance of SOC and potential of such effects to increase the CO_2 emission during transport from the perspective of settling velocity. This chapter is planned to be submitted to the *Soil Discussions.*

Chapter 3 presents the results of ***Field Experiment 2*** in terms of SOC erosion and mineralization during transport. This chapter mainly describes the sensitivity of eroded sediment to accumulated rainfall impact and discusses the effect of aggregation on quality of sediment associated SOC. This manuscript is intended to be submitted to *Catena*.

Chapter 4 describes the design and rationale of a RADD approach in ***Laboratory Experiment 1*** to generate quasi-natural sediment. This chapter illustrates the importance of aggregation in determining the settling velocity distribution of sediment and suggests the potential application of the RADD approach to generate quasi-natural sediment. Chapter 3 was published in *Geographica Helvetica 2015, 70, 167–174; doi:10.5194/gh-70-167-2015.*

Chapter 5 presents the results of ***Laboratory Experiment 2***. It extends the RADD-ST approach to various soils with different degrees of aggregation on the basis of Chapter 4. This chapter aims to illustrate the feasibility and sensitivity of the RADD-ST approach. Chapter 5 was published in *Hydrology 2015, 2, 176-192; doi:10.3390/hydrology2040176*.

Chapter 6 summarizes the key findings from Chapters 2-5, and evaluates whether the research questions identified in Chapter 1 are properly addressed. The potential research outlook is also discussed in the end of this chapter.

Chapter 2

Potential fate of SOC eroded from a naturally crusted soil surface under wind-driven rainfall

Liangang Xiao, Wolfgang Fister, Philip Greenwood, Yaxian Hu and Nikolaus J. Kuhn

Manuscript in preparation, planned to submit to *Soil*

Abstract

Improving the assessment of the impact of soil erosion on carbon (C) cycling requires a better understanding of the redistribution of eroded sediment and associated soil organic carbon (SOC) across agricultural landscapes. Recent studies conducted on dry-sieved aggregates in a laboratory have reported that aggregation can dramatically skew SOC redistribution and its subsequent fate by increasing settling velocities of individual mineral particles. However, the erodibility of a soil in the field is more spatially and temporally variable due to the impacts of tillage, wetting-drying cycles, freezing, and biological effects. It is not entirely clear whether soil changes in natural surface conditions could impact on the characteristics of eroded sediment, thereby diminishing the effect of aggregation on the fate of the eroded SOC. Improving the evaluation of the fate of the eroded SOC therefore requires taking into account natural soil surface conditions in the field.

This study was aimed to investigate the potential fate of the SOC eroded from a naturally developed soil surface. Short term wind driven storms simulated with a portable wind and rainfall simulator (PWRS) were conducted on a crusted soil in the field. The sediments eroded were fractionated with a settling tube according to their potential transport distances. The sediment mass, SOC concentration and cumulative CO_2 emission of each fraction were identified to evaluate the effect of aggregation on the SOC distribution across sediment fractions. The results show: 1) 53% of eroded sediment and 62% of the eroded SOC from the natural surface in the field would deposit across landscapes, which were six times and three times higher compared to that implied by mineral grains; 2) the preferential deposition of SOC-rich fast-settling sediment potentially released approximately 50% more CO_2 than the same layer of the non-eroded original soil, indicating an additional CO_2 emission at depositional site after erosion events; 3) the CO_2 emission from the slow-settling fraction was three times greater compared to the bulk soil, suggesting the SOC associated with this fraction is very active after erosion events. Overall, the results of the field study confirm the trends observed in the laboratory that aggregation could profoundly impact on the potential fate of the eroded SOC across landscapes

compared to that suggested by mineral grain distribution. The preferential deposition of SOC-rich aggregates can further contribute to an increased CO_2 emission and strengthen the C source effect at depositional site. Furthermore, the CO_2 emissions from all transported fractions were on average 163 mg CO_2-C g^{-1} C during 80 days incubation, 70% higher compared to the 96 mg CO_2-C g^{-1} C the bulk soil. This indicates that the additional atmospheric CO_2 release during redistribution must be taken into account when calculating the C budget.

Keywords: aggregation, crust, wind driven storm, settling velocity, fate of the eroded SOC

2.1 Introduction

2.1.1 C dynamics and sediment redistribution

The net effect of soil erosion in the global carbon cycle has received increasing attention from soil and environmental-scientists (e.g. Stallard, 1998; Harden et al., 1999; Polyakov and Lal, 2004; Berhe et al., 2007; Van Oost et al., 2007; Kuhn et al., 2009; Quinton et al., 2010; Van Oost et al., 2012; X. Wang et al., 2014 Hu and Kuhn, 2014). However, it remains controversial whether the lateral redistribution of C across landscapes lead to a vertical C sink or C source since the expansion of agriculture (e.g. Lal, 2004; Van Oost et al., 2012). Currently, C dynamics on eroded lands are mostly assessed by comparing soil organic carbon (SOC) inventories at eroding sites to that at depositional sites (Van Oost et al., 2007; Quinton et al., 2010; Van Oost et al., 2012). These calculations are based on underlying assumptions of 1) the SOC content is temporally stationary and can be related to soil erosion rate to back-calculate the SOC erosion, and 2) the SOC content is spatially stationary when eroded sediment moves across landscapes (e.g. Van Oost et al., 2007). However, several recent reports have showed a temporary-dynamic pattern of the SOC content in the long term (Kuhn et al., 2009), as well as a spatial enrichment and/or depletion of SOC in sediment that differ from original soils (Quinton et al., 2001; Kuhn et al., 2009; Schiettecatte et al., 2008; Z. Wang et al., 2010; Kuhn and Armstrong, 2012; Hu and Kuhn, 2014). Therefore, without considering the SOC contents of soils at the time of erosion and understanding the differentiation of sediment between source and sink area during redistribution, the approach of using SOC inventories of slope scale to back-calculate C fluxes caused by erosion would lead to biased estimate (Kuhn et al., 2009).

Improving the assessment of the impact of soil erosion on C cycling therefore requires a better understanding of the movement of eroded sediment and associated SOC across agricultural landscapes (Kuhn et al., 2009; Kirkels et al., 2014). Apart from sediment concentrations and hydraulic conditions (Beuselinck et al., 2000), the transport distance of an eroded particle is determined by its settling velocity (Kinnell, 2001; Loch, 2001; Van Oost et al., 2004; Kuhn, 2013). Therefore, many erosion models apply the settling velocity of mineral grains as a key parameter when simulating the redistribution of sediment and sediment associated SOC (e.g. Fentie et al., 1999; Van Oost et al., 2004). However, sediment is not always eroded as dispersed mineral particles, but mostly in the form of aggregates (Walling, 1988). Aggregation profoundly increases the settling velocity of individual mineral grains that are incorporated into aggregates, as well as the transport distance of associated SOC (Hu and Kuhn, 2014). For aggregated sediment, using the settling velocity based on mineral grains may lead to a biased estimate of the redistribution of sediment associated SOC. Consequently, the uncertainties of calculating the lateral redistribution of sediment and associated SOC may further lead to a biased estimate of the vertical C release from the eroded SOC during redistribution (Billings et al., 2010; Hu and Kuhn, 2016). Therefore, the role of sediment aggregation requires further investigation in order to evaluate the redistribution and subsequent fate of the eroded SOC more

appropriately.

2.1.2 Erodibility changes and field conditions

Previous studies (Hu et al., 2013; Hu and Kuhn, 2014; Xiao et al., 2015a; Xiao et al., 2015b) have examined the transport fate of aggregated sediment and associated SOC based on settling velocity. For example, Xiao et al. (2015b) used a raindrop aggregate destruction device (RADD) to break down the dry-sieved aggregate and found that aggregation could increase the average settling velocity by six times. Hu and Kuhn (2014, 2016) reported that aggregation of dry-sieved aggregates would profoundly skew the SOC redistribution towards landscapes by facilitating the settling velocity of eroded sediment and consequently increase mineralization potential of the deposited SOC. While the observations highlight the necessity to account for the effect of aggregation on the redistribution of sediment associated SOC and C dynamics, they were conducted under ideal conditions in the laboratory: soils sampled from the field were artificially dry-sieved to aggregates of small size (e.g. < 8 mm), leading to a uniform and smooth soil surface. However, the natural soil surface development always involves more complex processes and factors than the soil surface prepared in the laboratory, such as tillage, wetting and drying cycles, vegetation cover, and animal activities (e.g. earthworms) (Le Bissonnais et al., 1996; Fox et al., 1998), resulting in much different and variable soil conditions (Kuhn et al., 2003). For instance, a prominent process on the natural soil surface is the development of a crust over almost one year after the soil disturbance caused by tillage at the time of planting (Slattery and Bryan, 1994; Torri et al., 1998; Salles et al., 2000). The development of the crust in the field may considerably alter the soil erodibility by reducing the infiltration rate and increasing soil cohesion (Chen et al., 1980; Moore and Singer, 1990; Robinson and Phillips, 2001; Kuhn, 2007). It is not entirely clear whether soil changes induced by the formation of the crust under natural circumstances could impact on the characteristics of sediment, thereby diminishing the effect of aggregation on the fate of the eroded SOC. Although the crust development and formation can be simulated using dry-sieved aggregates under single rainfall in the laboratory (e.g. Le Bissonnais et al., 1995; Kuhn et al, 2003), the further application of simulated crusted soil surface in the laboratory for generating natural sediment is still limited due to the lack of long-term natural impacts mentioned above. In addition to the changed soil erodibility, the adoption of the dry-sieved aggregates also significantly reduces the soil surface roughness as compared to that in the field (Hu et al., 2013a). The reduced roughness in turn results in more diffused runoff and thus a shallower water film on the soil surface, which may change the detachment and transport of the sediment compared to the field. Furthermore, the soil depth of the flume test is much shallower than that in the field, which can also profoundly alter the hydrological responses and consequently the erosional responses during rainfall events. For instance, the infiltration capacity of the flume test in the laboratory is significantly reduced as compared to that in the field because of the restricted flow of water within the shallower soil body (X. Wang et al., 2014). This would in turn lead to a higher runoff rate on the artificially prepared soil surface than the natural field, which can further impact on the detachment and transport of sediment.

Overall, the soil surface developed in the laboratory offers a convenient approach to investigate the erosion processes. However, the preferential study of a flat-shallow surface with uniform aggregates would overlook the important spatial and temporal variability of soil conditions found in the field (Freebairn et al., 1991; Le Bissonnais et al., 1995; Fox et al., 1998). This possibly leads to a biased estimate of sediment detachment and movement. It is thus necessary to conduct an investigation in the field to take into account the importance of natural soil conditions on the redistribution and fate of eroded sediment and SOC.

2.1.3 Aim of this study

In order to quantitatively identify the potential fate of SOC eroded from a naturally crusted soil surface, a rainfall simulation was conducted in the field. A portable wind and rainfall simulator (PWRS) was used to test the sensitivity of sediment properties and subsequent C emissions to kinetic energy of rainfall. The sediments eroded from the natural bare surface were fractionated with a settling tube according to their potential transport distances. The CO_2 emissions of the fractionated sediment were then identified during 80 days incubation. The settling velocity distribution of aggregated sediment was compared with that of corresponding dispersed mineral grains, so as to evaluate the effect of aggregation on spatial redistribution of eroded sediment and SOC.

2.2 Materials and methods

2.2.1 Study site description

The study site is located in Witterswil, Switzerland (47°29' N, 7°30' E). The average annual temperature in Witterswil is 9.7 °C. The average annual rainfall is 817 mm (Climate-Data.org, 2014). The soil at this site is a silty loam, characterized as a Luvisol (FAO/ISRIC/ISSS, 1998). The soil has been under continuous crop farming for more than 20 years, most recent several years with wheat-maize rotations. A previous study has shown that this area is prone to erosion because of intensive agriculture, especially during the period when the bare soil surface is exposed directly to rainfall impact after harvesting (Croft et al., 2012). At the time the experiment was conducted in October, 2013 (Figure 2.1), the soil surface had been exposed to natural impacts of rainfalls, wetting-drying cycles, freezing, and animal activities (e.g. earthworms) in the field for almost one year since the last tillage when wheat was planted in the fall of the previous year. Most large aggregates formed by tillage had been destroyed into remnant loose aggregates and a flat cohesive layer of structural crust had developed as a result of interactions between rainfall, runoff and erosion (Figure 2.2a). Such conditions represent a soil surface that is particularly prone to erosion because the formation of the crust can considerably increase the runoff rates and the frequency of runoff events by reducing the infiltration (Chen et al., 1980; Moore and Singer, 1990). It was therefore considered as an ideal soil condition to assess the detachment and transport of sediment associated SOC as well as to compare the results to those from dry-sieved aggregates.

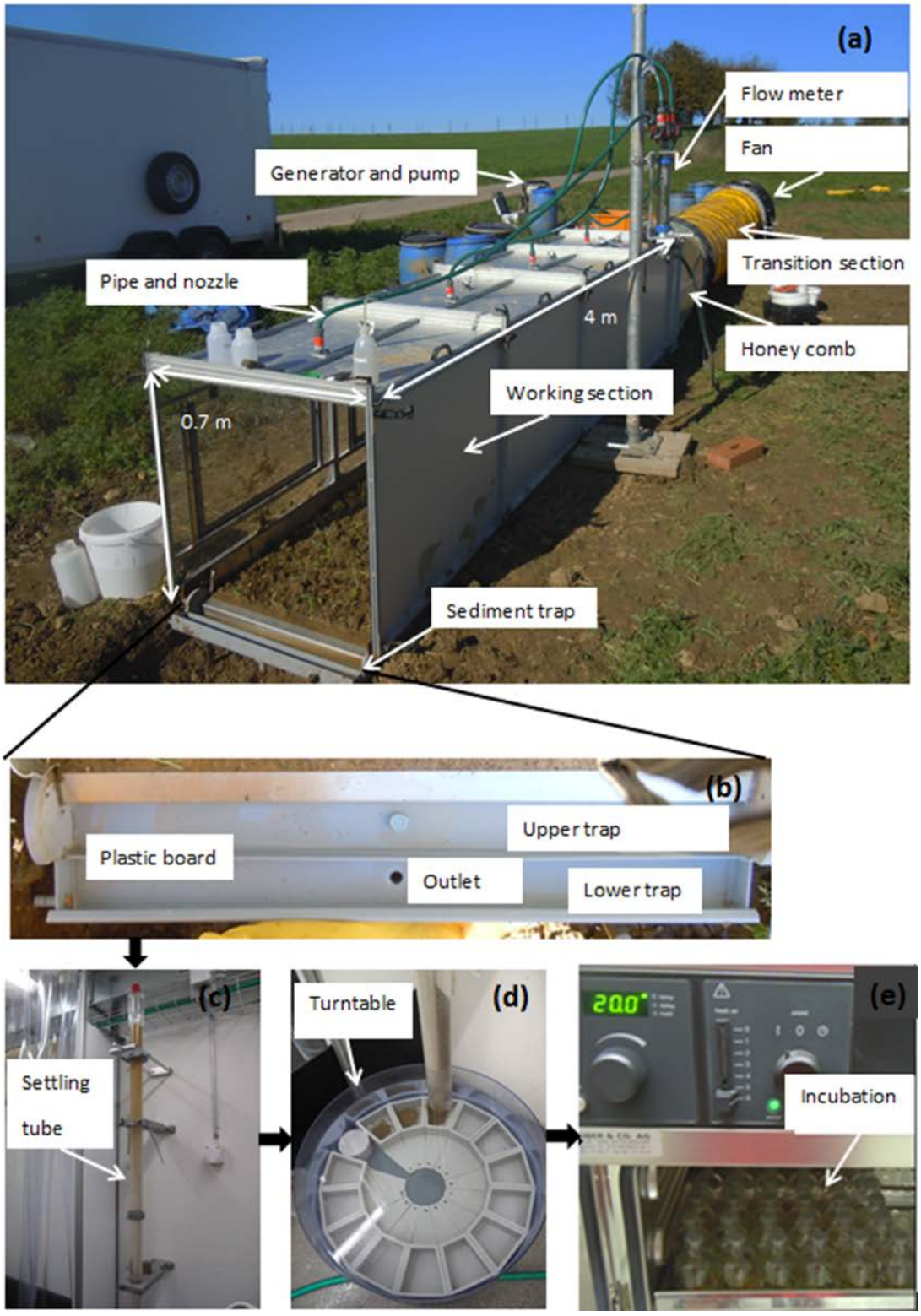

Figure 2.1 The experimental procedures: the rainfall simulation with a portable wind and rainfall simulator (PWRS) (a), the sediment trap (b), the settling tube apparatus (c), the turntable to collect the fractionated sediment (d), and incubation of the fractionated sediments (e).

2.2.2 Field rainfall simulation with a portable wind and rainfall simulator (PWRS)

A portable wind and rainfall simulator (PWRS) was used in the rainfall simulations in this study. The application of the PWRS enabled to simulate the natural erosive force as realistically as possible (Cornelis et al., 2004; Ries et al., 2014). Detailed information of the PWRS has been described in Fister et al. (2012). In brief, the PWRS consists of a fan to generate wind, a honeycomb and transition section to reduce the turbulences of wind, and a 4*0.7 m working section along which rainfall simulations can be conducted (Figure 2.1a). A water flow from a calibrated electric pump was distributed to the four spraying nozzles, which were installed 0.7 m above the soil surface on the roof of the tunnel. The four spraying nozzles were separated about 0.7 m away from each other along the tunnel, to fully and uniformly cover the entire four-meter working section. The four-meter plot was prolonged than the flumes used in the laboratory (e.g. Hu and Kuhn, 2014). It thus provided longer transport distance for eroded sediment to simulate a more comparable sediment transport process as that in natural erosion events.

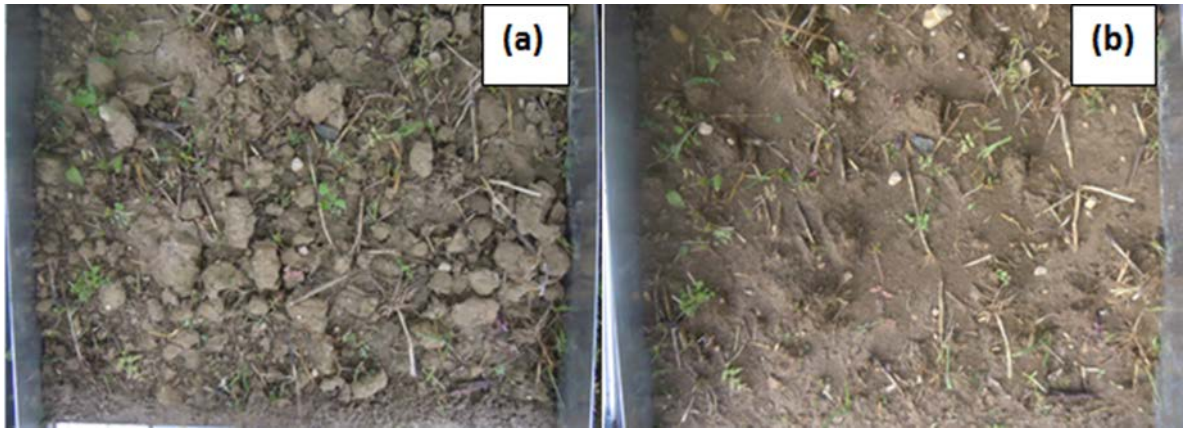

Figure 2.2 Soil surface before simulated rainfall (a) and after simulated rainfall (b)

A sediment trap was installed at the end of working section to collect sediment and runoff. Given that an aim of this study is to investigate the potential redistribution of eroded sediment, it is necessary to separate the coarse sediment that would deposit across landscapes from the fine sediment in suspension that would be preferentially transported further. The sediment trap was thus equally separated into upper and lower sub-traps by placing a vertically standing plastic board (5 mm shorter than the height of the sediment trap) in the middle (Figure 2.1b). When runoff and sediment flew into the sediment traps during rainfall events, the fast settling coarse aggregates would first pre-settle in the upper trap. The exceeding fine suspensions could then flow over the plastic board into the lower trap and then channeled into collection bottles. However, we observed certain amount of coarse aggregates (ca. 20%) would be flown over the board with runoff because of turbulent flow. To be more accurate, both the sediment deposited in the upper trap and sediment in suspension was fractionated with a settling tube (details see section 2.3).

A windless rainfall with an intensity of 30mm h^{-1} lasting for one hour was first conducted to pre-wet the soil. The cumulative kinetic energy of the pre-wetting rainfall, detected by a Joss–Waldvogel disdrometer, was on average 40 J m^{-2}. The pre-wetting enabled the soil to reach a saturation that facilitated faster runoff development during the actual test, given the greater infiltration capacity in the field than the soil prepared in the laboratory. No runoff and sediment was generated during this run of pre-wetting rainfall. After a 20-minute break, a wind driven storm was applied for 10 minutes with a rainfall intensity of 100 mm h^{-1} and a wind velocity of 5.2 m s^{-1}. The kinetic energy of the raindrops was on average 180 J m^{-2} h^{-1}. A rainfall with an intensity of 100 mm h^{-1} lasting 10 minutes is unlikely in the Witterswil area, where precipitation intensity is mostly less than 35 mm h^{-1} (recurrence interval of 0.33 years (MeteoSwiss, 2013)). However, given that the kinetic energy of simulated rainfall is typically lower than that during natural precipitation, increasing the rainfall intensity is commonly used as a compensatory approach to generate conditions that are more comparable to natural precipitation (Iserloh et al., 2012; Hu and Kuhn, 2014). A pretest had shown that a thorough breakdown of the aggregate requires a cumulative kinetic energy of about 75 J m^{-2}. Therefore, simulated rainfall of 100 mm h^{-1} lasting 10 minutes after the pre-wetting rainfall, corresponding to a total cumulative kinetic energy of ca. 70 J m^{-2}, were considered reasonable. The runoff from the wind driven storm was collected with standard sized bottles of 250 ml. After the rainfall events, the aggregates deposited in the upper trap was carefully washed into collectors, transported back to University of Basel Geography laboratory and stored in a cooling chamber (ca. 4 °C) for further tests. A previous test has shown that the aggregates are quite stable once eroded and moved into the trap, so the transfer process from the sediment trap to the laboratory did not initiate cause further breakdown of aggregates. Soil moisture and roughness were measured three times, i.e. before and after the pre-wetting rainfall, and after the wind driven storm. The soil moisture was identified with a TDR100 soil moisture meter. The soil roughness was measured using the chain method developed by Saleh (1993). In brief, a 50 cm long chain was placed across the soil surface. The horizontal chain length reduction caused by roughness was calculated as soil roughness, expressed in percentage (%).

2.2.3 Settling tube test

A 1.8 m long settling tube apparatus was used to fractionate both the eroded sediment collected from upper and lower traps (Figure 2.1c, d). The settling velocity distributions from both the upper and lower traps were then proportionally merged to calculate the overall settling velocity distribution of eroded sediment. The settling tube used in this study is similar to the Griffith tube (Hairsine and McTainsh, 1986; Loch, 2001; Hu et al., 2013b) and consists of four major components: a settling tube, an injection device, a turntable, and a control panel (Figure 2.1c, d). Detailed information about the setup and operation of the settling tube has been described in Hu et al. (2013b). In order to relate the settling velocity to particle diameter, Hu et al. (2013b) also proposed a concept of Equivalent Quartz Sizes (EQS) to represent the diameter of a nominal spherical quartz particle that would fall with the same velocity as the aggregated particle for which fall velocity is measured. Based on the EQS

concepts in Hu et al. (2013b) and the settling equation proposed by Gibbs et al. (1971), six particle size classes were selected: EQS of > 500 µm, 250 to 500 µm, 125 to 250 µm, 62 to 125 µm, 32 to 62 µm, and < 32 µm (Table 2.1). According to the findings reported by Starr et al. (2000), we assume that fractions of EQS > 62 µm would be possibly re-deposited across landscapes, while fractions of EQS < 62 µm would stay suspended and therefore is possibly to be transported to aquatic systems.

Table 2.1 Settling time intervals, settling velocity, equivalent quartz size (EQS), and possible fate of each fraction based on the conceptual model developed by Starr et al. (2000).

Time intervals (s)	Settling velocity (m s^{-1})	EQS (µm)	Possible fate
Before 20	>0.09	> 500	
20-40	0.045-0.09	250-500	
40-120	0.015-0.045	125-250	Deposited across landscapes
120-600	0.003-0.015	62-125	
600-1800	0.001-0.003	32-62	Possible to rivers
After 1800	<0.001	<32	

2.2.4 Sediment respiration measurements

After the fractionation, the sediment eroded from the crusted surface in the field was incubated to predict the mineralization potential after an erosion event. Approximately, 1-2 grams of fresh aggregates was immediately transferred into 60 ml bottles for sediment respiration tests (Figure 2.1e). Sediment respiration rates were measured based on the method described in Robertson et al. (1999) and Zibilske (1994). In brief, the sediment samples in the 60 ml bottles were incubated at 20 °C in a dark environment. All the bottles were kept open for ca. 12 hours to exclude the initial CO_2 pulses. Three replicates of the original undisturbed soil aggregates (ca. five grams) were also prepared in the same way to generate reference. Before performing measurements, all the bottles were then sealed with airtight rubber stoppers. Gaseous samples were taken immediately from headspace air at the top of each vials using syringe. The CO_2 concentration was then measured with a SRI 310C gas chromatograph. This method of sampling was repeated again after ca. 10 hour of incubation. The rate of CO_2 emission was determined based on the difference between the two samples before and after incubation. As a previous study had shown that CO_2 emissions from sediment were most active in the first 10 days after erosion (Hu and Kuhn, 2014), respiration measurements were repeated on day 1, 2, 4, 6, 11, 17, 24, 31, 38, 45, 52, 66, 80. During the 80 days, the variation of sediment moisture was constrained within 1% of variation by adding water every 3 days.

2.2.5 Mineral particle size distribution

In order to compare the differences between aggregated sediment settling velocity distribution and the soil texture derived settling velocity distribution, 25 grams of aggregated sediment was dispersed into mineral grains using a Sonifier 250 (Branson, USA), and then wet-sieved into six size classes listed

above (section 2.3). The energy dissipated in the water/soil suspension was ca. 60 J ml^{-1}, which could thoroughly disperse the aggregates (Xiao et al., 2015a).

2.2.6 Soil and sediment analysis

After settling fractionation and ultrasonic dispersion, all the EQS and dispersed soil fractions were dried at 40 °C and weighed. The SOC concentration of each EQS and dispersed soil fraction was determined using a Leco 612 carbon analyzer following the method of Hu et al. (2013a). The SOC mass distribution across the EQS and dispersed mineral grain classes was calculated by multiplying the SOC concentration of each class with their individual weight proportions. The cumulative respiration rates of each settling class and the original soils were calculated by adding up their hourly rates after linearly extrapolating the respiration rates per hour to 24 hours, and further to daily intervals (method adapted from Robertson et al., 1999; Zibilske, 1994; Hu and Kuhn, 2014). The CO_2 emissions across the EQS classes were also calculated by multiplying the CO_2 emissions of each class with their individual weight proportions.

2.3 Results

The erosional responses under the wind driven storm are listed in Table 2.2. In brief, runoff started in two minutes after the rainfall started, and kept increasing in the following 8 minutes. During the 10-minute wind driven storm, total runoff and sediment discharges were on average 3.5 l and 73 g, respectively (Table 2.2).

Figure 2.3 shows the EQS distribution of eroded sediment from the crusted surface in the field and its corresponding mineral grain fractions. About 53% of the sediment eroded from the crusted surface was of EQS > 62 µm, which was strongly contrasting against that only 10% indicated by mineral grain size distribution (Figure 2.3).

Table 2.2 Summary of the erosional responses to wetting rainfall and wind storm. Numbers in the brackets represent standard deviations.

Moisture			Roughness		Runoff		Sediment
Original (%)	After wetting (%)	After storm (%)	Original (%)	After storm (%)	Total runoff (l)	Runoff coefficient (%)	Total sediment
23.1 (6.1)	33.9 (1.8)	35.5 (4.3)	19.7 (5.3)	11.3 (2.7)	3.5 (1.4)	19.1 (7.6)	73.0 (67.4)

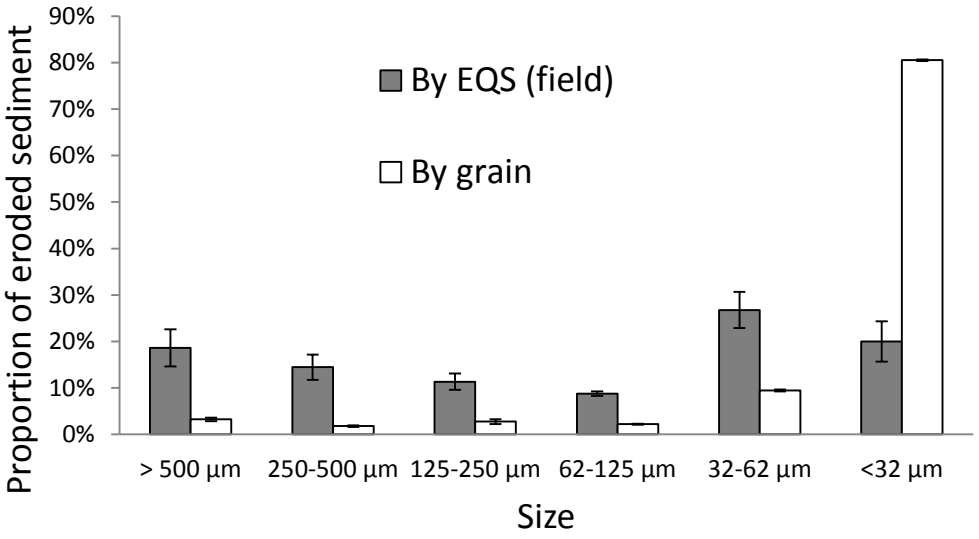

Figure 2.3 The weight distribution of the six Equivalent Quartz Size (EQS) fractions and six mineral grain fractions. See Table 2.1 for the potential fate of sediment and associated SOC. Bars represent standard errors.

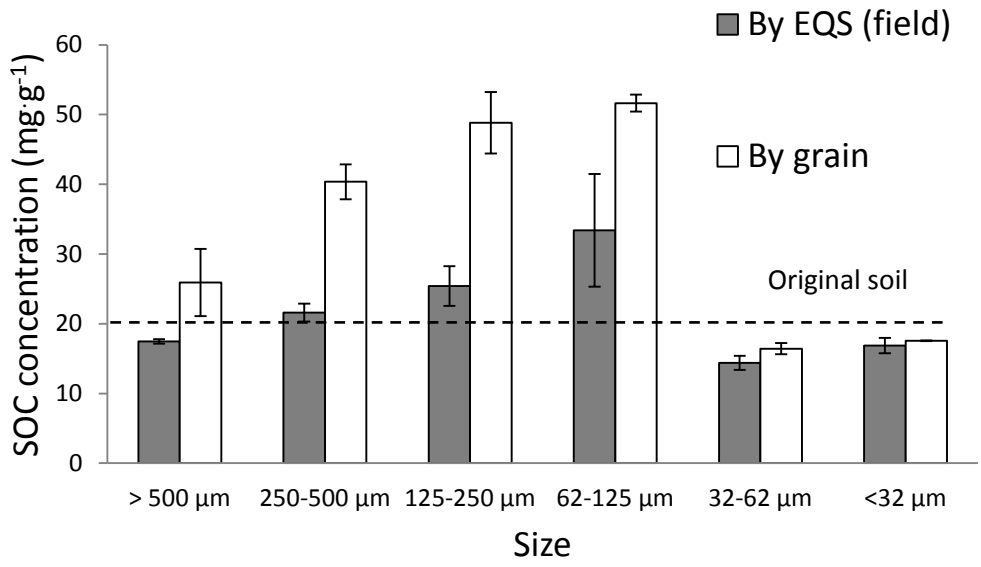

Figure 2.4 Soil organic carbon (SOC) concentration across Equivalent Quartz Size (EQS) fractions fractionated by the settling and across grain size classes dispersed by ultrasound. See Table 2.1 for the potential fate of sediment and associated SOC. Bars represent standard errors.

The SOC concentrations of each EQS fraction and mineral grain fraction are presented in Figure 2.4. Generally, the EQS fractions > 62 μm had equivalent or higher SOC concentration compared to the original soil. The highest SOC concentration was found in EQS of 62-125 μm, while the lowest concentration were found in the two finest EQS fractions. After multiplying the weight distribution of the sediment fractions (Figure 2.3) with their SOC concentrations (Figure 2.4), the distribution of SOC across EQS and mineral grain size fractions are shown in Figure 2.5. For the sediment from the field, the fractions of EQS > 62 μm contained 62% of the eroded SOC, which was strongly contrasting against the 20% suggested by the mineral specific SOC distribution in mineral grains > 62 μm (Figure 2.5).

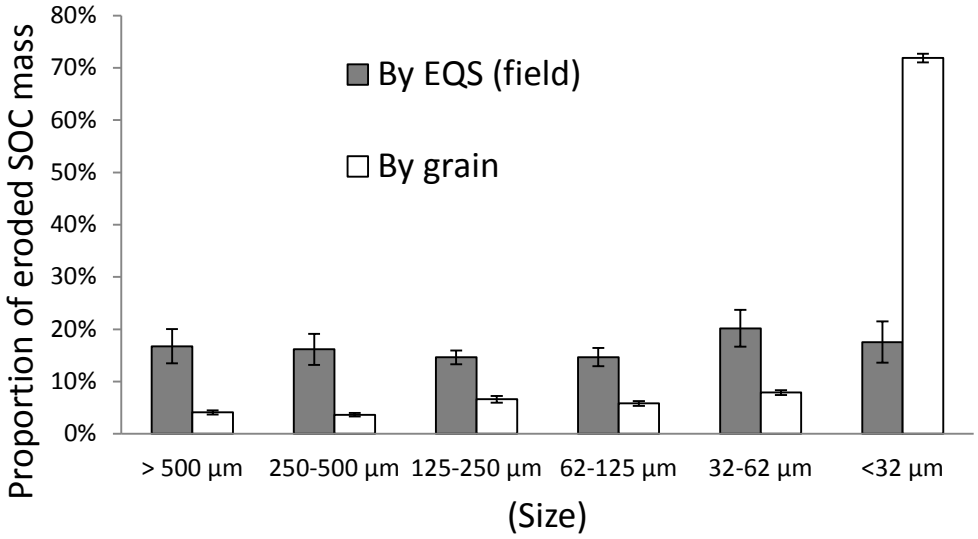

Figure 2.5 Soil organic carbon (SOC) mass distribution across Equivalent Quartz Size (EQS) fractions fractionated by the settling and across grain size classes dispersed by ultrasound. See Table 2.1 for the potential fate of sediment and associated SOC. Bars represent standard errors.

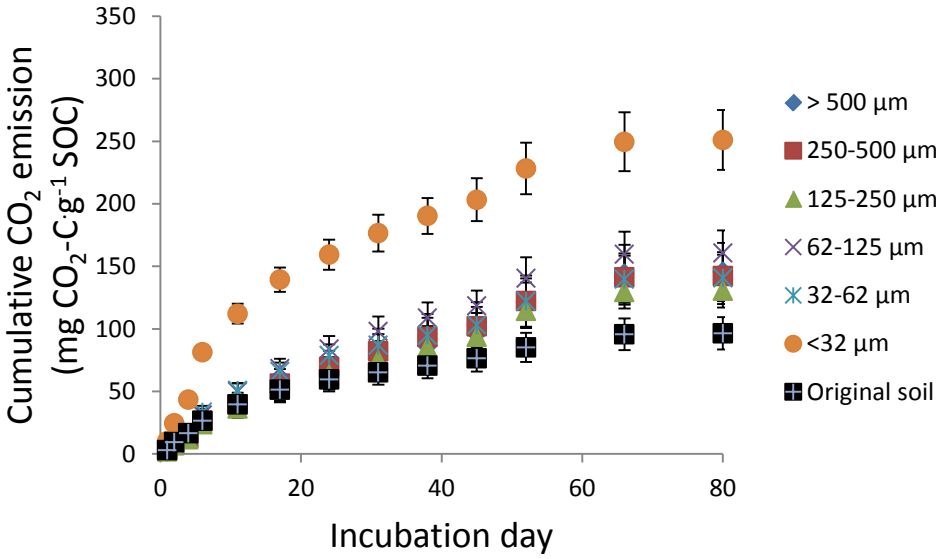

Figure 2.6 Cumulative CO_2 emissions of six Equivalent Quartz Size (EQS) fractions in the 80 days of incubation. See Table 2.1 for the potential fate of sediment and associated SOC. Bars represent standard errors.

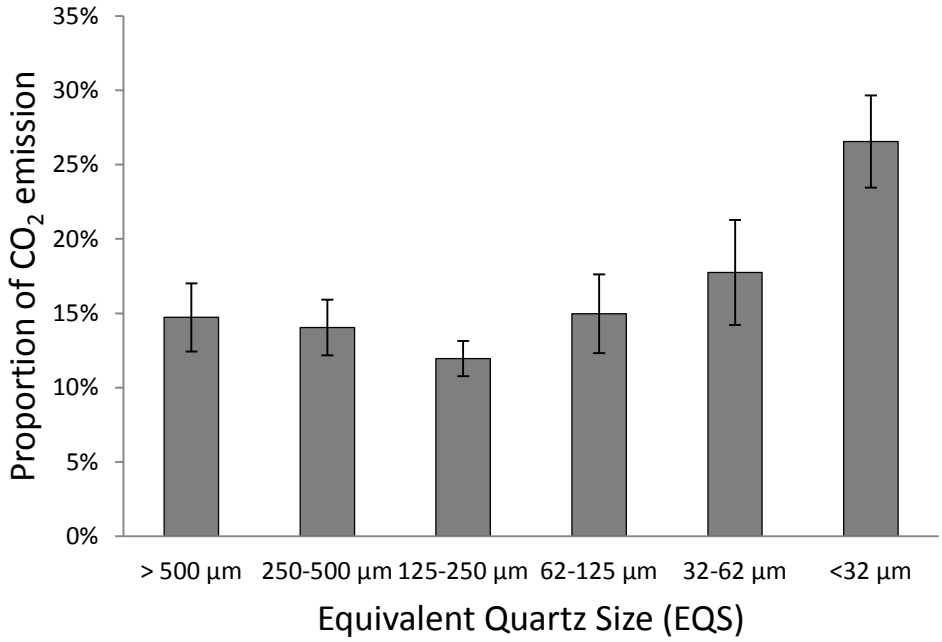

Figure 2.7 The potential shares of CO_2 emission from SOC of six Equivalent Quartz Size (EQS) fractions. See Table 2.1 for the potential fate of sediment and associated SOC.

The cumulative CO_2 emissions per gram of SOC associated with six EQS fractions were presented in Figure 2.6. The results show that the SOC in six EQS fractions were more susceptible to

mineralization than that in the original soils. The CO_2 emission from all transported fractions was on average 163 mg CO_2-C g^{-1} C during the 80 days incubation, 70% higher compared to the 96 mg CO_2-C g^{-1} C the bulk soil. Among the six EQS fractions, the greatest final cumulative CO_2 emission were observed in EQS < 32 μm, indicating the fine sediment was the most susceptible to mineralization (Figure 2.6). Figure 2.7 further shows the potential shares of CO_2 emission from eroded sediment of each fraction, out of which about 55% was mineralized from the SOC that was likely to be re-deposited across landscapes.

2.4 Discussion

2.4.1 Aggregation-induced skew of SOC deposition on crusted soil

Previous studies based on flume tests conducted in the laboratory reported that the aggregate would homogeneously breakdown (Hu and Kuhn, 2014; Hu and Kuhn et al., 2016). Finally, it leads to the formation of a new crust when interaction between rainfall, runoff and erosion achieves equilibrium under intensive rainfall (Hardy et al., 1983). However, this might not be the case in the field. On one hand, the in-situ observation only showed slight change of the crust after the rainfall simulation (Figure 2.2). This indicates the non-coherent washed-out layer, consisting of stable aggregates, has been largely removed during previous repeated erosion events (Kuhn et al., 2002). Consequently, the washed-in layer is gradually exposed to form the crust, resulting in a reduced erosion rate due to the increased cohesion and thus the lower erodibility (Torri et al., 1998; Kuhn et al., 2003). On the other hand, we did observe a considerable decrease of the size of remnant aggregates by the end of rainfall simulation (Figure 2.2), which finally led to the decreased roughness of the soil surface (Table 2.2). The results further demonstrate that the removal of the washed-out layer as well as the formation of a new crust lasts for a significant part of the erosion season (Kuhn et al., 2002). Such a dynamic erosion process was still prominent by the time of experiment (i.e. end of October). The contrasting responses of the crust and the remnant aggregates to the rainfall in the field illustrate the important effects of spatial and temporal variation of surface conditions on sediment detachment that has been overlooked in the laboratory.

The results further show that the potential deposition of the eroded sediment and SOC from the crusted surface are 6 times and 3 times higher compared to that implied by mineral grains, respectively (Figure 2.3; Figure 2.5). Despite the different processes of sediment detachment between the flume test and the field test, the contrasting distributions of eroded sediment and SOC between EQS fractions and mineral grain fractions confirm the observation based on the flume test that aggregation can potentially skew the SOC redistribution towards deposition across landscapes (Hu and Kuhn, 2014; Hu and Kuhn et al., 2016). Furthermore, due to the preferential deposition of SOC-rich fractions (Figure 2.4), the potential SOC stock of the top 25 cm layer at depositional site, in theory composed of fractions of EQS > 62 μm, would be 9.4 kg m^{-2} (bulk density assumed 1.65 g cm^{-1}). This is 13.2%

higher than that of the same depth of non-eroded original soil (Table 2.3). It thus challenges the previous assumption that the SOC concentration is unchanged during transport when calculating the C-flux based on C inventories of eroding sites and depositional site (e.g. Van Oost et al., 2007; Van Oost et al., 2012). Consequently, the preferentially deposited SOC-rich aggregates on the same nominal foot-slope potentially releases approximately 50% more CO_2 than the same layer of the non-eroded original soil (Table 2.3). The results are also in accordance with the previous studies conducted under laboratory conditions by Hu and Kuhn (2014, 2016) who estimated the SOC at depositional site would be enriched by ca. 12% and the potential mineralization of SOC would be increased by 100%. The consistent results illustrate that even though the soil surface is mostly protected by the crust, the amount of sediment detached as aggregate is still considerable, possibly due to the contribution of the remnant aggregates survived from previous erosion events. Therefore, we argue that the effect of aggregation on sediment redistribution is very prominent in erosion events and thus cannot be ignored when assessing the redistribution of the eroded SOC and C dynamics. Without considering the skewing deposition and enrichment of SOC at depositional sites caused by aggregation (e.g., in Dlugoß et al., 2012), it would consequently lead to an underestimation of C mineralization (Hu and Kuhn, 2014) (Figure 2.8).

Table 2.3 Comparison of soil organic carbon (SOC) stock and average CO_2 emission between the top layer of 25 cm from a temporary depositional site which is theoretically composed of only four Equivalent Quartz Size (EQS) classes, and the original soil in the same top layer of 25 cm. Density 1.65 g cm^{-3} is applied here to have a preliminary comparison because bulk densities for sediment fractions of different sizes are not available (NA).

	EQS (µm)	Proportion (%)	SOC concentration (mg g^{-1})	CO_2 emission (mg g^{-1} SOC)	Average SOC stock difference (%)	Average CO_2 emission difference (%)
Deposited fraction	> 500	34.3	17.5	145.5	+13.2	+50
	250-500	26.9	21.6	142.2		
	125-250	21.5	25.4	130.5		
	62-125	17.3	33.4	160.6		
Original soil	NA	NA	20.0	96.5	NA	NA

2.4.2 Potential mineralization from slow-settling sediment

In addition to the increased CO_2 emission from the fast-settling fractions at depositional sites, the potential fate of slow-settling fraction (i.e. the silt and clay fraction) that is possibly transported to aquatic systems also bears a large amount of uncertainties. Previous studies reported that the potential

mineralization from the slow-settling fraction was quite limited (e.g. Z. Wang et al., 2013). They attributed the low CO_2 emission to that the main component of SOC in the silt and clay fraction (< 53 µm) is mineral associated organic carbon (MOC), which is more stable than particulate organic carbon (POC) associated with coarse sediment (Six et al, 2002). However, our results based on incubation test show that the mineralization rate of the SOC in the slow-settling fraction of EQS < 32 µm was much higher compared to the other fractions, especially during the initial period of incubation (Figure 2.6). The fraction of EQS < 32 µm only contained 18% of the eroded SOC (Figure 2.5), but contributed up to 27% of total CO_2 emission (Figure 2.7), suggesting the SOC associated with this fraction is very active after erosion events. The actually high CO_2 mineralization from the fraction of EQS < 32 µm illustrates that, in addition to the recalcitrant MOC, there must be some labile SOC component that plays a more critical role in determining the CO_2 emission from the silt and clay fraction. Very likely, the labile SOC is the free silt-clay sized POC fragments that are not completely decomposed (Jacinthe et al., 2002). The free silt-clay sized labile SOC thus has a high risk of mineralization after erosion events, which has been underestimated by Z. Wang et al. (2013), at least for some soils. The high CO_2 mineralization from the silt-clay sized labile SOC has important implications for the long-term fate of the eroded SOC after erosion. Even though that we assume the aggregates of EQS < 32 µm are likely to be transported to aquatic systems, this does not mean that all eroded fine sediment would be transported to rivers during single rainfall event (Polyakov and Lal, 2004; Jacinthe et al., 2004). The redistribution of sediment and SOC is a complex process which involves drying, wetting, breakdown, and re-aggregation in repeated cycles of erosion, transport and deposition (Starr et al. 2000).The active life span of the small aggregates associated SOC might be long enough to contribute more additional CO_2 emission before finally reaching aquatic systems. Therefore, the potential fate of slow-settling fraction that is possibly transported to aquatic systems deserves more credit to the calculation of C budget (Li et al., 2015; Nadeu et al., 2015), possibly attributing more C loss from the soil to the atmosphere.

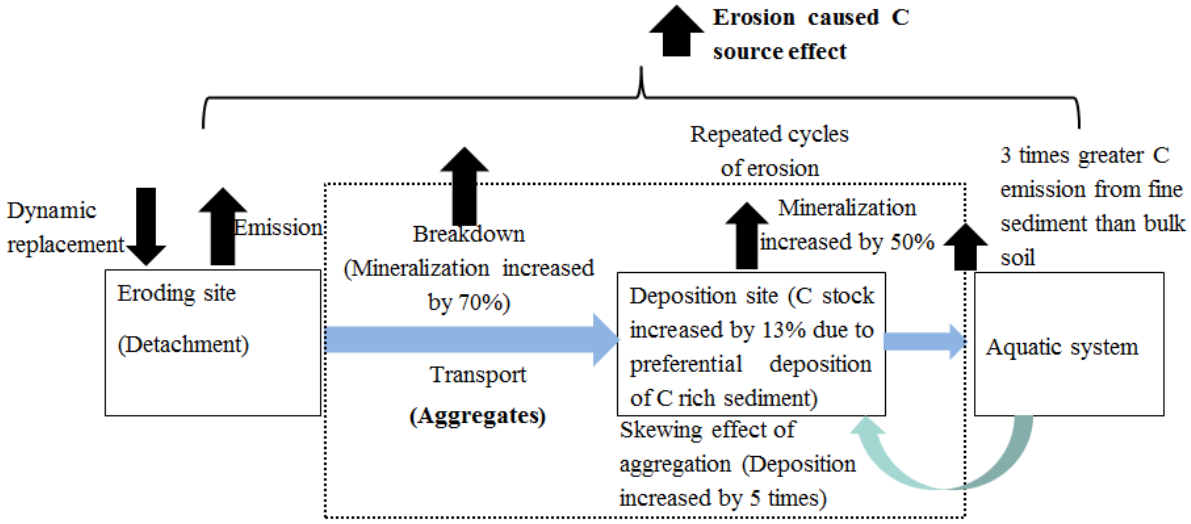

Figure 2.8 Conceptual diagram illustrating the mineralization risk of C eroded from the natural soil surface. The blue arrows represent water flow; the black arrows represent C fluxes; the green arrow represents the skewing effect of aggregation.

2.5 Conclusion

The aim of this study was to assess the potential fate of the SOC eroded from a naturally developed soil surface. The results on one hand demonstrate that the field situation can considerably change the erosion processes as compared to that based on the flume test in the laboratory. On the other hand, the field investigation confirms the previous studies conducted in the laboratory which illustrated that aggregation could significantly skew the redistribution of the eroded SOC towards deposition compared to that implied by mineral grain distribution. The preferential deposition of SOC-rich aggregates can further contribute to an increased CO_2 emission and strengthen the C source effect at depositional site. In addition to the SOC deposited across landscapes, the SOC associated with the slow-settling fraction that is possibly transported to aquatic systems also has a high risk to be mineralized after erosion events. This finding contrasts against the studies that reported the SOC associated with the silt and clay fraction was quite recalcitrant, which may underestimate the C mineralization potential during transport. Overall, the results suggest that aggregation plays an important role in the potential terrestrial SOC redistribution and erosion induced C cycling (Figure 2.8). Unless the impact of redistribution of the eroded SOC on C dynamic is adequately addressed, the erosion-induced carbon sink or source effects are still far from being fully understood.

Chapter 3

Effect of aggregation on transport of eroded sediment and SOC under wind-driven rainfall

Liangang Xiao, Wolfgang Fister, Philip Greenwood, Yaxian Hu and Nikolaus J. Kuhn

Manuscript in preparation, planned to submit to *Catena*

Abstract

The redistribution of eroded sediment and the associated soil organic carbon (SOC) plays a critical role in global carbon (C) cycling. Apart from sediment concentrations and hydraulic conditions, the transport distance of an eroded particle is determined by its settling velocity. Recent studies conducted in a laboratory have illustrated that aggregation can dramatically increase the settling velocities of individual mineral particles, and thus skew the redistribution and subsequent fate of eroded SOC. However, little is known about potential effect of aggregation on the quality of the redistributed SOC. Moreover, as compared to soil conditions in a laboratory, the erodibility of a soil in the field is inherently more spatially and temporally variable, due to the impacts of tillage, rainfalls, wetting-drying cycles, freezing, thawing and many biological processes. For example, rainfall kinetic energy will affect the breakdown of aggregates and the development of a crust. It is not entirely clear, however, whether changes in natural surface conditions could impact on the characteristics of sediment, and thereby diminish the effect of aggregation on the fate of the eroded SOC.

To fill the above knowledge gaps, four consecutive rainfall simulations were conducted using a portable wind and rainfall simulator (PWRS) on a natural soil surface after harvesting. The eroded sediments were fractionated into six different size-classes by a settling tube apparatus in order to predict their potential transport distances. To further examine the effect of aggregation on sediment transport, the same mass of sediment was also dispersed and sieved into the same six classes to form a comparison in size distribution. The SOC content and quality were measured for each settled and dispersed class to identify the effect of aggregation on the SOC distribution across sediment fractions. The cumulative CO_2 emission of each fraction was also measured during 80 days incubation to investigate the potential mineralization of C after erosion. Our results show that 1) the re-deposition of eroded SOC on hillslopes increased by a factor of three compared to that indicated by the mineral particle specific SOC distribution; 2) the underestimation of the proportion of eroded SOC deposited across landscapes can mainly be attributed to the underestimation of mineral-associated organic

carbon (MOC); 3) ca. 15% of the total eroded SOC was mineralized during incubation, which is approximately 50% more CO_2 than the same amount of disturbed bulk soil emitted; 4) the Equivalent Quartz Size (EQS) distribution of eroded sediment as well as the SOC concentration and mineralization potential of each fraction remained stable across the four rainfall simulations. Overall, our results illustrate that aggregation does not only skew the eroded SOC towards deposition but also profoundly impacts on the quality of the redistributed SOC by increasing the portion of MOC in deposited sediment, leading to an aggregate-specific, rather than mineral grain-specific, SOC redistribution. Further exposure of the deposited MOC due to aggregate breakdown in the following erosion events can potentially lead to additional CO_2 emissions that are currently unaccounted for. Moreover, the stable EQS distribution as well as the SOC concentration and mineralization potential of each fraction across four rainfall runs suggests that the settling information could be regarded as a stable parameter in erosion models. Therefore, it would be highly beneficial to develop a computable parameter that integrates aggregate settling velocity and the associated SOC distribution. Such an achievement would vastly simplify the parameterization processes and thus serve to optimize current erosion models.

Keywords: aggregation, crust, consecutive rainfall, settling velocity, erosion modelling

3.1 Introduction

3.1.1 C dynamics and sediment redistribution

The dynamics of soil erosion on C cycling have received increasing attention from soil and environmental-scientists (e.g. Stallard, 1998; Harden et al., 1999; Polyakov and Lal, 2004; Berhe et al., 2007; Van Oost et al., 2007; Kuhn et al., 2009; Quinton et al., 2010; Van Hemelryck et al., 2010; Hu and Kuhn, 2014, X. Wang et al., 2014). Yet, it remains controversial whether the redistribution of C across landscapes and associated impact on agro-ecosystem productivity has resulted in a net C sink or C source (e.g. Stallard, 1998; Lal, 2004; Van Oost et al., 2007). Currently, C dynamics on eroded lands are mostly assessed by comparing SOC inventories at eroding sites to that at depositional sites (e.g. Van Oost et al., 2007; Quine and Van Oost, 2007; Quinton et al., 2010). Calculations using SOC inventories of slope-scale to back-calculate C fluxes caused by erosion have been questioned, because they are based on the assumption that soil loss during transport, and dynamic replacement of SOC are static (e.g. Van Oost et al., 2007). However, Kuhn et al (2009) show that SOC erosion rates do not have the same temporal pattern as soil erosion rates over the long term (e.g. during the Holocene period), since erosion profoundly affects the soil C content profile and thus the C content of sediment over time. This illustrates that SOC erosion is temporally dynamic rather than stationary in the long term. Moreover, the use of SOC inventories to calculate C fluxes also relies on the assumption that sediment properties during transport and after deposition are spatially static, i.e. no-selective transport and deposition (Fiener et al., 2015). In fact, within the transport pathways that link eroding sites to depositional sites, entrainment and transportation processes nearly always involve selective removal of fine and light sediment, as well as the preferential deposition of coarse and heavy sediment (Schiettecatte et al., 2008; Kuhn et al., 2009; Z. Wang et al., 2010). Some recent studies have reported that ignoring the differentiation of sediment and sediment associated SOC during redistribution may lead to a substantial misinterpretation of erosion-induced C fluxes (Kuhn, 2013; Hu and Kuhn, 2014).

3.1.2 The effect of aggregation on sediment redistribution

Improving our understanding of soil erosion and its impact on C cycling necessitates discriminating sediment according to its transport distance during redistribution across agricultural landscapes (Kuhn et al., 2009; Kirkels et al., 2014). Apart from sediment concentrations and hydraulic conditions, that include flow velocity, flow depth, and turbulence within the overland flow itself (Beuselinck et al., 2000), the transport distance of eroded particles is determined by their settling velocity (Kinnell, 2001; Loch, 2001; van Oost et al., 2004; Kuhn, 2013). Therefore, many erosion models consider the settling velocity of mineral grains as a key parameter when simulating the redistribution of sediment and

sediment associated C. Examples of such models include the Griffith University Erosion System Template (GUEST) model (Fentie et al., 1999) and the Multi-class Sediment Transport and Deposition (MSTD) model (van Oost et al., 2004). Despite this assumption, however, sediment is not always eroded as dispersed mineral particles, but instead, is transported mostly in the form of aggregates (Walling, 1988). For aggregated sediment, the settling velocity based on mineral grains is unable to accurately reflect the natural settling behavior of sediment, because aggregation dramatically alters the size, density, shape and roughness of individual aggregates as compared with mineral grains (Hu et al., 2013b). Previous studies conducted on a simulated seedbed in a laboratory-based setting (e.g. Hu and Kuhn, 2014; Xiao et al., 2015a) examined the effect of aggregation on the fate of eroded sediment and associated SOC during transport. For example, Hu and Kuhn (2014, 2016) compared the SOC distribution of sediment eroded from a simulated seedbed in the laboratory with that of mineral grains and found that aggregation would profoundly skew those fractions remaining onremaining on landscapes by increasing the settling velocity of eroded sediment. More recently, Xiao et al. (in preparation) further took into account the effects of natural soil surface conditions and found that aggregation, even on a crusted soil, could profoundly impact the transportation and ultimately the potential fate of eroded SOC across landscapes.

3.1.3 Knowledge gaps

While those previous findings mentioned above confirm the necessity to account for the effect of aggregation on SOC spatial redistribution, the effect of aggregation on the quality of redistributed SOC have not been thoroughly examined. Generally, two types of SOC can be distinguished in soils, i.e. mineral-associated organic carbon (MOC) and particulate organic carbon (POC) (Tisdall and Oades, 1982, Elliott, 1986), with the former being more recalcitrant with respect to mineralization than the latter (Z. Wang et al., 2010). Aggregation potentially reduces the settling velocity, and therefore the potential transport distance of both MOC and POC, that are incorporated into aggregates. The combination of MOC and POC with different respiration activities in aggregates may thus lead to contrasting mineralization potential during redistribution, as compared to that indicated by mineral grain distribution. However, little is known about the effect of aggregation on the quality of the redistributed SOC and consequently on its potential fate in the environment.

In addition, the average settling information based on a single rainfall simulation was used to predict the potential fate of eroded sediment and associated SOC in previous studies (e.g. Hu and Kuhn, 2014, 2016). However, the natural soil surface conditions during erosion events are actually very sensitive to interactions between the raindrop impact and the soil surface (Kuhn et al., 2003). For example, the cumulative effect of raindrop impacts causes the breakdown of existing aggregates and the development of a new crust, leading to the formation a smooth but cohesive layer (Le Bissonnais et al., 1995). It is not entirely clear whether the soil surface changes during repeated rainfall in the field, especially the formation of crusts, could influence on the characteristics of particles resulting from detachment and thereby diminish the effects of aggregate on the fate of eroded SOC. Moreover, it is

well documented that SOC is often selectively eroded together with fine sediment (e.g. Kuhn, 2007; Schiettecatte et al., 2008; Kuhn et al., 2012; Z. Wang et al., 2010). The preferential removal of SOC could theoretically lead to the depletion of the SOC content in the soil surface layer after progressively receiving more rainfall. This may consequently impact on the amount of SOC eroded in the following erosion events. Therefore, the significance of the increased kinetic energy on the soil surface changes as well as on the sediment properties in soil erosion experiments, particularly on SOC erosion, needs to be systematically investigated. This is not only important in order to gain a better understanding of the redistribution of sediment associated SOC, but it is also critical to the parameterization of erosion models. For instance, if the sediment properties are dynamic as cumulative rainfall increases, all factors related to erosion process must be properly accounted for in order to avoid a large amount of uncertainty in the further application of modeling SOC redistribution across landscapes. Alternatively, if sediment properties are stable during a given rainfall event, they could be regarded as stable parameters, which will significantly simplify the parameterization process.

3.1.4 Aim of this study

This study is a follow-up to investigations undertaken by both Hu and Kuhn (2014, 2016) and Xiao et al. (in preparation), and the aims are: 1) to identify the effect of aggregation of crusted soil surface on the quality and mineralization of sediment associated SOC; and 2) to assess the sensitivity of sediment properties to cumulative kinetic energy in a series of simulated rainfall events. Four rainfall simulations were conducted on a naturally crusted soil surface to generate quasi-natural sediment. Sediment eroded from the field was fractionated using a settling tube according to their Equivalent Quartz Size (EQS) and thus potential transport distance across an agricultural landscape. The SOC content and the quality of the fractionated sediment were then identified, so as to be able to re-evaluate the effect of aggregation on the potential spatial redistribution of eroded SOC.

3.2 Materials and methods

3.2.1 Study site description

The experiment was conducted on a silty loam, characterized as a Luvisol (FAO/ISRIC/ISSS, 1998), in Witterswil, Switzerland (47°29' N, 7°30' E). The study site description and soil properties are presented in Table 3.1. A previous study has shown that this area is prone to erosion because of intensive agriculture, especially during the period when the bare soil surface is exposed directly to rainfall impact after harvesting (Croft et al., 2012). At the time the experiment was performed, in October, 2013, the soil surface had been exposed to natural impacts of rainfalls, wetting-drying cycles, freezing, and animal activities (e.g. earthworms) in the field for almost one year since the last tillage when wheat (*triticum*) was planted in the fall of the previous year. Most large aggregates induced by tillage had been destroyed into remnant loose aggregates and a flat cohesive layer of structural crust had developed as a result of interactions between rainfall, runoff and erosion. Such surface conditions

represent a soil condition that is particularly prone to erosion because the formation of the crust can considerably increase runoff rates and the frequency of runoff events by reducing infiltration (Chen et al., 1980; Moore and Singer, 1990).

3.2.2 Rainfall simulation

3.2.2.1 Portable wind and rainfall simulator (PWRS)

A portable wind and rainfall simulator (PWRS) was used in the rainfall simulations in this study. Detailed information about the PWRS has previously been described in Fister et al. (2012). Generally, the PWRS consists of a fan to generate wind, a honeycomb and transition section to reduce the wind turbulence, and a 4*0.7 m long working section along which rainfall simulations can be performed (Figure 3.1a). A flow meter was used to control the water flow pumped by the electric pump from the water supply barrels. The water flow was then distributed to the four separate spraying nozzles, which were installed 0.7 m above the soil surface on the roof of the tunnel. The four spraying nozzles were separated about 0.7 m away from each other along the tunnel, to fully and uniformly cover the entire working section.

Figure 3.1. The experimental procedures: the rainfall simulation with a portable wind and rainfall simulator (PWRS) (a), the sediment trap (b), the settling tube apparatus (c), and the turrntable to collect the fractionated deposited sediment (d).

3.2.2.2 Sediment trap

A sediment trap was installed at the end of working section to collect sediment and runoff (Figure 3.1b). Given that an aim of this study is to investigate the potential redistribution of eroded sediment, it is necessary to separate the coarse sediment that would deposit across landscapes from the fine sediment in suspension that would be preferentially transported further. In order to pre-separate the fine suspended fractions from the fast settling coarse aggregates, the sediment trap was equally separated into upper and lower sub-traps with a vertically standing plastic board in the middle. The plastic board is five mm shorter than the height of the sediment trap (Figure 3.1b), so that the fast settling coarse aggregates would first pre-settle in the upper trap when runoff and sediment was entrained and transported into the sediment traps during rainfall events. The fine suspension was then able to flow over the plastic board into the lower trap, whereupon it was then channeled into a series of collection bottles marked in numeric order. By pre-separating the fine suspensions away from the coarse aggregates, it was also possible to reduce the sample size of the fast settling aggregates to a reasonable amount, thus facilitating the settling tube fractionation work to be performed using the following steps (details see section 3.2.3).

3.2.2.3 Rainfall tests

A series of rainfall simulation each consisting of three replicates were conducted at the study site in October 2013. Windless rainfall with an intensity of 30 mm h^{-1} lasting for one hour was first conducted to pre-wet the soil. The cumulative kinetic energy of the pre-wetting rainfall, detected by a Joss–Waldvogel disdrometer, was on average 40 J m^{-2}. The pre-wetting induced an initial crust and soil settling processes that facilitated faster runoff development during the actual test. No sediment was generated during the pre-wetting run. After a 20-minute break, four rainfall runs (each of 10-minute duration) were conducted. The first, second, and fourth rainfalls were wind driven storms with a rainfall intensity of 100 mm h^{-1} and a wind velocity of 5.2 m s^{-1}. The kinetic energy of the wind-driven raindrops was on average 180 J m^{-2} h^{-1}. The third rainfall was windless but with the same rainfall intensity as the other three rainfall runs. The average kinetic energy of the windless raindrops was 163 J m^{-2} h^{-1}. The time break between each rainfall was 20-minute. Such configuration of rainfall patterns allowed us not only to investigate the sediment composition change as rainfall proceeds but also to investigate the influence of wind on sediment yield. During each rainfall test, runoff as well as fine sediment was collected continuously with standard sized bottles of 250 ml, and the time to fill up each bottle was also recorded in order to calculate the runoff rate. During the 20-minute break after each run of rainfall, sediment deposited in the upper trap was carefully washed into one litter bottle. All the samples were transported back to the University of Basel Geography Laboratory and stored in a cooling chamber at ca. four Celsius (°C) to await further tests. A previous test has shown that the aggregates are quite stable once eroded and moved into the trap, so the transfer process from the

sediment trap to the laboratory did not initiate further breakdown of aggregates.

To investigate the effects of cumulative rainfall on soil conditions, soil surface roughness and soil moisture were assessed. The soil roughness was measured using the chain method developed by Saleh (1993). In brief, a 50 cm long chain was placed across the soil surface. The horizontal chain length reduction caused by roughness was calculated as soil roughness, expressed in percentage (%). The soil moisture was identified with a TDR100 soil moisture meter. Both the soil surface roughness and soil moisture were measured three times during the rainfall simulation, i.e. before rainfall, after the first rainfall, and after the fourth rainfall.

3.2.3 Settling tube test

A settling tube apparatus was used to fractionate the sediment collected from the field (Figure 3.1c). The settling tube used in this study is similar to the Griffith tube (Hairsine and McTainsh, 1986; Loch, 2001; Hu et al., 2013b). Detailed information about the setup and operation of the settling tube has been described in Hu et al. (2013b). Based on the concept of Equivalent Quartz Sizes (EQS) described in Hu et al. (2013) and the settling equation proposed by Gibbs et al. (1971), six particle size classes were selected: EQS of > 500 μm, 250 to 500 μm, 125 to 250 μm, 62 to 125 μm, 32 to 62 μm, and < 32 μm (Table 3.2). According to the findings reported by Starr et al. (2000), we assume that fractions of EQS > 62 μm would be re-deposited across landscapes, whereas fractions of EQS < 62 μm would stay in suspension and therefore can be considered likely to be transported to aquatic ecosystems. Pre-tests showed that that more than 80% of the fine suspension overflown into the lower trap are of EQS < 62 μm, confirming that the cutoff of EQS < 62 μm to predict the potential fate of eroded sediment adopted in this study is valid. Given the limited volume of the injector of the settling tube, the coarse sediments collected in the upper trap were directly transferred to the injector and fractionated through the tube, while the fine suspension collected through the lower traps were first pre-settled for 12 hours in buckets (> 30 cm in depth). The supernatant and remaining suspended sediment (corresponding to EQS < 3 μm) was then decanted off and added to the EQS < 32 μm fraction remaining in suspension in the settling tube. To fully reflect the settling velocity distribution of all sediment collected, the settling velocity distributions of sediment from both the upper and lower traps were then proportionally merged based on the weight ratio.

Table 3.1 Study site description and soil properties.

Soil management	Average annual temperature (°C)/ rainfall (mm)	Slope (%)	SOC (%)	Sand (%)	Silt (%)	Clay (%)	Water stable aggregate (WSA) > 250 μm (%)
Maize /wheat rotations for 20 yrs	9.7/ 817	8.0 (0.1)	2.0 (0.1)	8.4 (1.0)	53.5 (0.7)	38.1 (1.5)	50.3 (4.7)

Table 3.2 Settling time intervals, settling velocity, equivalent quartz size (EQS), and possible fate of each fraction based on the conceptual model developed by Starr et al. (2000).

Time intervals (s)	Settling velocity (m/s)	EQS (μm)	Possible fate
Before 20	>0.09	> 500	
20-40	0.045-0.09	250-500	Deposited across landscapes
40-120	0.015-0.045	125-250	
120-600	0.003-0.015	62-125	
600-1800	0.001-0.003	32-62	Possible transfer to rivers
After 1800	<0.001	<32	

Table 3.3 Summary of moisture and soil surface roughness. Values in parenthesis represent standard deviations.

Moisture				Roughness		
Original (%)	After wetting (%)	After 1st rainfall (%)	After 4th rainfall (%)	Original (%)	After 1st rainfall (%)	After 4th rainfall (%)
23.1 (6.1)	33.9 (1.8)	35.5 (4.3)	36.67 (3.5)	19.7 (5.3)	11.3 (2.7)	8.0 (4.3)

3.2.4 Mineral particle size distribution

In order to assess the effect of aggregation on sediment composition, the EQS distribution of aggregated sediment was compared with the size distribution of mineral grains. The sediment was dispersed into mineral grains according to Kaiser et al. (2012). Approximately 25 g sediment was immersed in 50 ml of distilled water and then subjected to ultrasound dispersion using a Sonifier Model 250 (Branson, USA). The energy dissipated in the water/soil suspension was ca. 60 J ml^{-1}. The dispersed particles were then wet-sieved into six different class-sizes, corresponding to the EQS fractions described in 2.3.

3.2.5 Soil and sediment analysis

After fractionation and ultrasonic dispersion, all the EQS and dispersed soil fractions were dried at 40 °C. Approximately one gram of each dry sample was weighed from each fraction and ground for SOC measurement. SOC was determined using a Leco 612 at 550° C. To further determine the SOC quantity, the SOC was separated into two fractions using the method proposed by Cheng et al. (2010) and Z. Wang et al. (2013). Generally, three ml of sodium hexametaphosphate (5%) and sodium carbonate (0.7%) were added to one gram of dry soil from each sample each into a 25 ml bottle. After agitating for 18 h at 30 rpm, each dispersed sediment sample was washed through a 53 μm sieve. The material remaining on the sieve was collected by back-washing. We assume the amount of MOC in the fraction > 53 μm was very low because the specific surface area (SSA) of this fraction and the possibility for MOC to be bound to it was negligible in comparison to the clay fraction (Z. Wang et al., 2013). The organic carbon contained in the > 53 μm fraction was thus regarded as POC not bound to mineral surfaces, whereas the SOC in the fraction < 53 μm sieve was considered to be mineral-associated organic carbon (MOC). The SOC mass across EQS classes and mineral grain size classes were calculated by multiplying the SOC contents of each class with individual proportions.

3.2.6 Sediment respiration measurements

The sediment eroded from the crusted surface in the field was incubated to predict the mineralization potential after an erosion event. Approximately one-two grams of fresh aggregates was immediately transferred into 60 ml bottles and incubated at 20 °C in a dark environment for sediment respiration tests. Three replicates of the original undisturbed soil aggregates (ca. five grams) were also prepared in the same way to generate a reference value by calculating the mean of the three values. Before taking measurements, all the bottles were then sealed with airtight rubber stoppers in order that the resultant mineralized CO_2 would accumulate. Gaseous samples were taken immediately from headspace air at the top of each vial using a syringe. The CO_2 concentration was then measured with a SRI 310C gas chromatograph. This method of sampling was repeated again after ca. 10 hours of incubation. The rate of CO_2 emission was determined based on the difference between the two samples before and after incubation. Respiration measurements were repeated on days 1, 2, 4, 6, 11, 17, 24, 31, 38, 45, 52, 66,

80. During the 80 days, the variation of sediment moisture was constrained within 1% of change by adding water every 3 days. The cumulative CO_2 emissions of each settling class and the original soils were calculated by summing their hourly rates after linearly extrapolating the respiration rates per hour to 24 hours, and further to daily intervals (method adapted from Robertson et al., 1999; Zibilske, 1994; Hu and Kuhn, 2014).

3.3 Results

3.3.1. Erosional response during rainfall

The relationship between runoff and sediment during the four rainfall runs is shown in Figure 3.2. Overall, the results show that both runoff and sediment increased gradually from the first run to the fourth run. No considerable decline of runoff and sediment yield was observed for the third run consisting of windless rainfall only, as compared to the second and the fourth wind-driven runs with rainfall. Weight ratios between sediment deposited in the sediment trap and that transported in suspension for all the four rainfall runs are shown in Figure 3.3. More than 60% of eroded sediment was deposited in the trap, whereas the other 40% was transported in suspension. The proportions of sediment in the trap and that in suspension did not change significantly across four rainfall runs ($P > 0.05$, one way-ANOVA).

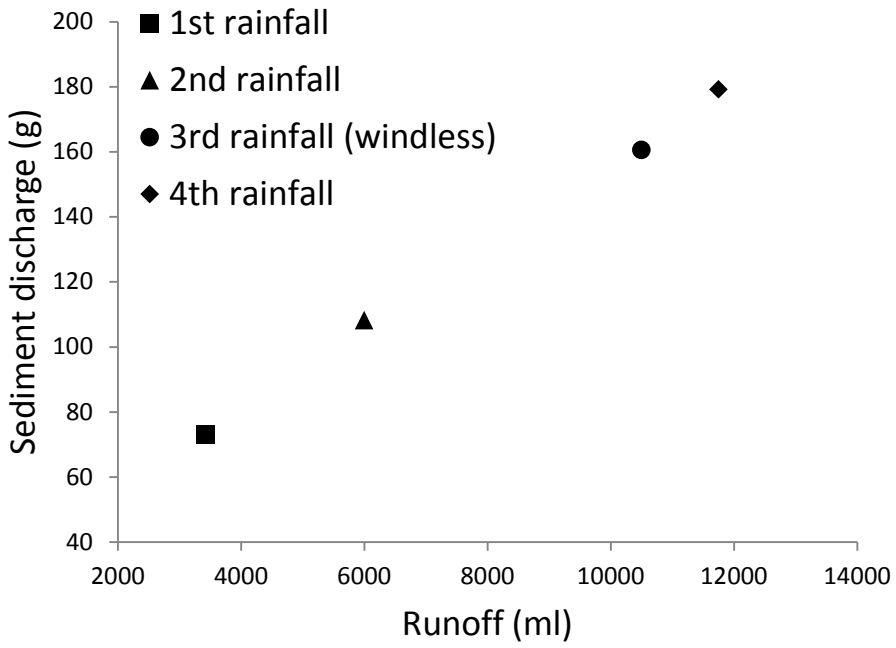

Figure 3.2 Relationship between runoff sediment recovered both from the trap and in suspension

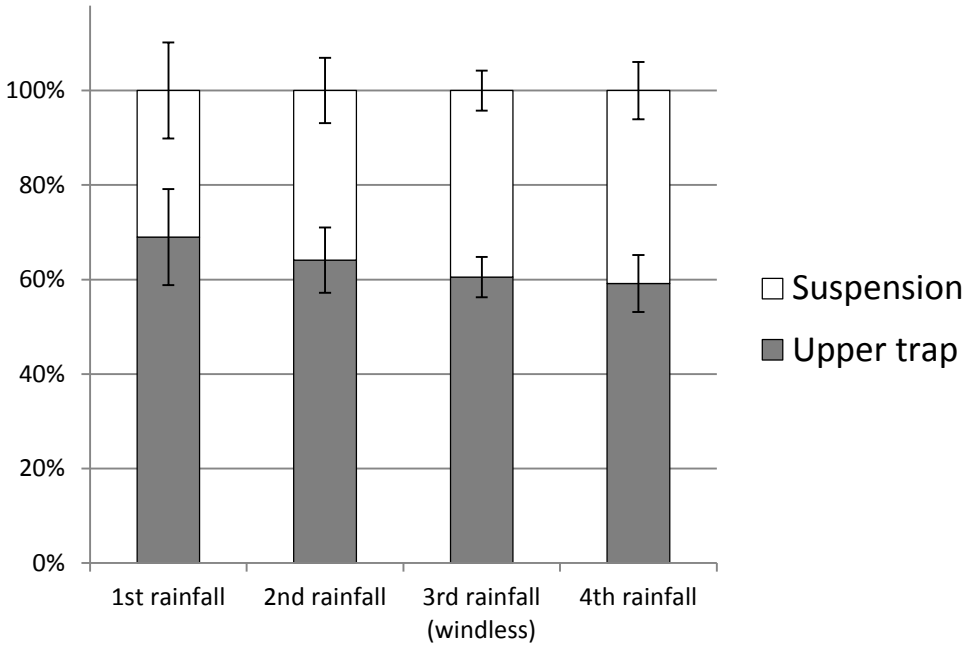

Figure 3.3 Weight percentage of sediment in upper trap and in suspension. Bars represent standard errors.

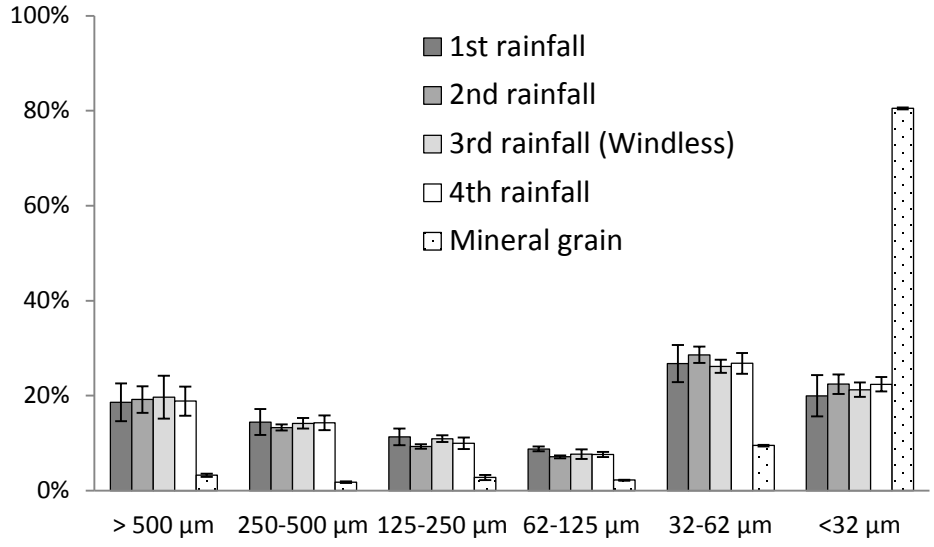

Figure 3.4 EQS distribution of aggregated sediment and corresponding dispersed mineral grains. Bars represent standard errors.

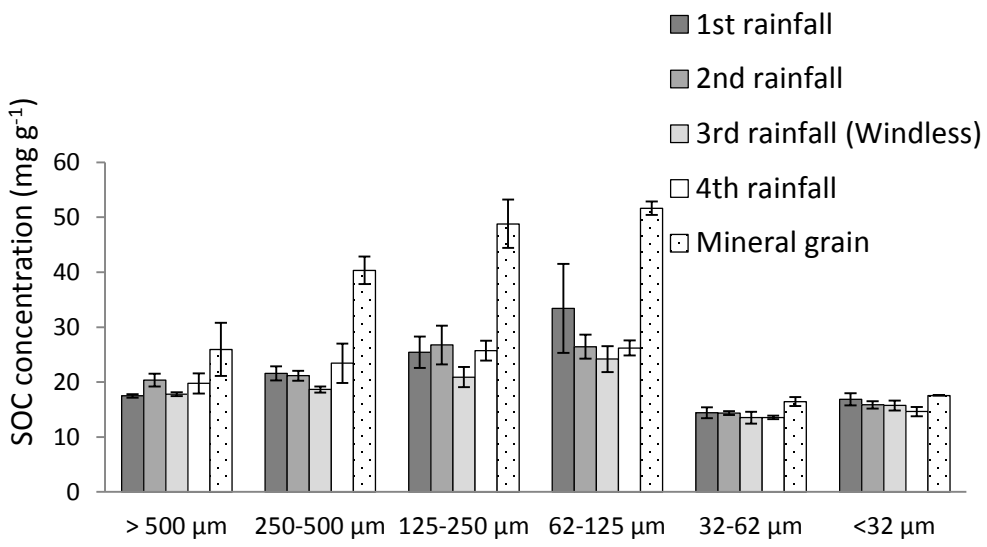

Figure 3.5 SOC concentrations across EQS fractions and mineral grain fractions. Bars represent standard errors.

3.3.2 EQS distribution of eroded sediment

Figure 3.4 shows the overall EQS distributions of aggregated sediment of the four rainfall runs and their corresponding mineral grain size distribution. The EQS distributions of aggregated sediment were not significantly different among the four rainfall runs ($P > 0.05$, one way-ANOVA), but differed markedly from the distribution of mineral grain fractions ($P < 0.05$). For the aggregated sediment, ca. 50% of the fractionated fractions were of EQS > 62 µm, which strongly contrasts against the 10% indicated by the mineral grain distribution.

3.3.3 SOC distribution and quality of eroded sediment

The SOC concentrations of aggregated EQS fractions and corresponding mineral grain fractions are presented in Figure 3.5. For each aggregated EQS fraction, SOC concentrations were not significantly different among the four rainfall runs ($P > 0.05$, one way-ANOVA) (Figure 3.5). However, for the fractions with EQS 250-500 µm, the SOC concentrations of aggregated sediment were significantly lower than that of corresponding mineral grain fractions ($P < 0.001$). In addition, the SOC quality of aggregated sediment fractions with EQS > 62 µm was also different from that of the corresponding mineral grain fractions (Figure 3.6): approximately 80% of eroded MOC was contained in the aggregated fractions of EQS > 62 µm, whereas only POC was identified in the mineral grain fractions of > 62 µm. Overall, aggregated sediment with an EQS size range of > 62 µm contained 60% of the eroded SOC, which contrasted with only ca. 20% of SOC being associated with mineral grain > 62 µm (Figure 3.7).

3.3.4 SOC mineralization during long-term incubation

Figure 3.8 shows the cumulative CO_2 emissions per gram of SOC associated with six EQS fractions across four rainfall runs. The cumulative CO_2 emissions from the same fractions among the four rainfall runs were not significantly different ($P > 0.05$, one way-ANOVA). Among the six EQS fractions, the greatest final cumulative CO_2 was emitted by EQS < 32 μm, indicating the MOC associated with the silt and clay fraction was the most susceptible to mineralization. Overall, about 15% of the total eroded SOC was mineralized into CO_2, which is approximately 50% more than the same amount of the non-eroded original soil.

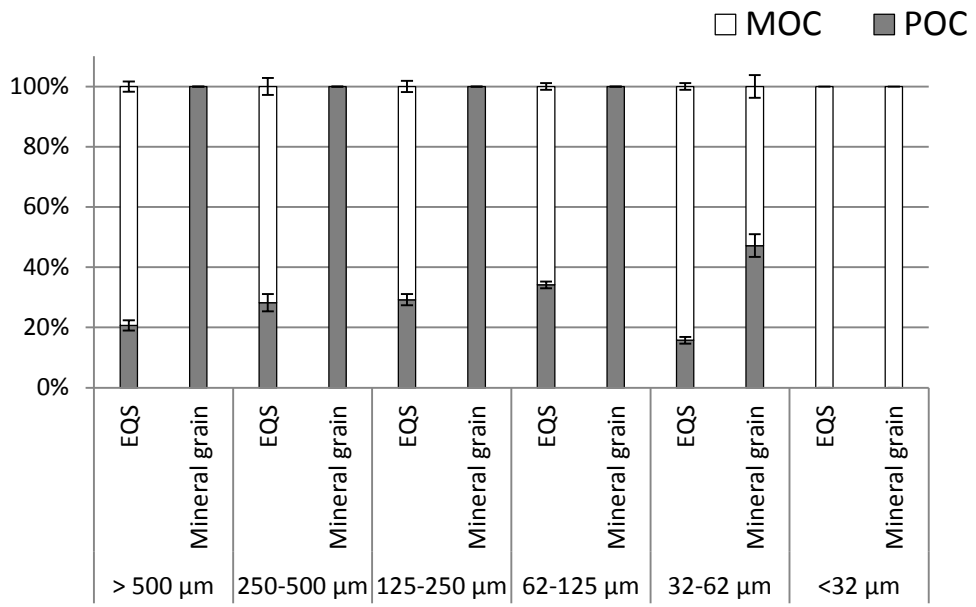

Figure 3.6 MOC and POC ratios of each EQS fraction and mineral grain fraction. Bars represent standard errors.

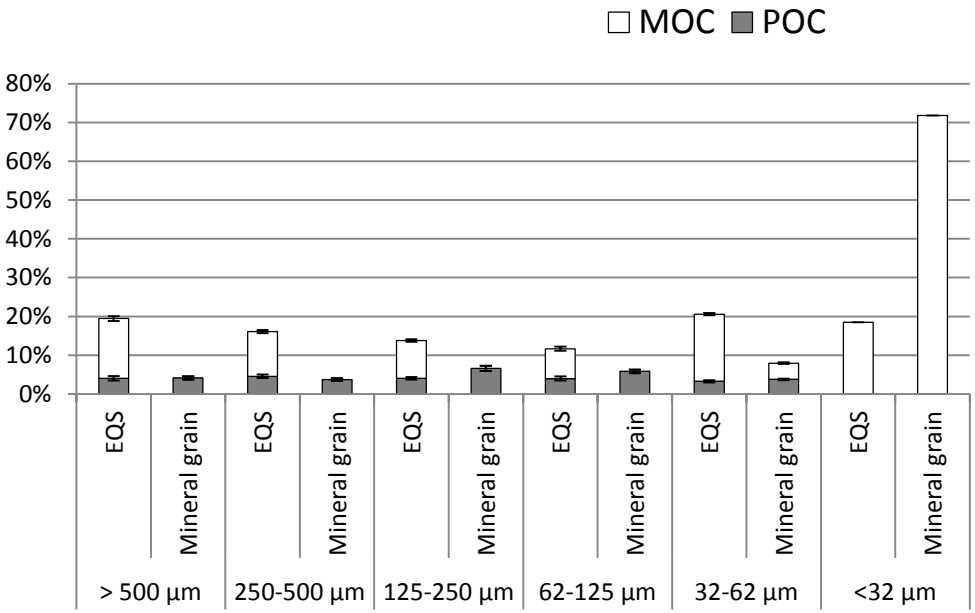

Figure 3.7 SOC mass distributions across EQS fractions and mineral grain fractions. Bars represent standard errors.

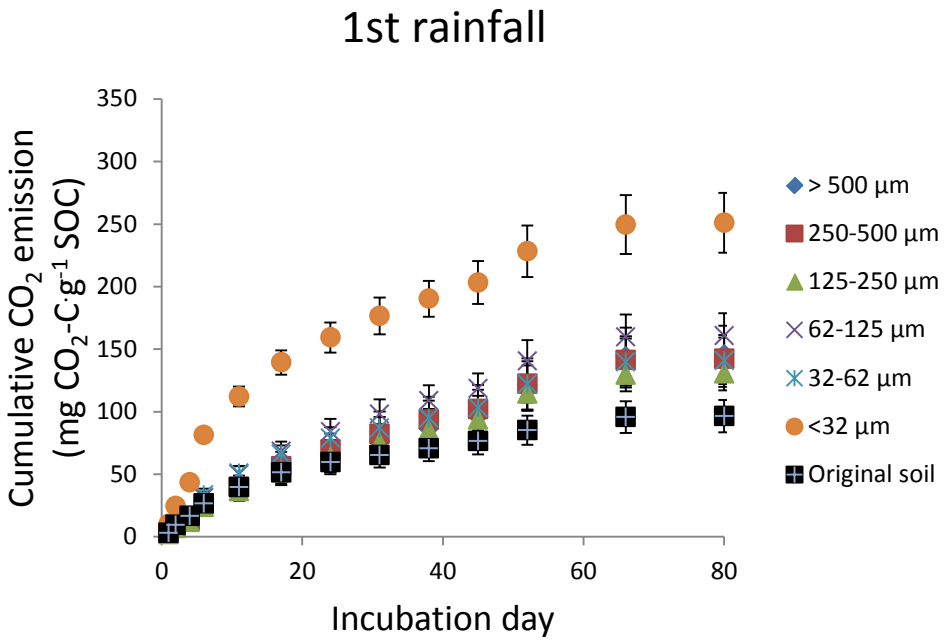

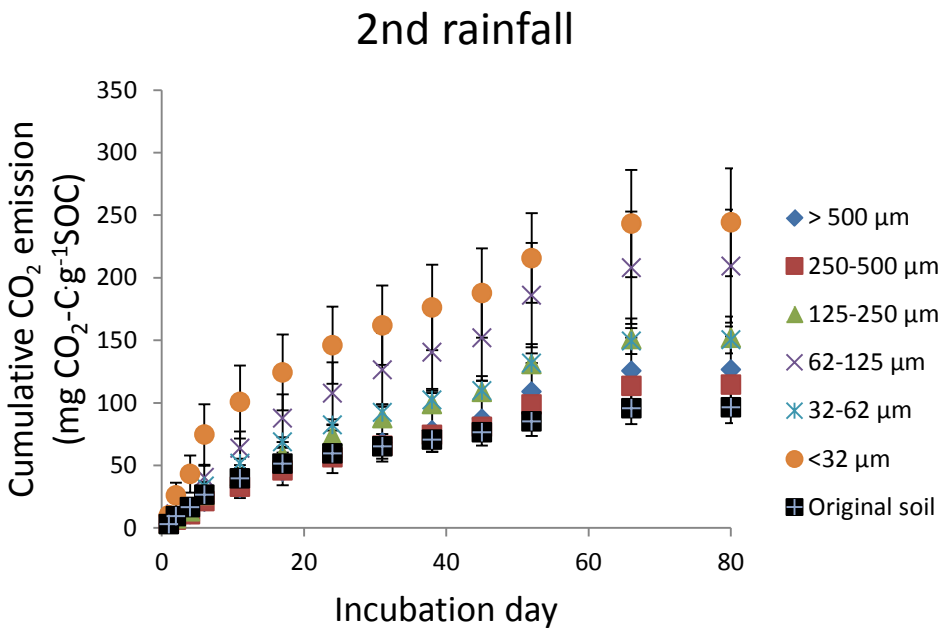
2nd rainfall
Cumulative CO2 emission (mg CO2-C·g-1SOC)
350
300
250
200
150
100
50
0
0
20
40
60
80
Incubation day
> 500 µm
250-500 µm
125-250 µm
62-125 µm
32-62 µm
<32 µm
Original soil

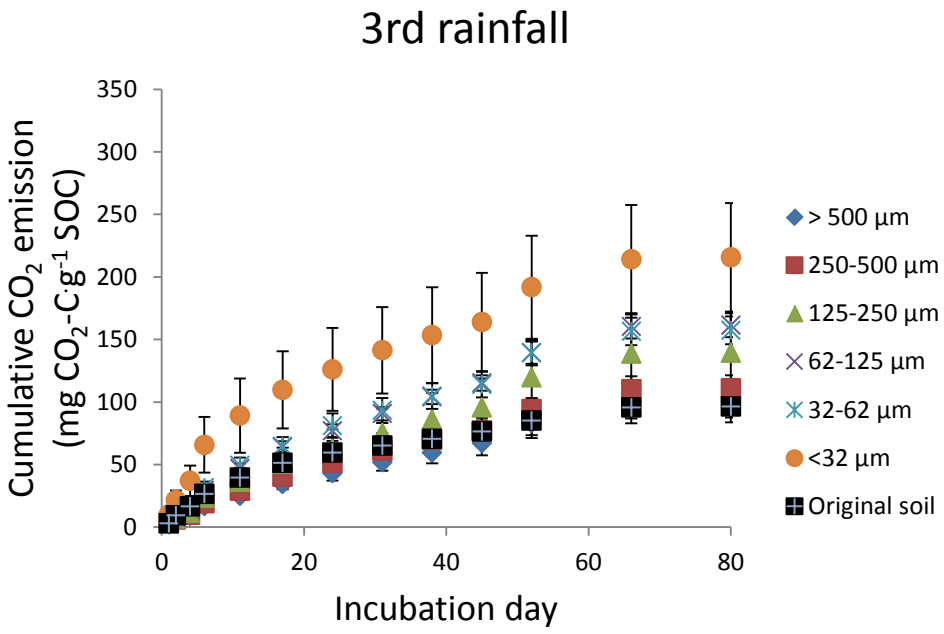
3rd rainfall
Cumulative CO2 emission (mg CO2-C·g-1 SOC)
350
300
250
200
150
100
50
0
0
20
40
60
80
Incubation day
> 500 µm
250-500 µm
125-250 µm
62-125 µm
32-62 µm
<32 µm
Original soil

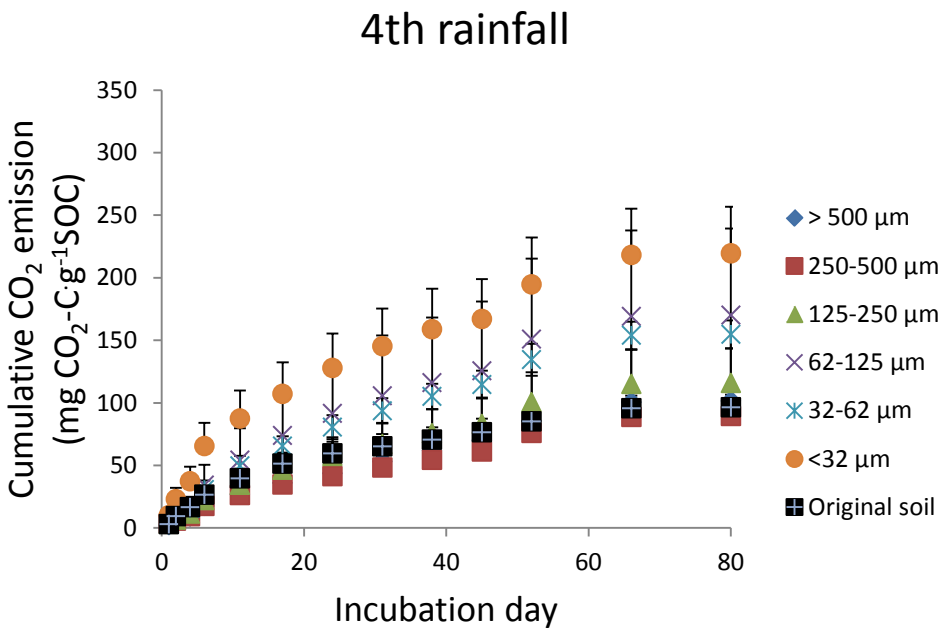

Figure 8 Cumulative CO_2 emissions of six Equivalent Quartz Size (EQS) fractions in the 80 days of incubation. Bars represent standard errors..

3.4 Discussion

3.4.1 Overall dynamics of runoff, erosion and sediment properties.

Detachment and transportation of aggregates over the four rainfall runs led to a continuous decline in soil surface roughness (Table 3.3), as well as a gradual increase of both runoff and sediment when comparing the first rainfall to the fourth rainfall. The gradual increase of runoff and sediment suggests that the effects of wind on runoff and sediment yields are negligible (Figure 3.2). This contrasts with a previous study conducted on a sandy soil which showed that wind can profoundly increase runoff and sediment yields (Iserloh et al., 2013). The limited effect of wind observed in this study might be attributed to the different degrees of aggregation. For poorly aggregated soils (e.g. in Iserloh et al., (2013)), wind-driven rainfall can easily exceed the threshold needed to increase sediment detachment and erosion due to the lower aggregate stability. However, for well aggregated soil, especially on a more cohesive crusted soil surface in this study, higher aggregate stability raises the threshold of wind effects, so that increasing the kinetic energy of raindrops through wind did not necessarily promote the detachment of aggregates and contribute to additional sediment yield. The result supports the argument made by Ries et al. (2014) in which the natural variability of soil-surface related characteristics is essential for a comprehensive assessment of the effect of wind on soil erosion. Our study particularly emphasizes that the effect of aggregation, especially on the crust formation, must be taken into account in wind-driven erosion events.

Contrasting against the changing soil surface conditions and the increasing sediment yield, the composition of eroded sediment was very stable as cumulative rainfall increased. This could be

illustrated by the stable proportions of sediment in the trap and the sediment in suspension (Figure 3.3), as well as the similar EQS distribution of eroded sediment across the four rainfall runs (Figure 3.4). In addition to the stable sediment composition, the SOC concentration (Figure 3.5) as well as the SOC mineralization potential (Figure 3.8) of each fraction also remained unchanged across the four rainfall runs. Such results illustrate that changing surface conditions under repeated rainfalls are unlikely to have an immediate impact on the characteristics of eroded sediment in a single erosion event once a crust has formed

3.4.2 Skewing effect of aggregation on sediment and SOC redistribution

Despite the stable EQS distribution across the four rainfall runs, sediment EQS distributions of all the four rainfall runs strongly contrast against the mineral particle size distribution. If applying mineral grain size distribution to predict the redistribution of eroded sediment based on the 62 μm cutoff threshold established by Starr et al. (2000), the re-deposition of sediment across landscapes would have been underestimated by five times the actual amount (Figure 3.4). Accordingly, the re-deposition of sediment associated SOC across landscapes would have been underestimated by three times (Figure 3.7). The effect of aggregation on the potential transport of eroded sediment and associated SOC are comparable with the previous report on another silt loam from the same region (Hu and Kuhn, 2014; Xiao et al., 2015b). They conducted a rainfall simulation on a simulated seedbed in the laboratory-based setting and found the re-deposition of eroded SOC was six times higher than that suggested by mineral grains. The comparable results between the predictions based on seedbed in the laboratory and natural soil surface in the field highlights that the effect of aggregation, even on crusted soil surface, can potentially increase the settling velocity and thus skew the deposition of aggregated sediment and the associated SOC towards the terrestrial systems.

3.4.3 Effect of aggregation on SOC quality and mineralization

The POC potentially deposited across landscapes accounted for 20% of total eroded SOC based on the EQS distribution. This is similar to the 17% of total eroded SOC indicated by mineral grain distribution (Figure 3.7). However, the MOC potentially deposited across landscapes accounts for ca. 70% of the total SOC measured in this study, which is in strongly contrast to the fact that no MOC would be deposited across landscapes, as suggested by mineral grain distribution (Figure 3.6). Such contradictory estimates on the spatial re-distribution of eroded MOC illustrate that the effect of aggregation on skewing the redistribution of SOC towards deposition across landscapes was exerted mainly through increasing the portion of MOC in the deposited sediment. In other words, the underestimation of eroded SOC deposited across landscapes can mainly be attributed to the underestimation of MOC. Furthermore, many studies have reported that the MOC is less active as compared to POC (Six et al., 2002), and thereby can only contribute limited CO_2 emissions during transport (e.g. Z. Wang et al., 2013). However, the actual C mineralization data based on 80-day incubation of this study clearly illustrates that MOC associated with the silt and clay fraction is very

active after erosion events and has the highest CO_2 emission potential among all fractions of eroded sediment (Figure 3.8). The results suggest that the release of the silt and clay fraction due to aggregate breakdown activates the mineralization potential of the associated MOC and increases the average CO_2 emission of eroded sediment. Iterative/stepwise movement of sediment from the site of first erosion to a permanent deposition site can involve a complex pattern of mobilization and deposition, each associated with drying and formation of new aggregates (Starr et al. 2000). The deposition of MOC across landscapes caused by aggregation would therefore undergo further exposure in repeated cycles of erosion, transport and deposition during subsequent erosion events. This will potentially have a large influence on the C dynamics by continuously contributing additional CO_2 emission. Over all, since most soils, and thus sediments, are in an aggregated form, the effect of aggregation on the transport distance of eroded MOC observed in this study illustrates that current C balance should ascribe more credit to the potential C mineralization of deposited MOC across landscapes, and accordingly attribute less MOC loss to aquatic systems. The effect of aggregation on both the quality and quantity of redistribution of eroded SOC must be properly accounted for in slope-scale C balances.

3.5 Conclusion

This study investigated the aggregation of a crusted soil surface on the settling behavior, and thus potential transport fate, of eroded sediment under simulated wind-driven rainfall using a portable wind and rainfall simulator (PWRS). Our results illustrate that the effect of aggregation, even for crusted soil surfaces, could considerably reduce the potential transport distance of eroded sediment and associated SOC. This could potentially skew the redistribution of eroded SOC towards deposition across landscapes. The underestimation of the proportion of eroded SOC deposited across landscapes can mainly be attributed to the underestimation of mineral-associated organic carbon (MOC). Furthermore, the MOC associated with silt and clay fractions released due to aggregate breakdown is very active, which will certainly increase CO_2 emissions during repeated cycles of re-aggregation and subsequent breakdown. Overall, the results illustrate that aggregation profoundly affects the redistribution and quality of eroded SOC across agricultural landscapes, thereby introducing a further error onto current carbon balances.

While aggregation affects SOC movement and its subsequent fate, the effect of aggregation on the settling velocity distribution of eroded sediment, as well as the SOC concentration and mineralization potential of each fraction, remain stable across cumulative rainfalls. It is thus promising to develop a constant parameter integrating aggregate settling velocity and the associated SOC distribution for soil and SOC erosion modeling. In combination with sediment yield data, such an integrated parameter could be adopted to efficiently model the potential distribution of eroded sediment and associated SOC. In this manner, this approach can not only contribute to optimizing current erosion models, by taking into account the effect of aggregation as compared to the current application of mineral grain

size (e.g. van Oost et al., 2004), but also considerably simplify the parameterization process for erosion models. Obviously, the settling fractionation based on field and laboratory tests with flumes (e.g. Hu and Kuhn, 2014 and this study), even if well-designed to cover a wide range of rainfall conditions, still represents far too much work to be able to test all soils under all scenarios. Therefore, the development of a simple proxy, such as that demonstrated above, is urgently needed to generate similar sediment as that eroded from the natural surface.

Chapter 4

The use of a raindrop aggregate destruction device (RADD) to evaluate sediment and SOC transport

Liangang Xiao, Yaxian Hu, Philip Greenwood, Nikolaus J. Kuhn

Published in Geographica Helvetica, 70, 167–174, 2015

Abstract

Raindrop impact and subsequent aggregate breakdown can potentially change the movement behavior of soil fractions and thus alter their transport distances when compared against non-impacted aggregates. In a given water layer, the transport distance of eroded soil fractions, and thus that of the associated substances across landscapes, such as soil organic carbon (SOC) and phosphorous, are determined by the settling velocities of the eroded soil fractions. However, using mineral size distribution to represent the settling velocities of soil fractions, as often applied in current erosion models, would ignore the potential influence of aggregation on the settling behavior of soil fractions. The destructive effects of raindrops impacting onto aggregates are also often neglected in current soil erosion models. Therefore, the objective of this study is to develop a proxy method to effectively simulate aggregate breakdown under raindrop impact, and further identify the settling velocity of eroded sediment and the associated SOC.

Two agricultural soils with different sandy and silty loam textures were subjected to rainfall using a raindrop aggregate destruction device (RADD). The aggregates sustained after raindrop impact were fractionated by a settling tube into six different classes according to their respective settling velocities. The same mass amount of bulk soil of each soil type was also dispersed and sieved into the same six classes, to form a comparison in size distribution. The SOC content was measured for each settled and dispersed class. Our results show that: 1) for an aggregated soil, applying dispersed mineral grain size distribution, rather than its actual aggregate distribution, to soil erosion models would lead to a biased estimation on the redistribution of eroded sediment and SOC; 2) the RADD designed in this study effectively captures the effects of raindrop impact on aggregate destruction and is thus able to simulate the quasi-natural sediment spatial redistribution; 3) further RADD tests with more soils under standard rainfall combined with local rainfalls are required to optimize the method.

Keywords: Raindrop impact, aggregate breakdown, settling velocity, sediment redistribution

Geogr. Helv., 70, 167–174, 2015
www.geogr-helv.net/70/167/2015/
doi:10.5194/gh-70-167-2015

+ GEOGRAPHICA HELVETICA +

The use of a raindrop aggregate destruction device to evaluate sediment and soil organic carbon transport

L. Xiao, Y. Hu, P. Greenwood, and N. J. Kuhn

Physical Geography and Environmental Change Group, Department of Environmental Sciences, University of Basel, Klingelbergstrasse 27, 4056 Basel, Switzerland

Correspondence to: L. Xiao (liangang.xiao@unibas.ch)

Received: 29 September 2014 – Revised: 27 May 2015 – Accepted: 31 May 2015 – Published: 15 June 2015

Abstract. Raindrop impact and subsequent aggregate breakdown can potentially change the movement behaviour of soil fractions and thus alter their transport distances when compared against non-impacted aggregates. In a given water layer, the transport distances of eroded soil fractions, and thus that of the associated substances across landscapes, such as soil organic carbon (SOC) and phosphorous, are determined by the settling velocities of the eroded soil fractions. However, using mineral size distribution to represent the settling velocities of soil fractions, as often applied in current erosion models, would ignore the potential influence of aggregation on the settling behaviour of soil fractions. The destructive effects of raindrops impacting onto aggregates are also often neglected in current soil erosion models. Therefore, the objective of this study is to develop a proxy method to effectively simulate aggregate breakdown under raindrop impact, and further identify the settling velocity of eroded sediment and the associated SOC.

Two agricultural soils with different sandy and silty loam textures were subjected to rainfall using a raindrop aggregate destruction device (RADD). The aggregates sustained after raindrop impact were fractionated by a settling tube into six different classes according to their respective settling velocities. The same mass amount of bulk soil of each soil type was also dispersed and sieved into the same six classes, to form a comparison in size distribution. The SOC content was measured for each settled and dispersed class. Our results show the following: (1) for an aggregated soil, applying dispersed mineral grain size distribution, rather than its actual aggregate distribution, to soil erosion models would lead to a biased estimation on the redistribution of eroded sediment and SOC; (2) the RADD designed in this study effectively captures the effects of raindrop impact on aggregate destruction and is thus able to simulate the quasi-natural sediment spatial redistribution; (3) further RADD tests with more soils under standard rainfall combined with local rainfalls are required to optimize the method.

1 Introduction

Erosion is generally considered as a three-step process that includes detachment, transport, and deposition (Lal, 2005; van Oost et al., 2007). After being detached (Le Bissonnais, 1996; Legout et al., 2005), soil particles may experience selective deposition across landscapes, or be further transported to aquatic systems (Stallard, 1998; Starr et al., 2000; Lal, 2005; Kuhn et al., 2009). Hence, the destruction of soil aggregates during detachment, transport, and deposition can potentially affect the transport distance of eroded soil fractions. Discrimination of eroded soil fractions according to their likely transport distances, therefore, is essential to fully understand the movement of eroded sediment (van Oost et al., 2004), and thus the redistribution patterns of sediment-bound substances such as organic carbon and phosphorous across landscapes (Quinton et al., 2001; Lal, 2004; van Oost et al., 2007; Kuhn and Armstrong, 2012; Hu and Kuhn, 2014).

Apart from flow velocity, depth, and turbulence, the transport distance of a certain particle is closely related to its settling velocity (Kinnell, 2001, 2005; Kuhn, 2013). Settling velocity converted from mineral grain size distribution (e.g. Stokes, 1851; Gibbs et al., 1971; Hallermeier, 1981; Diet-

Table 1. Particle parameters adopted in currently used erosion models.

Studies	Name or purpose of model	Particle type	Classes	Particle range
van Oost et al. (2004)	MCST	grain	10	0.9–91.35 µm
Lu et al. (2006)	Modelling sediment delivery	grain	3	Clay (< 4 µm), silt (4–50 µm), sand (50–1000 µm)
Pieri et al. (2007)	WEPP	grain	3	Coarse sand, fine sand, clay
De Baets et al. (2008)	EUROSEM	grain	1	42 µm (median size)

rich, 1982; Cheng, 1997; Ferguson and Church, 2004) has been applied to erosion models (Table 1). However, soil is not always eroded as individual mineral grains, but it is mostly eroded in the form of aggregates (Walling, 1988; Nadeu et al., 2011). The settling velocities of aggregated soil fractions are different from those of individual mineral grains. For instance, aggregation could considerably increase the sizes of soil fractions by combining mineral grains into aggregates, and thus facilitate their settling velocities. In addition, the upper limits of mineral grain size classes used in current erosion models are often smaller than the actual aggregate sizes. For example, the largest mineral grain size class used in the model by van Oost et al. (2004) is only 90 µm (Table 1), which is much smaller than the largest naturally eroded aggregates (e.g. > 500 µm reported by Hu and Kuhn, 2014). Furthermore, the settling velocity of a mineral grain and aggregate of the same size are also different due to differences in their respective shape and density (Dietrich, 1982; Loch, 2001). Therefore, using the actual settling velocities of eroded aggregates, rather than that converted from dispersed mineral grain size distribution, could contribute to providing more accurate input into erosion models.

Field investigations and simulated rainfall experiments under laboratory conditions are the two common methods for collecting natural or quasi-natural eroded aggregates (Croft et al., 2012a). For example, Hu and Kuhn (2014) used a 150×80 cm flume under simulated rainfall to generate quasi-natural sediment to predict the transport fate of sediment and soil organic carbon (SOC) eroded from a silty loam (Fig. 1a). However, these methods are often too time consuming and resource demanding to be of practical use. Hence, as an alternative solution, data on aggregate size distribution, based on wet-sieving, have occasionally been used in erosion models to represent settling velocity distribution of soil fractions (e.g. Angima et al., 2003). However, calculating settling velocity solely based on aggregate size ignores the potential influence of porosity, irregular shape, and the involvement of organic matter on the settling behaviour of wet aggregates. In addition, wet-sieving does not account for the potential effects of raindrop impact on aggregate breakdown (e.g. mechanical breakdown, slaking, dispersion, and liquefaction, Le Bissonnais, 1996) and, thus, possible changes on settling velocities of soil fractions. Therefore, it is crucial to develop a simple but efficient proxy method to effectively capture the potential influence of raindrop-impact-induced aggregate breakdown on the transport distance of sediment and eroded SOC.

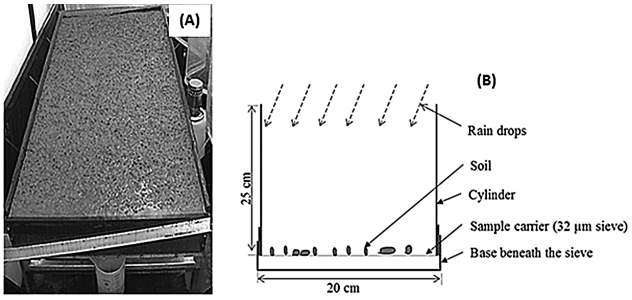

Figure 1. The flume used by Hu and Kuhn (2014) **(a)** and the raindrop aggregate destruction device (RADD) used in this study **(b)**.

This study aims to develop a raindrop aggregate destruction device (RADD) for use as a sensitive proxy, to effectively simulate aggregate breakdown under raindrop impact, and further identify the settling velocity of eroded sediment and the associated SOC. Two soils with contrasting textures – one a poorly aggregated sandy soil and the other a well-aggregated silty loam – were first broken down using the RADD to generate raindrop-impacted soil particles, which were then fractionated using a settling tube apparatus. The influence of aggregation on settling velocity distribution was then highlighted by comparing the settling velocity distributions of the aggregates and/or grains of the two soils, as well against their mineral grain size distributions. The effectiveness of this RADD proxy method was then assessed by comparing the settling velocity distribution of the aggregated silty loam generated from the RADD with that of the same silty loam from a flume experiment conducted by Hu and Kuhn (2014).

2 Materials and methods

2.1 Soil samples and preparations

Two soils – one a sandy soil from Denmark and one a silty loam from Switzerland – were used in this investigation. The sandy soil from Denmark, characterized as a Luvisol (FAO/ISRIC/ISSS, 1998), was collected in September 2011 from a conventionally managed farm under a rotation of wheat and maize in Foulum (56°30′ N, 9°35′ W), central Jutland, in northern Denmark. The silt loam from Switzerland,

Table 2. Texture, SOC content and stable aggregates greater than 250 µm (%) of the Foulum and Möhlin bulk soils. Numbers in brackets represent standard deviations.

Soils	Sand (%)	Silt (%)	Clay (%)	SOC (mg g^{-1})	Stable aggregates > 250 µm (%)
Möhlin	16.14 (0.34)	77.00 (0.36)	6.85 (0.04)	9.60 (0.10)	66.85 (0.47)
Foulum	77.19 (0.40)	21.00 (0.38)	1.81 (0.02)	11.00 (0.30)	No stable aggregate

recognized as a Luvisol (FAO/ISRIC/ISSS, 1998), was collected in March 2012 from a conventionally managed farm supporting a rotation of wheat, rape, grass and maize located in the Möhlin region (47°33′ N, 7°50 W) of north Switzerland. The selective properties of the two soils are summarized in Table 2. Although the sampling time of each soil was different, the two soils were ploughed before sampling, which provided similar field surface conditions. In addition, both sampling sites are prone to erosion due to intensive agriculture (Olsen and Kristensen, 1998; Croft et al., 2012b). Due to contrasting aggregation conditions, the two soils were expected to generate different size distributions after direct raindrop impact, which very likely leads to different movement patterns and thus different redistribution patterns of SOC across the landscape.

After sampling, the two soils were air-dried at a temperature of 20 °C for ca. 2 weeks until 10 % water content was reached. Such air-dried aggregates can resemble soil surface conditions and have been widely used in raindrop splash experiments (Legout et al., 2005). The well-aggregated Möhlin soil was then dry-sieved through an 8 mm mesh, to exclude over-sized aggregates which may excessively resist raindrop impact and thus skew the proportion of coarse aggregates that survive raindrop impact. Whilst this process may, in retrospect, skew the aggregate distribution of the Möhlin soil towards finer size, this result in an over-representation of fine particles, most of which may remain in suspension in overland flow when transport processes occur. However, the standard-sized clods can ensure a comparable reaction to accumulating raindrop impact. As the Foulum soil was very poorly aggregated with no aggregates exceeding 8 mm, it was considered to be standard-sized and thus was not dry-sieved. It should be noted that the pre-treatment is flexible. Where other aggregate moisture or seasonality conditions are applied, pre-treatment protocols should be accordingly adjusted.

2.2 Raindrop aggregate destruction device and rainfall simulation

A raindrop aggregate destruction device (RADD) (Fig. 1b) was designed to simulate the physical process when aggregates are subject to direct raindrop impact. To fulfil this, the RADD must meet two requirements: firstly, it must ensure that sufficient raindrops impact on the aggregate surfaces without being attenuated by surface flow; secondly, a certain degree of water ponding is necessary to mimic natural soil surface conditions that are essential to initiate overland flow during an erosion event. Based on the above premises, the RADD developed in this study consists of three parts. The first is a sample carrier – a 32 µm diameter sieve to hold the dry soil samples prior to raindrop impact, as well to collect aggregates/particles surviving raindrop impact. In addition, the sieve also allows free drainage, which prevents over accumulation of surface water, but ensures that a certain degree of ponding occurs. The second is a base beneath the sample carrier to collect fine particles and redundant water passing through the sieve. The third is a 25 cm tall cylinder embracing the sample carrier, which is 20 cm higher than the surface of the carrier and is designed to prevent the removal and loss of splashed particles (Fig. 1b).

A total of 25 g (dry weight) of each soil was distributed uniformly on the sample carrier of the RADD to fully cover the sieve, and then subjected to simulated rainfall (Fig. 1b). This configuration ensured maximum exposure of the aggregates to the impacting raindrops, as well as generating sufficient materials in order to perform settling fractionation tests. During rainfall experiments, the depth of ponding water in the sample carrier was ca. 1–2 mm (operator's on-site observation), which is representative of overland flow during the flume test conducted by Hu and Kuhn (2014). Given that these estimates were so small, the proportion of material lost to raindrop splash erosion was not accounted for in this study.

Simulated rainfall was generated using a Lechler full cone nozzle (type +460.728.30.CE), with a fall height of 2 m over the RADD, with an average intensity of 35 mm h^{-1}. Average drop size was ca. 2.2 mm, with a kinetic energy of 105 J m^{-2} h^{-1}, measured using a Joss–Waldvogel disdrometer. Because the Möhlin soil is more aggregated and the size distribution is thus more sensitive to raindrop impact than the Foulum soil, simulated rainfall scenarios were chosen to more resemble precipitation conditions in the Möhlin region. Precipitation with an intensity of 35 mm h^{-1} is very common in the Möhlin region, and has a return period of 0.33 years (MeteoSwiss, 2013). Previous research has shown that ensuring complete aggregate breakdown requires a kinetic energy of 150 J m^{-2} (Hu and Kuhn, 2014). Such kinetic energy corresponds to natural precipitation at the above intensity for 15 min (Iserloh et al., 2012). Given that the kinetic energy of simulated rainfall is typically lower than that during natural

precipitation (Iserloh et al., 2012; Hu and Kuhn, 2014), increasing the intensity or prolonging the duration of an event is commonly used as a compensatory approach to generate conditions that are more comparable to natural precipitation. In addition, rainfall kinetic energy is a more relevant variable than cumulative rainfall when investigating soil surface dynamics (Torri et al., 1999). Therefore, simulated rainfall of 35 mm h^{-1} lasting for 90 min with a cumulative kinetic energy about 150 J m^{-2} was chosen in this study to sufficiently break down aggregates. Furthermore, in order to observe the sensitivity of aggregation to increasing kinetic energy, rainfall events with increasing durations of 15, 30, 45, 60, and 90 min were separately applied (not in a sequence) to the two soils in order to simulate the cumulative kinetic energy of 26, 52, 78, 104, and 156 J m^{-2}, respectively. During each rainfall event, three replications were conducted simultaneously for each soil.

Tap water with an electric conductivity of 2220 µs cm^{-1}, which was 5 times greater than local rainwater (462 µs cm^{-1}), was used for each test. Although higher electric conductivity of tap water may increase the dispersion of aggregates (e.g. Borselli et al., 2001), a preliminary study has shown its influence on aggregate breakdown of the two soils used in this study is negligible (Hu et al., 2013a).

2.3 Settling tube and settling velocity measurement

The settling tube used in this study is similar to the Griffith tube (Hairsine and McTainsh, 1986; Loch, 2001; Hu et al., 2013b) and consists of four major components: a settling tube, an injection device, a turntable, and a control panel (Fig. 2). Detailed information about the setup and operation of the settling tube has been described in Hu et al. (2013b). After destroyed by the increasing raindrop impact in the RADD, all soil fractions remaining on the carrier sieve were washed into the injector to conduct fractionation tests (Fig. 2). Given that the settling velocity distribution of aggregates is different from that of mineral grains, and cannot be directly converted from aggregate diameter, we used the concept of equivalent quartz size (EQS) to represent the diameter of a spherical quartz particle that would deposit with the same velocity as an aggregated particle (Loch, 2001; Hu et al., 2013b; Hu and Kuhn, 2014). Based on Stokes' law and the concept of EQS, six settling classes were chosen in this study to fractionate the raindrop-impacted soil fractions: 500 to 1000 µm, 250 to 500 µm, 125 to 250 µm, 62 to 125 µm, 32 to 62 µm, and < 32 µm (Table 3). The finest particles remaining suspended in the settling tube (of EQS < 32 µm), plus those collected in the base beneath the 32 µm sample carrier sieve during the raindrop impact simulation (Table 3), were pooled together and treated as one subsample (EQS < 32 µm).

Following the conceptual model proposed by Starr et al. (2000), which predicts that the fate of eroded SOC is a function of particle size, it is assumed in this study that

Figure 2. Settling tube apparatus used in this study. Detailed technical and operation information has been reported in Hu et al. (2013).

fractions of EQS > 62 µm would be potentially re-deposited across landscapes. In contrast, fine particles of EQS < 62 µm would be transported furthest from their point of origin and thus have the potential to enter aquatic systems (Table 3). There may be some discrepancies induced by the "primary silt-sized particles" measured in Starr et al. (2000) and the concept of EQS used in this study. Yet, for a certain particle, its EQS is either smaller than (as an aggregate) or equivalent to (as a mineral grain) its actual diameter (as measured in Starr et al., 2000). Therefore, it should be noted that taking 62 µm EQS measurement as a cut-off point by which the potential fate of eroded soil fractions may be determined could result in slightly underestimating re-deposition across landscapes.

2.4 Mineral grain size distribution

In order to compare the different size distributions of EQS fractions and that of mineral grains, 25 g of bulk soil from each soil type was dispersed using a Sonifier 250 (Branson, USA). The energy dissipated in the water–soil suspension was ca. 60 J mL^{-1}, which accords with the approach adopted by Kaiser et al. (2012). To correspond to the six EQS fractions fractionated by the settling tube, the dispersed soil fractions were then wet-sieved into six size classes listed above. Three replications were conducted for each soil.

Table 3. Settling time intervals, settling velocity, equivalent quartz size (EQS), class and possible fate of each fraction.

Time intervals (s)	Settling velocity ($m\,s^{-1}$)	EQS (μm)	Class	Possible fate
Before 20	> 0.09	> 500		
20–40	0.045–0.09	250–500	Fast-settling	Deposit on landscape
40–120	0.015–0.045	125–250		
120–600	0.003–0.015	62–125	Medium-settling	
600–1800	0.001–0.003	32–62	Slow-settling	Transport to river
After 1800	< 0.001	< 32		

2.5 Laboratory measurements

After the fractionation and ultrasonic dispersion, all the EQS and dispersed soil fractions were dried at 40 °C and weighed. The SOC concentration of each EQS and dispersed soil fraction was determined using a Leco 612 carbon analyzer following the method of Hu et al. (2013a). The SOC was burnt at 550 °C for 200 s and all carbon fractions were detected as CO_2. The SOC mass distribution across EQS and dispersed classes was calculated by multiplying the SOC concentration of each class with their individual weight proportions. Data analysis was carried out using Microsoft Excel 2010 and SPSS 16.0 software packages.

3 Results and discussion

3.1 Aggregation effects

The EQS distributions of the Möhlin and Foulum soils after raindrop impact using the RADD are shown in Fig. 3 and compared with the corresponding mineral grain size distribution. The EQS distributions differed profoundly between the aggregated Möhlin soil and the sandy Foulum soil (Fig. 3a, b). For the Möhlin soil, 45 to 73 % of the aggregated fractions were of EQS > 62 μm. This strongly contrasts the Möhlin mineral grain size distribution, which suggests that only 10 % of the mineral grains were of size > 62 μm (Fig. 3a). Consequently, up to 77 % of the total SOC was associated with the soil fractions of EQS > 62 μm (Figs. 4a and 5a), which would be re-deposited across landscapes following the 62 μm cut-off proposed by Starr et al. (2000) (Table 3). It strongly contrasts the 10 % SOC contained in the mineral grains of size > 62 μm (Figs. 4a, 5a). If estimated by mineral-grain-specific SOC distribution, this would underestimate the re-deposition of aggregated SOC across landscapes by up to 67 %. Such discrepancies highlight that the effects of aggregation can potentially facilitate the settling velocity and thus reduce the likely transport distances of aggregated sediment and the associated SOC, hence skewing their deposition towards the terrestrial systems. For the sandy Foulum soil, the EQS distribution was well matched with the mineral grain size distribution, illustrating the absence of aggregation effects to alter soil size distribution (Fig. 3b). This consequently resulted in a roughly consistent SOC distribution across EQS and mineral grain classes (Figs. 4b, 5b). No significant difference was detected for each class ($P > 0.05$) (Fig. 4b).

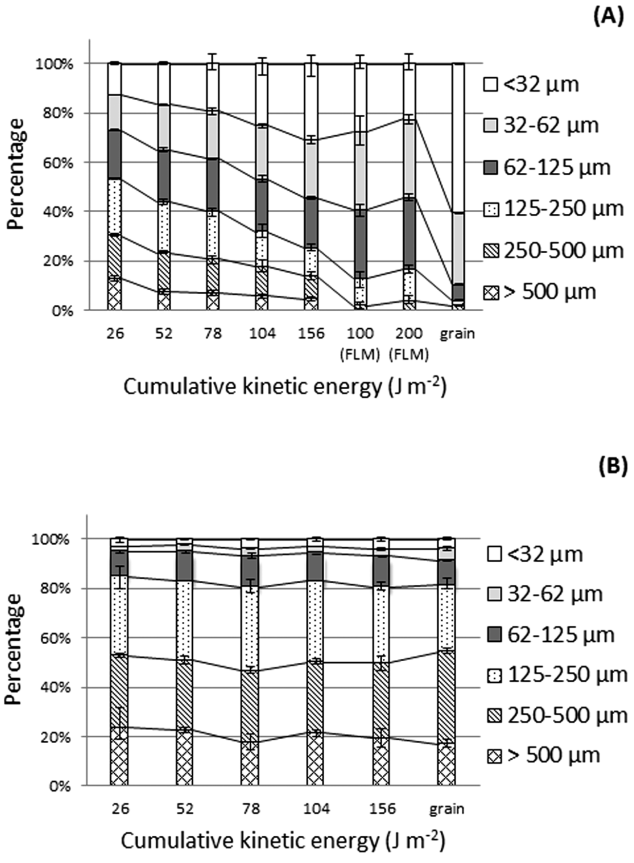

Figure 3. The equivalent quartz size (EQS) distributions of **(a)** the Möhlin soil and **(b)** the Foulum soil after different cumulative kinetic energy. The columns "100 (FLM)" and "200 (FLM)" represent the EQS distribution of eroded sediment from a flume (FLM) (Hu and Kuhn, 2014) after 100 and 200 $J\,m^{-2}$ of cumulative kinetic energy impact. "Grain" represents the grain size distribution by wet-sieving after ultrasonic dispersion. Upper and lower bars represent maximum and minimum values, respectively.

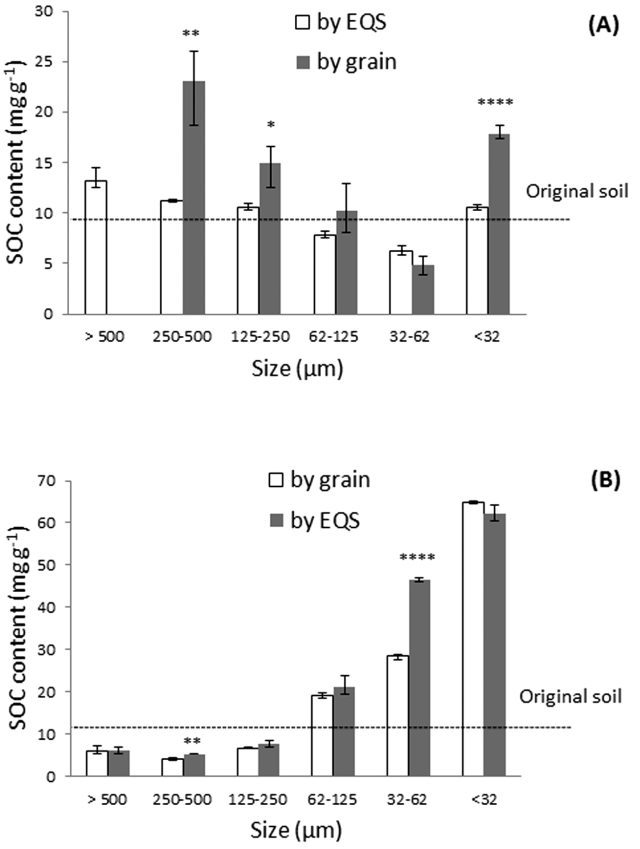

Figure 4. Soil organic carbon (SOC) content across equivalent quartz size (EQS) fractions fractionated by the settling and across grain size classes dispersed by ultrasound of **(a)** the Möhlin soil and **(b)** the Foulum soil. The "*" indicates significant difference at $P<0.05$ level, the "**" indicates significant difference at $P<0.01$ level, and the "****" indicates significant difference at $P<0.0001$ level between SOC content of each fraction by EQS and by grain. Upper and lower bars represent maximum and minimum values, respectively.

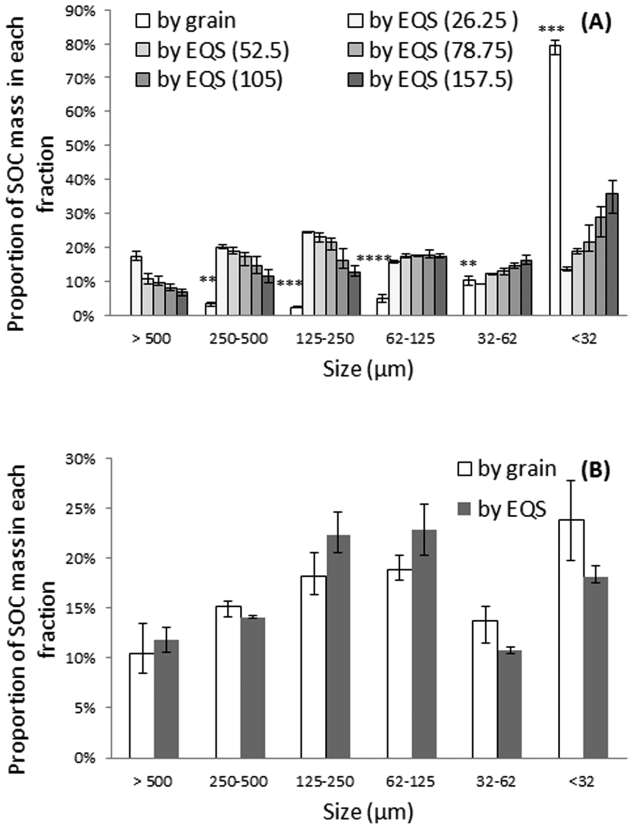

Figure 5. The soil organic carbon (SOC) mass of different fractions of **(a)** the Möhlin soil and **(b)** the Foulum soil. The numbers in the brackets are the cumulative kinetic energy of each rainfall ($J\,m^{-2}$). The "**" indicates significant difference at $P<0.01$ level, the "***" indicates significant difference at $P<0.001$ level, and the "****" indicates significant difference at $P<0.0001$ level between SOC mass proportion by grain and by equivalent quartz size (EQS). Upper and lower bars represent maximum and minimum values, respectively.

3.2 Sensitivity to accumulative kinetic energy

The sensitivity of EQS size distribution to increasing kinetic energy also differed between the Möhlin and Foulum soils (Fig. 3). For the Möhlin soil, fractions of EQS < 62 μm increased significantly as the kinetic energy accumulated from 26 to 156 $J\,m^{-2}$ ($P<0.01$) (Fig. 3a), but the increased kinetic energy had only minor influences on the EQS distribution of the Foulum soil (Fig. 3b). The significant changes in EQS distribution are probably due to the destruction of the Möhlin aggregates of EQS > 125 μm upon raindrop impact. This may induce the gradual release of more fine particles as kinetic energy increases (Legout et al., 2005). However, for the Foulum soil, because of the sandy characteristics and thus lack of aggregation effects (Table 2), soil fractions did not act in response to the higher kinetic energy associated with impacting raindrops. The different soil responses between the Möhlin and the Foulum soil against raindrop impact suggest that a simple texture measurement is sufficient to predict the likely transport distances of soil fractions for poorly aggregated soils. However, investigating the natural breakdown processes of well-aggregated soils requires a proxy, such as the RADD developed in this study, to efficiently simulate quasi-natural sediment.

3.3 Effectiveness of the RADD

The effectiveness of the RADD, as a proxy method for generating quasi-natural sediment, can also be verified by the comparable EQS distributions for the same Möhlin soil (Fig. 3a) collected from the RADD in this study (when receiving kinetic energy of 156 $J\,m^{-2}$) and that from the previous flume experiment (Hu and Kuhn, 2014). For all the settling classes, except that of EQS > 250 μm, the proportional EQS distributions are quite similar between RADD-destroyed aggregates in this study and the sediment generated from the flume and

reported by Hu and Kuhn (2014). The lack of fractions of EQS > 250 µm in the flume experiment reported by Hu and Kuhn (2014) is mainly because not all the dispersed aggregates were transported out of the flume. Instead, some aggregates > 250 µm were deposited across the surface. Therefore, our results suggest that the simple RADD is an effective proxy to simulate aggregate breakdown upon direct raindrop impact and generate quasi-natural sediment in a simple and more time-efficient way. It also demonstrates the possibility of contributing to generating a more representative input to erosion models. For example, in the Multi-Class Sediment Transport model (MCST) (van Oost et al., 2004), instead of inputting the settling velocity classes calculated from mineral grain size distributions, it is possible to directly apply the actual aggregate settling information identified by RADD to predict soil erosion risk. Moreover, if further applying such effective proxy to SOC distribution, the RADD also promises the potential to develop a SOC erodibility index with a reasonable resemblance to natural SOC erosion processes. While our results are limited by the preliminary experiments having been conducted on only two soil types, other factors such as seasonality (Le Bissonnais, 1996) and transport process under various water flow conditions (Wang et al., 2014) were also not accounted for; the RADD provides a proxy method to effectively separate the complex erosion process into individual processes. This therefore offers an opportunity to identify the potential effects of aggregation and raindrop impact on the spatial distribution of sediment and eroded SOC in a more efficient manner when compared to the traditional approach, based on mineral-grain-specific SOC distribution.

4 Conclusions

This study aimed to develop a simple method using raindrop aggregate destruction device (RADD) as a proxy to generate quasi-natural sediment, and to further identify the effects of aggregation on the settling velocity of sediment and the associated SOC. The settling distributions of an aggregated loamy soil and a poorly aggregated sandy soil were different from each other. In particular, the settling-specific SOC distribution for the aggregated loamy soil strongly contrasted its mineral-grain-size-specific SOC distribution. The aggregated SOC potentially re-deposited within terrestrial systems was up to 67 % more than that estimated by mineral-grain-size-specific SOC distribution. This clearly demonstrates the risk of underestimating SOC redistribution within terrestrial systems if ignoring the effect of aggregation or neglecting the dynamics of aggregate breakdown upon raindrop impact. This highlights the necessity for an effective proxy such as the RADD developed in this study as a means of generating quasi-natural sediment for well-aggregated soil. While our results from the RADD are only based on two soils, it demonstrates a possibility to contribute to generating a more representative input to erosion models. However, in the future, a wider range of soils with various aggregation characteristics should be investigated under more varied rainfall conditions in order to support the results observed in this study, and to thus help optimize the RADD apparatus during further research.

Acknowledgements. We are grateful to the support of China scholarship council (CSC) and University of Basel. The contribution of Ruth Strunk is also acknowledged. Particularly, we want to thank Marianne Caroni, who passed away but is still sorely missed in our group.

Edited by: M. Hoelzle
Reviewed by: three anonymous referees

References

Angima, S. D., Stott, D. E., O'Neill, M. K., Ong, C. K., and Weesies, G. A.: Soil erosion prediction using RUSLE for central Kenyan highland conditions, Agric. Ecosyst. Environ., 97, 295–308, 2003.

Borselli, L., Torri, D., Poesen, J., and Sanchis, P.: Effects of water quality on infiltration, runoff and interrill erosion processes during simulated rainfall, Earth Surf. Process. Landf., 26, 329–342, 2001.

Cheng, N. S.: Simplified settling velocity formula for sediment particle, J. Hydraul. Res., 123, 149–152, 1997.

Croft, H., Kuhn, N. J., and Anderson, K.: On the use of remote sensing techniques for monitoring spatio-temporal soil organic carbon dynamics in agricultural systems, Catena, 94, 64–74, 2012a.

Croft, H., Anderson, K., and Kuhn, N. J.: Reflectance anisotropy for measuring soil surface roughness of multiple soil types, Catena, 93, 87–96, 2012b.

De Baets, D., Torri, D., Poesen, J., and Meersmans, J.: Modelling increased soil cohesion due to roots with EUROSEM, Earth Surf. Process. Land., 33, 1948–1963, 2008.

Dietrich, W. E.: Settling velocity of natural particles, Water Resour. Res., 18, 1615–1626, 1982.

FAO/ISRIC/ISSS: World Reference Base for Soil Resources, FAO: Rome, 1998.

Ferguson, R. I. and Church, M.: A simple universal equation for grain settling velocity, J. Sediment Res., 74, 933–937, 2004.

Gibbs, R. J., Matthews, M. D., and Link, D. A.: The relationship between sphere size and settling velocity, J. Sediment Petrol., 41, 7–18, 1971.

Hairsine, P. B. and McTainsh, G. H.: The Griffith tube: a simple settling tube for the measurement of settling velocity of soil aggregates, AES working paper 3/86, Griffith University, Brisbane, 1986.

Hallermeier, R. J.: Terminal settling velocity of commonly occurring sand grains, Sedimentology, 28, 859–865, 1981.

Hu, Y. and Kuhn, N. J.: Aggregates reduce transport distance of soil organic carbon: are our balances correct?, Biogeosciences, 11, 6209–6219, doi:10.5194/bg-11-6209-2014, 2014.

Hu, Y., Fister, W., and Kuhn, N. J.: Temporal variation of SOC enrichment from interrill erosion over prolonged rainfall simulations, Agriculture, 3, 726–740, 2013a.

Hu, Y., Fister, W., Rüegg, H. R., Kinnell, P. I. A., and Kuhn, N. J.: The use of Equivalent Quatz Size and settling tube apparatus to fractionate soil aggregates by settling velocity, Geomorphol. Tech. Online Ed. Br. Soc. Geomorphol., Section 1.1.1, 2013b.

Iserloh, T., Fister, W., Seeger, M., Willger, H., and Ries, J. B.: A small portable rainfall simulator for reproducible experiments on soil erosion, Soil Tillage Res., 124, 131–137, 2012.

Kaiser, M., Berhe, A. A., Sommer, M., and Kleber, M.: Application of ultrasound to disperse soil aggregates of high mechanical stability, J. Plant. Nutr. Soil. Sci., 175, 521–526, 2012.

Kinnell, P. I. A.: Particle travel distances and bed and sediment compositions associated with rain-Impacted flows, Earth. Surf. Proc. Land., 26, 749–758, 2001.

Kinnell, P. I. A.: Raindrop-impact-induced erosion processes and prediction: a review, Hydrol. Proc., 19, 2815–2844, 2005.

Kuhn, N. J.: Assessing lateral organic Carbon movement in small agricultural catchments, in: Mattertal – ein Tal in Bewegung, edited by: Graf, C., Publikation zur Jahrestagung der Schweizerischen Geomorphologischen Gesellschaft 29 Juni–1 Juli 2011, St. Niklaus. Birmensdorf, Eidg. Forschungsanstalt WSL, 151–164, 2013.

Kuhn, N. J. and Armstrong, E. K.: Erosion of organic matter from sandy soils: solving the mass balance, Catena, 98, 87–95, 2012.

Kuhn, N. J., Hoffmann, T., Schwanghart, W., and Dotterweich, M.: Agricultural soil erosion and global carbon cycle: controversy over?, Earth. Surf. Proc. Land., 34, 1033–1038, 2009.

Lal, R.: Soil carbon sequestration impacts on global climate change and food security, Science, 304, 1623–1627, 2004.

Lal, R.: Soil erosion and carbon dynamics, Soil Till. Res., 81, 137–142, 2005.

Le Bissonnais, Y.: Aggregate stability and assessment of soil crustability and erodibility: I. Theory and methodology, Eur. J. Soil Sci., 47, 425–437, 1996.

Legout, C., Leguedois, S., and Le Bissonnais, Y.: Aggregate breakdown dynamics under rainfall compared with aggregate stability measurements, Eur. J. Soil Sci., 56, 225–237, 2005.

Loch, R. J.: Settling velocity – a new approach to assessing soil and sediment properties, Comput. Electron. Agr., 31, 305–316, 2001.

Lu, H., Moran, C. J., and Prosser, I. P.: Modelling sediment delivery ratio over the Murray Darling Basin, Environ. Model. Softw., 21, 1297–1308, 2006.

MeteoSwiss: Monthly total precipitation during April, May, and June at Station Arisdorf near Möhlin from 1985 to 2012, 2013.

Nadeu, E., De Vente, J., Martínez-Mena, M., and Boix-Fayos, C.: Exploring particle size distribution and organic carbon pools mobilized by different erosion processes at the catchment scale, J. Soil. Sediment., 11, 667–678, 2011.

Olsen, P. and Kristensen, P. R.: Using a GIS system in mapping risks of nitrate leaching and erosion on the basis of SOIL/SOIL-N and USLE simulations, Nutr. Cycl. Agroecosys., 50, 307–311, 1998.

Pieri, L., Bittelli, M., Wu, J. Q., Dun, S., Flanagan, D. C., Pisa, P. R., Ventura, F., and Salvatorelli, F.: Using the Water Erosion Prediction Project (WEPP) model to simulate field-observed runoff and erosion in the Apennines Mountain Range, Italy. J. Hydrol., 336, 84–97, 2007.

Quinton, J. N., Catt, J. A., and Hess, T. M.: The selective removal of phosphorus from soil: is event size important?, J. Environ. Qual., 30, 538–545, 2001.

Stallard, R. F.: Terrestrial sedimentation and the carbon cycling: coupling weathering and erosion to carbon burial, Global Biogeochem. Cy., 12, 231–257, 1998.

Starr, G. C., Lal, R., Malone, R., Hothem, D., Owens, L., and Kimble, J.: Modeling soil carbon transported by water erosion process, Land Degrad. Dev., 11, 83–91, 2000.

Stokes, G. G.: On the effect of the internal friction of fluids on the motion of pendulums, Trans. Camb. Phil. Soc., 9, 8–106, 1851.

Torri ,D., Regüés, D., Pellegrini, S., and Bazzoffi, P.: Within-storm soil surface dynamics and erosive effects of rainstorms, Catena, 38, 131–150, 1999.

van Oost, K., Beuselinck, L., Hairsine, P. B., and Govers, G.: Spatial evaluation of a multi-class sediment transport and deposition model, Earth. Surf. Proc. Land., 29, 1027–1044, 2004.

van Oost, K., Quine, T. A., Govers, G., De Gryze, S., Six, J., Harden, J. W., Ritchie, J. C., McCarty, G. W., Heckrath, G., Kosmas, C., Giraldez, J. V., Marques da Silva, J. R., and Merckx, R.: The impact of agricultural soil erosion on the global carbon cycle, Science, 318, 626–629, 2007.

Walling, D. E.: Erosion and sediment yield research – some recent perspectives, J. Hydrol., 100, 113–141, 1988.

Wang, J. G., Li, Z. X., Cai, C. F., and Ma R. M.: Particle size and shape variation of Ultisol aggregates affected by abrasion under different transport distances in overland flow, Catena, 123, 153–162, 2014.

Chapter 5

A combined Raindrop Aggregate Destruction Device-Settling Device (RADD-ST) approach to identify the settling velocity of sediment

Liangang Xiao, Yaxian Hu, Philip Greenwood, Nikolaus J. Kuhn

Published in Hydrology, 3, 176–192, 2015

Abstract

The use of sediment settling velocity based on mineral grain size distribution in erosion models ignores the effects of aggregation on settling velocity. The alternative approach, wet-sieved aggregate size distribution, on the other hand, cannot represent all destructive processes that eroded soils may experience under impacting raindrops. Therefore, without considering raindrop impact, both methods may lead to biased predictions of the redistribution of sediment and associated substances across landscapes. Rainfall simulation is an effective way to simulate natural raindrop impact under controlled laboratory conditions. Yet, very few methods have been developed to integrate rainfall simulation with the settling velocity of eroded sediment. This study aims to develop a new proxy, based on rainfall simulation, in order to identify the actual settling velocity distribution of aggregated sediment. A combined Raindrop Aggregate Destruction Device -Settling Tube (RADD-ST) approach was developed to 1) simulate aggregate destruction under a series of simulated rainfalls, and 2) measure the actual settling velocity distribution of destroyed aggregates. Mean Weight Settling Velocity (MWSV) of aggregates was used to investigate settling behaviors of different soils as rainfall kinetic energy increased. The results show the settling velocity of silt-rich raindrop impacted aggregates is likely to be underestimated by at least six times if based on mineral grain size distribution. The RADD-ST designed in this study effectively captures the effects of aggregation on settling behavior. The settling velocity distribution should be regarded as an evolving, rather than steady state parameter during erosion events. The combined RADD-ST approach is able to generate the quasi-natural sediment under controlled simulated rainfall conditions and is adequately sensitive to measure actual settling velocities of differently aggregated soils. This combined approach provides an effective tool to improve the parameterization of settling velocity input for erosion models.

Keywords: raindrop impact; aggregate breakdown; settling tube; settling velocity; modelling

Hydrology **2015**, *2*, 176-192; doi:10.3390/hydrology2040176

OPEN ACCESS

hydrology

ISSN 2306-5338

www.mdpi.com/journal/hydrology

Article

A Combined Raindrop Aggregate Destruction Test-Settling Tube (RADT-ST) Approach to Identify the Settling Velocity of Sediment

Liangang Xiao *, Yaxian Hu, Philip Greenwood and Nikolaus J. Kuhn

Physical Geography and Environmental Change Research Group, Department of Environmental Sciences, University of Basel, Klingelbergstrasse 27, 4056 Basel, Switzerland;
E-Mails: yaxian.hu@unibas.ch (Y.H.); philip.greenwood@unibas.ch (P.G.);
nikolaus.kuhn@unibas.ch (N.J.K.)

* Author to whom correspondence should be addressed; E-Mail: liangang.xiao@unibas.ch;
Tel.: +41-61-2673645; Fax: +41-61-2670740.

Academic Editors: Thomas Iserloh, Artemi Cerdà, Wolfgang Fister and Saskia Keesstra

Received: 3 August 2015 / Accepted: 13 October 2015 / Published: 16 October 2015

Abstract: The use of sediment settling velocity based on mineral grain size distribution in erosion models ignores the effects of aggregation on settling velocity. The alternative approach, wet-sieved aggregate size distribution, on the other hand, cannot represent all destructive processes that eroded soils may experience under impacting raindrops. Therefore, without considering raindrop impact, both methods may lead to biased predictions of the redistribution of sediment and associated substances across landscapes. Rainfall simulation is an effective way to simulate natural raindrop impact under controlled laboratory conditions. However, very few methods have been developed to integrate rainfall simulation with the settling velocity of eroded sediment. This study aims to develop a new proxy, based on rainfall simulation, in order to identify the actual settling velocity distribution of aggregated sediment. A combined Raindrop Aggregate Destruction Test-Settling Tube (RADT-ST) approach was developed to (1) simulate aggregate destruction under a series of simulated rainfalls; and (2) measure the actual settling velocity distribution of destroyed aggregates. Mean Weight Settling Velocity (MWSV) of aggregates was used to investigate settling behaviors of different soils as rainfall kinetic energy increased. The results show the settling velocity of silt-rich raindrop impacted aggregates is likely to be underestimated by at least six times if based on mineral grain size distribution. The RADT-ST designed in this study effectively captures the effects of aggregation on settling behavior. The settling

velocity distribution should be regarded as an evolving, rather than steady state parameter during erosion events. The combined RADT-ST approach is able to generate the quasi-natural sediment under controlled simulated rainfall conditions and is adequately sensitive to measure actual settling velocities of differently aggregated soils. This combined approach provides an effective tool to improve the parameterization of settling velocity input for erosion models.

Keywords: raindrop impact; aggregate breakdown; settling tube; settling velocity; modelling

1. Introduction

1.1. Soil Erosion and Sediment Settling Velocity

Soil erosion represents a major environmental and agricultural problem worldwide [1–4]. On the one hand, soil erosion has significant on-site effects on agricultural land, e.g., by destroying the substrate for plant growth, or at least reducing the effective rooting depth, and thus water supply and soil fertility [5–7]. On the other hand, sediment transported to watercourses has tremendous off-site effects with respects to stream degradation, disturbance to wildlife habitat, and direct cost for dredging, levee maintenance, and loss of reservoir storages capacity [8–14]. Moreover, given that a large amount of C, N, and P is eroded and redistributed across landscapes, the potential effects of soil erosion on biogeochemical cycling and consequently on global climate change, has also drawn increasing attention [15–19]. However, the redistribution of eroded sediment as well as associated substances across landscapes is far from fully understood, and has largely impeded making an accurate estimation of the environmental impacts of soil erosion [18–22]. Improving our understanding of soil erosion and its impact on environment sustainability therefore requires a better understanding of the behavior of eroded soil as sediment during transport and deposition across agricultural landscapes [18,20,23].

The redistribution of sediment and associated substances across landscapes is determined by the transport distances of differently-sized sediment fractions [24,25]. Numerical models based on sediment transport distance have already contributed to improve our understanding of sediment redistribution [26–29]. However, the quality of the output depends highly on the quality of the input parameters, *i.e.*, the "gigo" ("garbage in = garbage out") principle. Among those parameters, settling velocity is a key factor in determining the transport distance of eroded particles in a given flow regime [24,30–33]: fast-settling fractions would be transported only short distances and preferentially deposited across landscapes, whereas slow-settling fractions would remain suspended in runoff and thus be more likely to be transported further and possibly to aquatic systems [18,34–36]. Improving the information on settling velocity of sediment in existing erosion models, as an advanced erodibility index, is therefore critical to understand the spatial redistribution of sediment and associated substances [21,37–42].

1.2. Parametrization of Settling Velocity

Settling velocity distributions based on dispersed mineral grains have been used in some erosion models to predict the redistribution of sediment and associated substances across landscapes (e.g., [29,43,44]). However, soil is not often eroded as individual mineral grains, but is mobilized mostly in the form of aggregates [36,45]. Aggregation increases effective particle size, but the settling velocity of a single mineral grain is also different from that of an aggregate of the same size, due to differences in its shape and density [27,46]. Using settling velocities based on mineral grain size distribution in erosion models therefore carries the risk of generating erroneous transport distance data. Alternatively, settling velocities can be calculated based on wet-sieved aggregate size distribution (e.g., [47]). However, wet-sieving fractionation cannot represent all processes of aggregate breakdown (e.g., mechanical breakdown, slaking, dispersion and liquefaction under raindrop impact) in the same way as experienced during natural rainfall [48,49]. Moreover, aggregate size distribution derived from wet-sieving fractionation ignores the potential influence of porosity, irregular shape, and the involvement of organic matter, and thus cannot accurately reflect the settling behavior of aggregates [27]. Furthermore, the inadequate representation of the actual settling behavior of aggregates in current soil erosion models may lead to a biased estimation on the redistribution of substances (e.g., C and P) associated with those aggregates. For instance, in current erosion investigations, soil organic carbon (SOC) erosion modeling is based on the assumption that SOC distributes uniformly across mineral grain (e.g., Revised Universal Soil Loss Equation (RUSLE) [50]), or aggregate size classes [51]. Hence, SOC erosion risk is often assessed by coupling the average SOC concentration of surface soil with mineral grain or aggregate size re-distribution [22]. However, SOC concentrations often differ among aggregate fractions in the soil matrix and thus also in eroded sediment, generating a settling velocity specific SOC distribution [30]. Therefore, disregarding the effects of aggregation on sediment settling velocity and associated SOC can lead to a biased estimation of SOC redistribution along sediment pathways after erosion.

To investigate the effects of aggregation on the spatial distribution of eroded soil and SOC across landscapes, sampling sediments (aggregated or not aggregated) in the field and studying their settling velocity distributions would provide the ideal input into soil erosion models. However, sediment composition and thus its settling velocity distribution also vary as erosion events proceed. Therefore, sampling sediment during and after natural rainfall events is not feasible to assess the risks associated with ignoring aggregation on sediment transport. As an alternative, rainfall simulation on micro-plot scale is a method widely used to systematically assess the generation of overland flow and sediment as well as to provide basic data for soil erosion modeling [52–56]. For example, Hu and Kuhn [30] used a settling tube apparatus to fractionate the aggregated silty loam eroded from a 150 cm × 80 cm flume after simulated rainfall events. From this, they predicted the potential transport distances of eroded sediment based on the settling behavior of the eroded soil fractions after crust formation. However, laboratory tests with flumes, even if well-designed to cover a wide range of rainfall conditions, still represent far too much work to be able to test all soils under all scenarios. Therefore, it is crucial to develop a simple, but efficient proxy method to: (1) generate natural or quasi-natural sediment under laboratory rainfall simulation; (2) provide sufficiently accurate settling velocity information of various soil types for erosion models with least effort input; and (3) use the settling velocity specific SOC distribution data to improve SOC erosion risk assessment.

2. The Design of RADT-ST Method

2.1. Experimental Rationale

An ideal settling velocity measurement of eroded sediment should involve quasi-natural destruction processes of aggregates followed by a settling velocity measurement, but avoiding any modification of sediment size distribution by selective deposition. To generate such sediments, a Raindrop Aggregate Destruction Test (RADT) (Figure 1a) can be used to simulate the physical process when aggregates are subject to direct raindrop impact under simulated rainfall events. Those raindrop impacted aggregates can then be fractionated by a settling tube (ST) apparatus (Figure 1b,c) according to their settling velocities. While the combined RADT-ST (Figure 2) is not designed to investigate soil erosion processes per se, it can capture the destructive effects of raindrop impact on aggregates and determine the actual settling behaviors of destroyed aggregates. The efficiency of the RADT-ST method to reflect the actual settling behavior of those raindrop destroyed aggregates can be evaluated by comparing the settling velocity distributions of those aggregates with that calculated from mineral grain size distributions and sediment eroded from an erosion plot (e.g., the flume in Hu and Kuhn [30]). The sensitivity of this method can be further examined by comparing the settling behaviors of soils with different degrees of aggregation in response to increasing cumulative raindrop kinetic energy. The effects of aggregation on the transport distance of sediment associated SOC can be evaluated by comparing the SOC distributions across destroyed aggregate fractions with that across mineral grain fractions. In this study, the use of a combined RADT-ST approach to generate such information on sediment is illustrated.

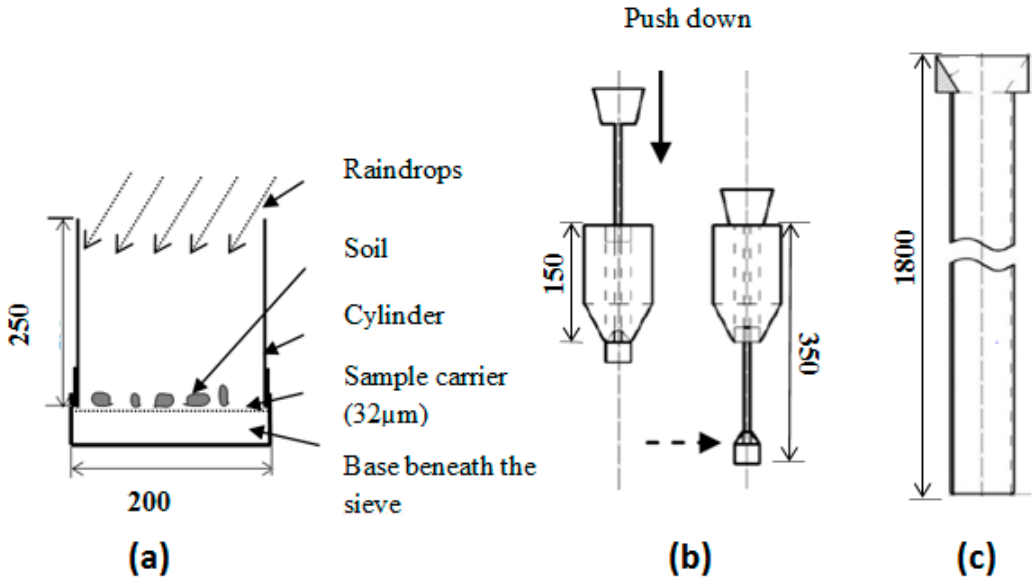

Figure 1. The sketch of the raindrop aggregate destruction test (RADT) used in this study (**a**); injection device (**b**); and settling tube (ST) apparatus (**c**) developed by Hu *et al.* [57]. All measurements given in mm.

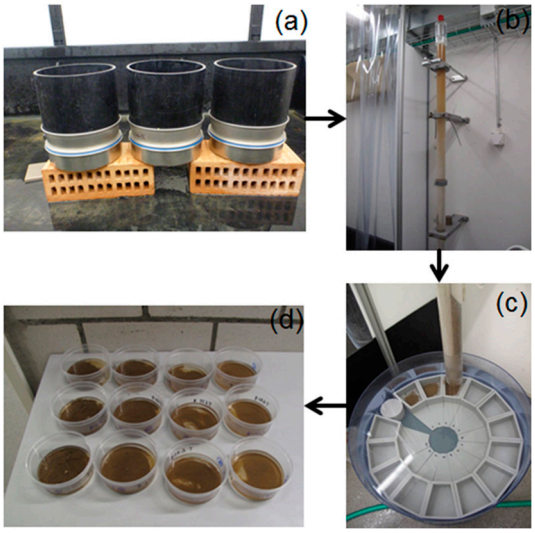

Figure 2. Experimental setup adopted in this study: (**a**) raindrop aggregate destruction test (RADT) test; (**b**) start of the settling tube (ST) test; (**c**) sample collection of each sediment fraction; and (**d**) transfer of samples from the turntable to beakers.

2.2. Raindrop Aggregate Destruction Test (RADT)

The RADT developed in this study consists of three parts (Figures 1 and 2):

(1) A sample carrier consisting of a 32-µm sieve to hold the dry soil samples prior to raindrop impact, and to collect aggregates surviving raindrop impact. The sieve can be uniformly covered by 25 g of soil, generating sufficient material to perform a settling tube fractionation. The sieve also allows a slow, but free drainage of water. This design ensures that a certain degree of ponding occurs, which resembles natural raindrop-impacted flow conditions [30], and prevents accumulation of surface water from forming a film, which attenuates the effect of raindrop kinetic energy on the soil surface [58,59].

(2) A base beneath the sample carrier to collect fine particles and redundant water passing through the sieve.

(3) A 25 cm tall cylinder embracing the sample carrier (the cylinder is 20 cm taller than the surface of the carrier). With this design, splashed particles can be caught on the sidewalls of the RADT and washed back to the base by rainwater, so that the RADT can capture all the sediment generated by raindrop impact.

2.3. Settling Tube (ST)

The settling tube (ST) apparatus used in this study is developed from the "Griffith"-tube described by Hairsine and McTainsh [37] and Loch [27]. Detailed information about the design and operation of the ST apparatus has been described in Hu *et al.* [57]. In brief, the ST apparatus consists of four major components (Figures 1 and 2):

(1) The actual settling tube with a water column through which soil fractions settle.

(2) An injection device to introduce soil into the tube.

(3) A turntable to collect separated sample fractions.

(4) A control panel to control the movement of the turntable.

After being introduced into the top of the tube by the injection device, the sediment sample is fractionated through the water column by settling velocity. Theoretically, the ST allows users to fractionate samples into a wide range of settling velocity classes through pre-set settling time intervals. However, for practical purposes, it is necessary to select the settling velocity fractions so as to generate sufficient sediment for each settling class in order to conduct further analysis. Meanwhile, the selected settling velocity distribution should also be related to the potential redistribution of sediment across landscapes. The concept of Equivalent Quartz Size (EQS) is thus introduced to represent the diameter of a spherical quartz particle that has the same velocity as the aggregated particle measured in the settling tube [27,30,57]. The soil sample can then be fractionated into six EQS classes corresponding to conventional size classes, *i.e.*, 500 to 1000 μm, 250 to 500 μm, 125 to 250 μm, 62 to 125 μm, 32 to 62 μm, and <32 μm. These EQS classes correspond to settling velocities of 90 to 180 mm·s^{-1}, 45 to 90 mm·s^{-1}, 15 to 45 mm·s^{-1}, 3 to 15 mm·s^{-1}, 1 to 3 mm·s^{-1}, and <1 mm·s^{-1} based on the settling equation proposed by Gibbs *et al.* [60], which was specifically developed for particles within these size ranges. From the perspective of sediment redistribution across a landscape, a particle size of 62 μm has been widely used as a cutoff to determine whether the eroded particles are deposited on hillslopes (>62 μm) or transported further downslope to enter aquatic ecosystems (<62 μm) (e.g., [30,34,61,62]). Therefore, a cut-off of EQS 62 μm (corresponding to a settling velocity of 3 mm·s^{-1}) can be applied to separate landscape deposition of eroded soil (with settling velocity >3 mm·s^{-1}) from that potentially transported into river systems (with settling velocity <3 mm·s^{-1}) (Table 1).

Table 1. Possible fate, settling velocity, and Equivalent Quartz Size (EQS) of each fraction, and ratio of the proportion of each fraction between mineral grain and aggregate (after being impacted by 156 J·m^{-2}). Values greater than 1 mean overestimation without considering aggregation, whereas values smaller than 1 mean underestimation without considering aggregation.

Possible Fate (Starr *et al.* [34])	Settling Velocity (mm·s^{-1})	EQS	Proportion of Mineral Grain/Proportion of Aggregate			
		(μm)	Möhlin	Weinan	Exeter	Eifel
Deposited across landscapes	90–180	500–1000	0.11	-	0.15	0.10
	45–90	250–500	0.15	-	0.29	0.23
	15–45	125–250	0.16	0.36	0.13	0.11
	3–15	62–125	0.60	0.69	0.29	0.37
Possible transfer to aquatic systems	1–3	32–62	0.80	1.00	0.71	0.63
	<1	<32	2.11	1.80	3.85	2.67

2.4. Mean Weight Settling Velocity (MWSV)

Ideally for comparison between various soil fractionation methods, the settling velocity distribution could be compiled into a single parameter enabling a simple, yet process-related comparison of soil settling behavior. Therefore, to compare the settling velocity distributions of various soils, the concept of Mean Weight Settling Velocity (MWSV), which follows the theory of Mean Weight Diameter

(MWD), is used in this study. The MWSV represents the settling velocity distribution of destroyed aggregates depicted in Equation (1):

$$\mathrm{MWSV} = \sum x_i \times y_i \quad (1)$$

where x_i is the settling velocity of each settling fraction (mm·s^{-1}), and y_i is the proportion of each settling fraction with respect to the total sample.

3. The Application of the RADT-ST Method

3.1. Soil Samples and Preparations

The RADT-ST method developed in this study was applied to four soils sampled from A horizon in cultivated fields in Switzerland, Germany, the UK and the Loess Plateau in China. Detailed information about sampling of the four soils is listed in Table 2. All four soils are classified as Luvisols with similar texture, but different degrees of aggregation (Table 3) and all supported a maize-wheat rotation under conventional tillage. The selection of the four soils was therefore considered suitable to compare the diverse effects of aggregation on sediment settling and to examine the sensitivity of the combined RADT-ST approach. After sampling, soils were air dried for two weeks at 20 °C until constant dry weight was achieved. They were then passed through an 8 mm diameter sieve. This size standard aimed to exclude big clods that would excessively resist raindrop impact because of their size, and thereby ensured comparable results when examining the reactions of different soils to raindrop impact. For specific erosion-related questions, alternative pre-treatments such as controlling different precedent moisture regimes and/or aggregate size variation might be required.

Table 2. The sampling time, sites and coordinates of the four soils.

	Sampling Date	Sampling Country	Coordinates
Möhlin	March 2012	Switzerland	47°33′N, 7°50′E
Weinan	February 2013	China	34°30′N, 109°30′E
Exeter	April 2013	UK	50°44′N, 3°31′W
Eifel	April 2013	Germany	50°02′N, 6°43′E

Table 3. Selected soil properties of the four soils. Numbers in brackets represent standard deviations. MWSV: Mean Weight Settling Velocity.

	Clay (%)	Silt (%)	Sand (%)	SOC mg·g^{-1}	Water Stable Aggregate (WSA) >250 µm (%)	MWSV of Mineral Grain (mm·s^{-1})
Möhlin	6.12 (0.06)	78.12 (0.13)	15.76 (0.19)	9.60 (0.10)	67.13 (0.61)	3.92 (0.49)
Weinan	6.78 (0.26)	72.52 (0.34)	20.70 (0.09)	4.31 (0.03)	48.00 (3.66)	3.13 (0.02)
Exeter	10.53 (0.47)	75.37 (1.70)	14.10 (1.23)	24.30 (0.04)	43.73 (1.82)	8.67 (1.26)
Eifel	9.04 (0.70)	79.15 (0.96)	11.81 (0.26)	19.40 (0.07)	54.42 (0.82)	4.71 (0.42)

3.2. RADT-ST Test Procedure and Rainfall Simulation

A total of 25 g (dry weight) of each soil was distributed uniformly across the sample carrier of the RADT, fully covering the sieve (Figure 2). For each soil, three RADT cylinders were placed next to

each other and simultaneously exposed to simulated rainfall. Details are described in the following paragraph. After raindrop impact induced destruction, all the soil fractions remaining on the sample carrier of the RADT were transferred into the settling tube (ST) apparatus to conduct settling fractionation. The settling velocity classes used in this experiment follow the protocol described in Section 2.3. To test the relevance of aggregation for transport of particulate substances, the SOC concentration of the four bulk soils (average SOC) and the respective EQS fractions (actual SOC) after the RADT-ST tests was measured using a LECO RC 612 (Mönchengladbach, Germany).

The rainfall was simulated using a Lechler full cone nozzle (type +460.728.30.CE, Lechler GmbH, Metzingen, Germany), with a fall height of 2 m over the sieve of the RADT. The intensity of the simulated rainfall was 35 $mm \cdot h^{-1}$ with an average raindrop size of 2.2 mm and an average kinetic energy of 105 $J\ m^{-2} \cdot h^{-1}$. A pre-test had shown that, to completely break down aggregates and form a soil crust that did not change visibly anymore on all the four soils, it required a kinetic energy of 150 $J \cdot m^{-2}$. Such kinetic energy corresponds to natural precipitation of approximately 35 $mm \cdot h^{-1}$ for 15 min [63] in the areas where the soils originated. The natural precipitation intensity of 35 $mm \cdot h^{-1}$ is common in the regions of the sampling sites, with a return period of 0.33 years [64] for the sampling sites of the European soils, and 0.39 years for the Weinan soil in China [65]. However, the kinetic energy of the simulated rainfall used in this study is lower than that natural precipitation of similar intensity [30,64]. Therefore, rainfall intensity or rainfall duration can be increased to generate a cumulative rainfall kinetic energy comparable to natural precipitation. Given that rainfall kinetic energy is more essential than cumulative rainfall amount in this study in terms of observing raindrop impact-induced soil surface changes [66], simulated rainfalls of 35 $mm \cdot h^{-1}$ lasting up to 90 min with a cumulative kinetic energy about 150 $J \cdot m^{-2}$ was used in this study. Such simulated rainfall can, therefore, assemble aggregate breakdown processes that are likely to experience during natural crust formation. In order to observe the sensitivity of the aggregate settling velocity of the sediment generated on the four soils during the crust formation, tests were carried out where the kinetic energy was systematically increased from 26 $J \cdot m^{-2}$, up to 59, 78, 104, and 156 $J \cdot m^{-2}$, which correspond to rainfall durations of 15, 30, 45, 60 and 90 min, respectively.

3.3. Mineral Grain Size Distribution

Comparing aggregated sediment settling velocity distribution to the soil texture derived settling velocity distribution allows an evaluation of the efficiency of the RADT-ST. The texture of the four soils was determined from a suspension of *ca.* 1 g of soil in 1000 mL of water, after pre-treatment with 5 mL of sodium hexametaphosphate and the further dispersed using ultrasound, with energy equivalent to 5.4 $J \cdot mL^{-1}$ for three minutes. The mineral grain size distributions of the four soils were then measured using a Malvern Mastersizer 2000 (Malvern Instruments Ltd., Malvern, UK). Mineral grains were divided into the same six size classes in accordance with the six EQS classes distinguished by the RADT-ST test described in Section 2.3. Subsequently, the MWSV based on mineral grain size distribution was also calculated to compare with that of the fractionated sediment aggregates.

4. Results and Discussion

The settling velocity distributions of the four soils after destruction and fractionation by RADT-ST are shown in Figure 3. Generally, for all four soils the mass of the fast-settling fractions decreased with cumulative rainfall kinetic energy, while the slow-settling fractions increased (Figure 3). This can be explained by the breakdown of large aggregates into smaller ones after being subjected to an increasing raindrop kinetic energy. For the Möhlin soil, a comparison of the RADT-ST results with the settling velocities of sediment generated from an eroding flume under laboratory simulated rainfalls [30] reveals a good agreement of the respective distributions after the maximum kinetic energy (156 $J \cdot m^{-2}$), except for the "missing" fast-settling fractions from the flume test (settling velocity > 45 $mm \cdot s^{-1}$) (Figure 3a). The good agreement between the two experiments shows that the RADT-ST method is a feasible approximation for sediment that is generated by raindrop-impacted flow. In fact, the "missing" fast-settling aggregates in sediment generated using a flume in Hu and Kuhn [30] are consistent with the differences between the two test procedures. These large aggregates are most likely those that moved slowly across the flume used by Hu and Kuhn [30] and thus did not all reach the outfall weir during the experiment. With the RADT-ST procedure, such scale-specific bias can be avoided in a simple and time-efficient manner.

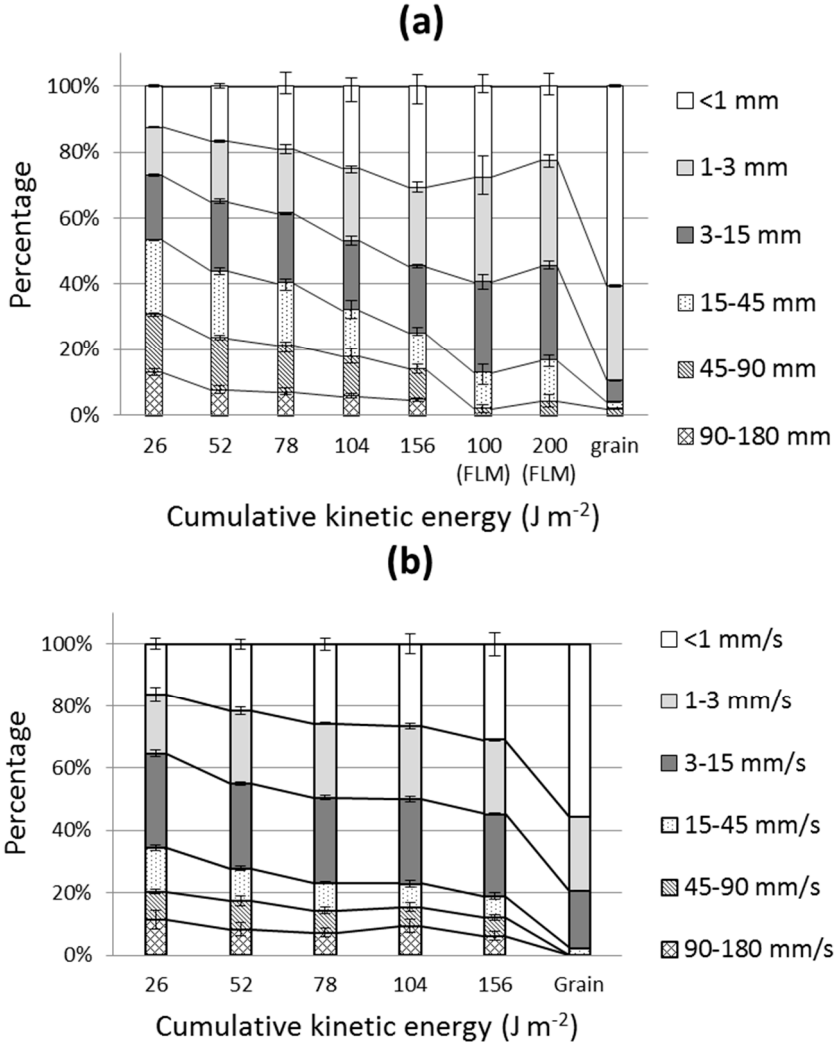

Figure 3. *Cont.*

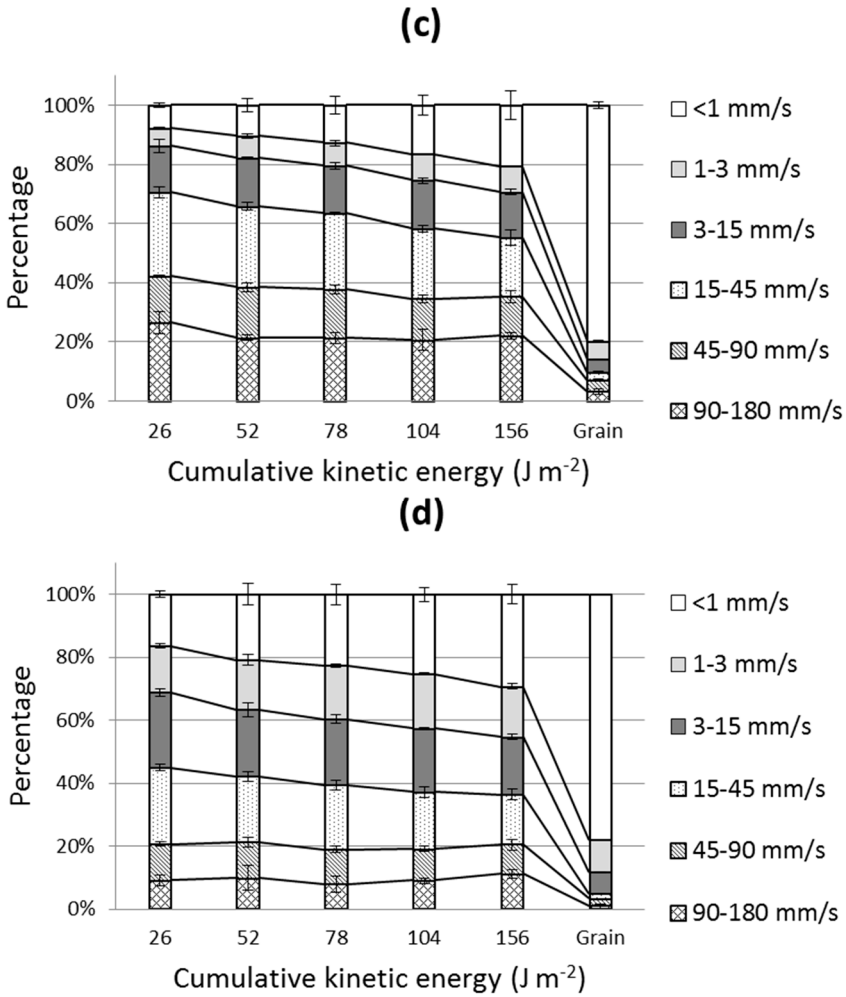

Figure 3. The settling velocity distributions after different cumulative kinetic energy of (**a**) the Möhlin soil; (**b**) the Weinan soil; (**c**) the Exeter soil and (**d**) the Eifel soil. "Grain" represents the settling distribution based on soil texture after dispersion. "100 (FLM)" and "200 (FLM)" represent the EQS distribution of eroded sediment from a flume (FLM) (Hu and Kuhn [30]) after 100 and 200 $J \cdot m^{-2} \cdot$of cumulative kinetic energy impact. Bars represent standard deviations.

The actual settling velocity distributions of the four soils were also distinctively different from that based on their mineral grain size distributions. For instance, aggregate fractions with a settling velocity < 3 $mm \cdot s^{-1}$ were two to four times less in amount than the mineral grains with equivalent settling velocity (Figure 3). Such differences were still evident even after the maximum cumulative kinetic energy (Figure 3), indicating that sediment would remain aggregated even throughout a prolonged erosion event or after multiple rainfall events. Therefore, if applying mineral grain size distribution into erosion models, the fractions potentially transferred into rivers (*i.e.*, settling velocity < 3 $mm \cdot s^{-1}$) would have been largely over-estimated, while those likely deposited across the terrestrial system (*i.e.*, settling velocity > 3 $mm \cdot s^{-1}$) would have been under-estimated. Furthermore, the MWSV of aggregates declined as cumulative kinetic energy increase (Figure 4). The ratios between the MWSV of aggregates and the MWSV of mineral grains were always larger than six for the four soils, suggesting that settling velocity based on mineral grain size distribution would have been underestimated by at least six times the actual amount (Figure 5). Our results therefore challenge the

way of using "average diameter of the soil particles" to calculate the redistribution of soils without considering the effects of aggregation in RUSLE [50]. The biased estimation on settling velocity of soil fractions would further lead to 2–5-fold under-representation of SOC deposited across landscapes (white bars in Figure 6). While coupling aggregate size distribution with average SOC content (e.g., [51]) can largely improve the calibration of soil erosion model (light grey bars compared to white bars in Figure 6), the settling velocity specific SOC distribution identified with the RADT-ST method represents an even more efficient proxy to reflect the potential redistribution of eroded SOC across landscapes (dark grey bars in Figure 6). It therefore represents a promising tool to integrate actual settling velocity specific SOC distribution into soil redistribution parameters for the purpose of optimizing soil erosion model outputs (e.g., the Multi-Class Sediment Transport model (MCST) used in [29]).

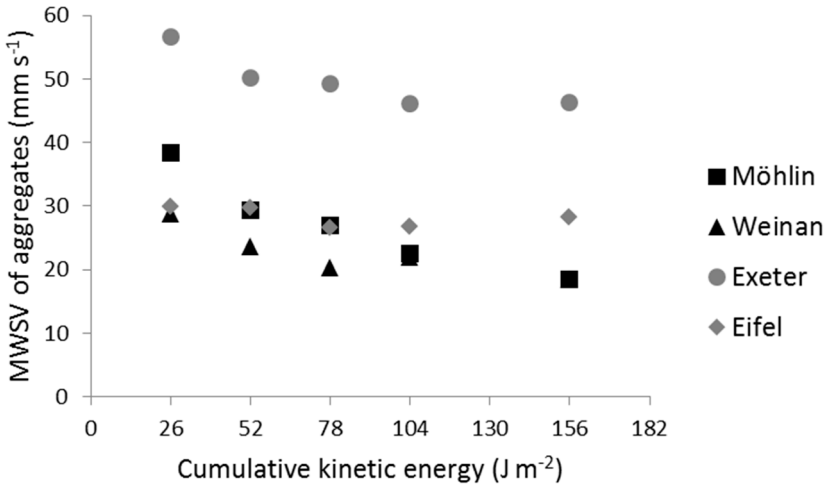

Figure 4. Mean Weight Settling Velocity (MWSV) of aggregates as cumulative kinetic energy increased.

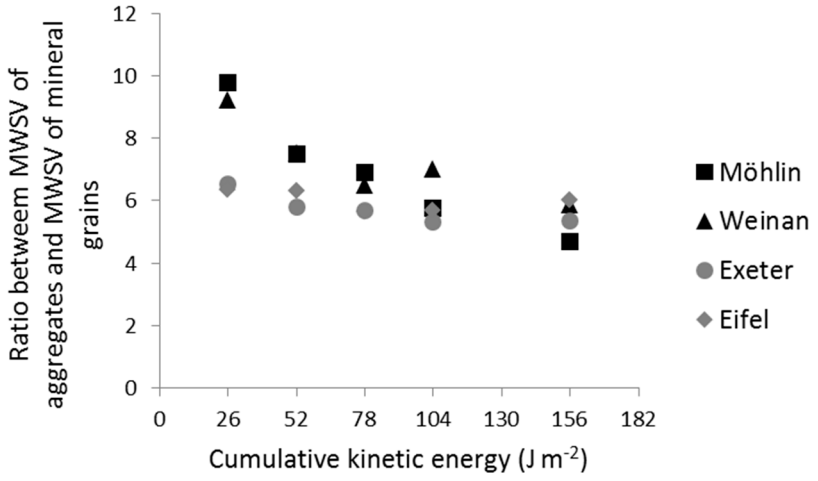

Figure 5. The ratios between Mean Weight Settling Velocity (MWSV) of aggregates and MWSV of mineral grains as cumulative kinetic energy increased.

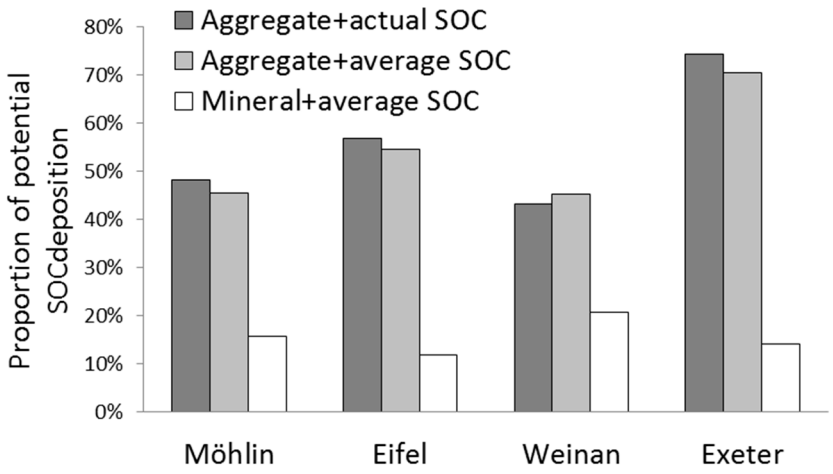

Figure 6. The proportions of potential SOC deposition calculated in different ways. The SOC distribution across EQS fractions and mineral grain fractions were first calculated. The SOC contained in fractions >62 μm was regarded as potentially depositional across landscapes (Starr *et al.* [34]). "Aggregate+actual" represents the SOC distribution that was calculated by multiplying the SOC concentration of each EQS fraction with their individual weight proportions. "Aggregate+average" represents the SOC distribution was calculated by multiplying the average SOC concentration of bulk soil with weight of each EQS fraction. "Mineral+average" represents the SOC distribution was calculated by multiplying the average SOC concentration of bulk soil with weight of each EQS fraction.

Apart from the general trends observed from the four soils, the RADT-ST can also capture minor differences between different types of soil. For instance, the MWSV reaction of the four soils, despite similar texture (Table 3), differed from each other as kinetic energy increased (Figure 4). Higher cumulative kinetic energy is required to reach equilibrium MWSV for the Möhlin soil (at least 156 $J \cdot m^{-2}$) than the other three soils, all of which were rapidly destroyed only after an initial kinetic energy of 52 $J \cdot m^{-2}$. This is consistent with the greater aggregate stability expressed by the Möhlin soil (Table 3) which can better preserve its aggregates from rapid destruction. Therefore, the differences among the four soils in aggregate breakdown over increasing kinetic energy clearly demonstrate that the RADT-ST method can serve as a new proxy that is adequately sensitive to detect the effects of different degrees of aggregation on sediment settling velocity. The RADT-ST derived settling velocity distribution could therefore be used to generate settling velocity datasets composing a wide range of soils, which in turn can be easily integrated into erosion models. The simplicity and feasibility of the RADT-ST under simulated rainfall conditions also avoid rigorous field sampling and sediment quality monitoring that is usually required to understand the relationship between soil properties and their settling behavior (e.g., [67]).

5. Conclusions

In order to rectify the bias of settling velocity distribution introduced by mineral grain size distribution, a combined Raindrop Aggregate Destruction Test-Settling Tube (RADT-ST) approach was developed to simulate the generation of sediment aggregates by raindrop impact under controlled simulated rainfall conditions, and to further determine their actual settling velocity distributions. Four types of soils with similar texture, but different degrees of aggregation, were used to examine the feasibility and

sensitivity of this RADT-ST approach. Through comparing the Mean Weight Settling Velocity (MWSV) of raindrop-destroyed aggregates with dispersed mineral grains, our results show that the settling velocity of the four soils and their SOC deposited across landscapes would have been underestimated by at least six times, if not considering the actual aggregate settling velocity distribution. This demonstrates the feasibility of the RADT-ST approach to capture the effects of aggregation onto sediment size and subsequent re-distribution. The feasibility of this approach was also illustrated by the comparable settling velocity distributions between aggregates collected from the RADT-ST in this study and that of the same soil collected from a previous flume experiment after receiving similar rainfall cumulative kinetic energy. Furthermore, the settling velocities gradually declined as raindrop kinetic energy increased, and the declining patterns differed between soils, clearly illustrating the sensitivity of the RADT-ST approach to detect subtle differences in soil erodibility properties. Overall, the RADT-ST approach developed in this study has the potential to provide actual settling information generated under relatively simple simulated rainfall conditions to optimize the parametrization of sediment behavior and quality in erosion models, such as the Multi-Class Sediment Transport model (MCST) [29]. If further extrapolated appropriately to a specific erosion scenario, the RADT-ST derived sediment quality parameters can also help to improve our understanding of sediment movement through watersheds and the environmental impacts of the heterogeneously distributed eroded substances.

Acknowledgments

We are grateful to the support of China scholarship council (CSC) and the University of Basel. The contribution of Ruth Strunk is also acknowledged.

Author Contributions

Nikolaus J. Kuhn and Liangang Xiao conceived and designed the experiments; Liangang Xiao performed the experiments; Liangang Xiao analyzed the data; and Liangang Xiao, Yaxian Hu and Philip Greenwood wrote the paper.

Conflicts of Interest

The authors declare no conflict of interest.

References

1. Pimentel, D.; Harver, C.; Resosudarmo, P.; Sinclair, K.; Kurz, D.; McNair, M.; Crist, S.; Shpritz, L.; Fitton, L.; Saffouri, R.; *et al.* Environmental and economic costs of soil erosion and conservation benefits. *Science* **1995**, *267*, 1117–1123.
2. Cerdà, A.; Giménez-Morera, A.; Bodí, M.B. Soil and water losses from new citrus orchards growing on sloped soils in the western Mediterranean basin. *Earth Surf. Process. Landf.* **2009**, *34*, 1822–1830.
3. Lieskovský, J.; Kenderessy, P. Modelling the effect of vegetation cover and different tillage practi-ces on soil erosion in vineyards: A case study en Vráble (Slovakia) using Watem/Sedem. *Land Degrad. Dev.* **2014**, *25*, 288–296.

4. Zhao, G.; Mu, X.; Wen, Z.; Wang, F.; Gao, P. Soil erosion, conservation, and Eco-environment changes in the Loess Plateau of China. *Land Degrad. Dev.* **2013**, *24*, 499–510.
5. Cerdà, A.; Flanagan, D.C.; le Bissonnais, Y.; Boardman, J. Soil erosion and agriculture. *Soil Tillage Res.* **2009**, *106*, 107–108.
6. Colazo, J.C.; Buschiazzo, D. The impact of agriculture on soil texture due to wind erosion. *Land Degrad. Dev.* **2015**, *26*, 62–70.
7. Lal, R. Soil erosion and the global carbon budget. *Environ. Int.* **2003**, *29*, 437–450.
8. Ritter, W.F.; Shirmohammadi, A. *Agricultural Nonpoint Source Pollution, Watershed Management and Hydrology*; Lewis Publishers: New York, NY, USA, 2001; p. 342.
9. Belsky, J.A.; Matzke, A.; Uselman, S. Survey of livestock influences on stream and riparian ecosystems in the western United States. *J. Soil Water Conserv*. **1999**, *54*, 419–431.
10. Greenwood, P.; Kuhn, N.J. Does the invasive plant, Impatiens glandulifera, promote soil erosion along the riparian zone? An investigation on a small watercourse in northwest Switzerland. *J. Soils Sediments* **2014**, *14*, 637–650.
11. Jordan, C.; McGuckin, S.O.; Smith, R.V. Increased predicted losses of phosphorus to surface waters from soils with high Olsen-P concentrations. *Soil Use Manag.* **2000**, *16*, 27–35.
12. Quinton, J.N.; Catt, J.A.; Hess, T.M. The selective removal of phosphorus from soil: Is event size important? *J. Environ. Qual.* **2001**, *30*, 538–545.
13. Kuhn, N.J.; Armstrong, E.K.; Ling, A.C.; Connolly, K.L.; Heckrath, G. Interrill erosion of carbon and phosphorus from conventionally and organically farmed Devon silt soils. *CATENA* **2012**, *91*, 94–103.
14. Baker, L.A. Introduction to nonpoint source pollution in the United States and prospects for wetland use. *Ecol. Eng.***1992**, *1*, 1–26.
15. Lal, R. Soil carbon sequestration impacts on global climate change and food security. *Science* **2004**, *304*, 1623–1627.
16. Van Oost, K.; Quine, T.A.; Govers, G.; de Gryze, S.; Six, J.; Harden, J.W.; Ritchie, J.C.; McCarty, G.W.; Heckrath, G.; Kosmas, C.; *et al.* The impact of agricultural soil erosion on the global carbon cycle. *Science* **2007**, *318*, 626–629.
17. Berhe, A.A.; Harte, J.; Harden, J.W.; Torn, M.S. The significance of the erosion-induced terrestrial carbon sink. *BioScience* **2007**, *57*, 337–346.
18. Kuhn, N.J.; Hoffmann, T.; Schwanghart, W.; Dotterweich, M. Agricultural soil erosion and global carbon cycle: Controversy over? *Earth Surf. Process. Landf.* **2009**, *34*, 1033–1038.
19. Quinton, J.N.; Govers, G.; van Oost, K.; Bardgett, R.D. The impact of agricultural soil erosion on biogeochemical cycling. *Nat. Geosci.* **2010**, *3*, 311–314.
20. Kirkels, F.M.S.A.; Cammeraat, L.H.; Kuhn, N.J. The fate of soil organic carbon upon erosion, transport and deposition in agricultural landscapes—A review of different concepts. *Geomorphology* **2014**, *226*, 94–105.
21. Fiener, P.; Auerswald, K.; van Oost, K. Spatio-temporal patterns in land use and management affecting stromflow response of agricultural catchments—A review. *Earth Sci. Rev.* **2011**, *106*, 92–104.

22. Kuhn, N.J. Assessing Lateral Organic Carbon Movement in Small Agricultural Catchments. Available Online: http://www.wsl.ch/dienstleistungen/publikationen/pdf/12491.pdf (accessed on 15 October 2015).
23. Lal, R.; Pimentel, D. Letter on "Soil Erosion: A carbon sink or source?" *Science* **2008**, *319*, 1040–1041.
24. Kinnell, P.I.A. Particle travel distances and bed and sediment compositions associated with rain-Impacted flows. *Earth Surf. Process. Landf.* **2001**, *26*, 749–758.
25. Kuhn, N.J.; Armstrong, E.K. Erosion of organic matter from sandy soils: Solving the mass balance. *CATENA* **2012**, *98*, 87–95.
26. Fiener, G.; Govers, G; van Oost, K. Evaluation of a dynamic multi-class sediment transport model in a catchment under soil-conservation agriculture. *Earth Surf. Process. Landf.* **2008**, *33*, 1639–1660.
27. Loch, R.J. Settling velocity—A new approach to assessing soil and sediment properties. *Comput. Electron. Agric.* **2001**, *31*, 305–316.
28. Van Oost, K., Govers, G.; Quine, T.A.; Heckrath, G.; Olesen, J.E.; de Gryze, S.; Merckx, R. Landscape-scale modeling of carbon cycling under the impact of soil redistribution: The role of tillage erosion. *Glob. Biogeochem. Cycles* **2005**, *19*, 1733–1739.
29. Van Oost, K.; Beuselinck, L.; Hairsine, P.B.; Govers, G. Spatial evaluation of a multi-class sediment transport and deposition model. *Earth Surf. Process. Landf.* **2004**, *29*, 1027–1044.
30. Hu, Y.; Kuhn, N.J. Aggregates reduce transport distance of soil organic carbon: Are our balances correct? *Biogeosciences* **2014**, *11*, 6209–6219.
31. Hairsine, P.B.; Rose, C.W. Rainfall detachment and deposition: Sediment transport in the absence of flow-driven processes. *Soil Sci. Soc. Am. J.* **1991**, *55*, 320–324.
32. Hairsine, P.B.; Rose, C.W. Modelling water erosion due to overland flow using physical principles: I. Uniform flow. *Water Resour. Res.* **1992**, *28*, 237–243.
33. Hairsine, P.B.; Rose, C.W. Modelling water erosion due to overland flow using physical principles: II. Rill flow. *Water Resour. Res.* **1992**, *28*, 245–250.
34. Starr, G.C.; Lal, R.; Malone, R.; Hothem, D.; Owens, L.; Kimble, J. Modeling soil carbon transported by water erosion process. *Land Degrad. Dev.* **2000**, *11*, 83–91.
35. Wang, Z.; Govers, G.; Steegen, A.; Clymans, W.; van den Putte, A.; Langhans, C.; Merckx, R.; van Oost, K. Catchment-scale carbon redistribution and delivery by water erosion in an intensively cultivated area. *Geomorphology* **2010**, *124*, 65–74.
36. Nadeu, E.; de Vente, J.; Martínez-Mena, M.; Boix-Fayos, C. Exploring particle size distribution and organic carbon pools mobilized by different erosion processes at the catchment scale. *J. Soils Sediments* **2011**, *11*, 667–678.
37. Hairsine, P.B.; McTainsh, G.H. *The Griffith Tube: A Simple Settling Tube for the Measurement of Settling Velocity of Soil Aggregates*; AES working paper 3/86; Griffith University: Brisbane, Australia, 1986.
38. Smith, R.E.; Quinton, J.; Goodrich, D.C.; Nearing, M. Soil-erosion models: Where do we really stand? *Earth Surf. Process. Landf.* **2010**, *35*, 1344–1348.
39. Proffitt, A.P.B.; Rose, C.W.; Lovell, C.J. Settling velocity characteristics of sediment detached from a soil surface by raindrop impact. *Catena* **1993**, *20*, 27–40.

40. Proffitt, A.P.B.; Rose, C.W. Soil erosion processes II. Settling velocity characteristics of eroded sediment. *Aust. J. Soil Res.* **1991**, *29*, 685–695.
41. Lovell, C.J.; Rose, C.W. Wake capture effects observed in a comparison of methods to measure particle settling velocity beyond Stokes' range. *J. Sediment. Petrol.* **1991**, *61*, 575–582.
42. Lovell, C.J.; Rose, C.W. The effects of sediment concentration and tube-diameter on particle settling velocity measured beyond Stokes' range: Experiment and theory. *J. Sediment. Petrol*. **1991**, *61*, 583–589.
43. Lu, H.; Moran, C.J.; Prosser, I.P. Modelling sediment delivery ratio over the Murray Darling Basin. *Environ. Model. Softw.* **2006**, *21*, 1297–1308.
44. Pieri, L.; Bittelli, M.; Wu, J.Q.; Dun, S.; Flanagan, D.C.; Pisa, P.R.; Ventura, F.; Salvatorelli, F. Using the Water Erosion Prediction Project (WEPP) model to simulate field-observed runoff and erosion in the Apennines Mountain Range, Italy. *J. Hydrol.* **2007**, *336*, 84–97.
45. Walling, D.E. Erosion and sediment yield research—Some recent perspectives. *J. Hydrol.* **1988**, *100*, 113–141.
46. Dietrich, W.E. Settling velocity of natural particles. *Water Resour. Res.* **1982**, *18*, 1615–1626.
47. Angima, S.D.; Stott, D.E.; O'Neill, M.K.; Ong, C.K.; Weesies, G.A. Soil erosion prediction using RUSLE for central Kenyan highland conditions. *Agric. Ecosyst. Environ.* **2003**, *97*, 295–308.
48. Le Bissonnais, Y. Aggregate stability and assessment of soil crustability and erodibility: I. Theory and methodology. *Eur. J. Soil Sci.***1996**, *47*, 425–437.
49. Levy, G.J.; Warrington, D.N.; Bhardwaj, A.K.; Mamedov, A.I. Changes in eroded material and runoff as affected by rain depth and aggregate slaking in three semiarid region soils. *Geophys. Res. Abstr.* **2007**, *9*, 05380.
50. Renard, K.G.; Foster, G.R.; Weesies, G.A.; Porter, J.P. Rusle: Revised universal soil loss equation. *J. Soil Water Conserv.* **1991**, *46*, 30–33.
51. Van Oost, K.; Verstraeten, G.; Doetterl, S.; Notebaert, B.; Wiaux, F.; Broothaerts, N.; Six, J. Legacy of human-induced C erosion and burial on soil-atmosphere C exchange. *Proc. Natl. Acad. Sci. USA* **2012**, *109*, 19492–19497.
52. Ries, J.B.; Iserloh, T.; Seeger, M.; Gabriels, D. Rainfall simulations—Constraints, needs and challenges for a future use in soil erosion research. *Z. Geomorphol. Suppl.* **2013**, *57*, 1–10.
53. Iserloh, T.; Ries, J.B.; Arnaez, J.; Boix Fayos, C.; Butzen, V.; Cerdá, A.; Echeverría, M.; Fernández-Gálvez, J.; Fister, W.; Gómez, J.A. European small portable rainfall simulators: A comparison of rainfall characteristics. *CATENA* **2013**, *110*, 100–112.
54. Kuhn, N.J.; Bryan, R.B.; Navar, J. Seal formation and interrill erosion on a smectite-rich Kastanozem from NE-Mexico. *CATENA* **2003**, *52*, 149–169.
55. Kuhn, N.J.; Bryan, R.B. Drying, soil surface condition and interrill erosion on two Ontario soils. *Catena* **2004**, *57*, 113–133.
56. Kuhn, N.J. Erodibility of soil and organic matter: Independence of organic matter resistance to interrill erosion. *Earth Surf. Process. Landf.* **2007**, *35*, 1344–1348.
57. Hu, Y.; Fister, W.; Rüegg, H.R.; Kinnell, P.I.A.; Kuhn, N.J. The Use of Equivalent Quartz Size and Settling Tube Apparatus to Fractionate Soil Aggregates by Settling Velocity. Available online: http://www.geomorphology.org.uk/sites/default/files/geom_tech_chapters/1.1.1_SettlingTube.pdf (accessed on 15 October 2015).

58. Kinnell, P.I.A. Sediment transport by medium to large drops impacting flows at subterminal velocity. *Soil Sci. Soc. Am. J.* **2005**, *69*, 902–905.
59. Kinnell, P.I.A. Raindrop-impact-induced erosion processes and prediction: A review. *Hydrol. Process.* **2005**, *19*, 2815–2844.
60. Gibbs, R.J.; Matthews, M.D.; Link, D.A. The relationship between sphere size and settling velocity. *J. Sediment. Petrol.* **1971**, *41*, 7–18.
61. Pert, M.R.; Walling, D.E. Particle size characteristics of fluvial suspended sediment. In *Recent Developments in the Explanation and Prediction of Erosion and Sediment Yield*; International Association of Hydrological Sciences (IAHS): Exeter, UK, 1982; pp. 397–407.
62. Polyakov, V.O.; Lal, R. Soil organic matter and CO_2 emission as affected by water erosion on field runoff plots. *Geoderma* **2008**, *143*, 216–222.
63. Iserloh, T.; Fister, W.; Seeger, M.; Willger, H.; Ries, J.B. A small portable rainfall simulator for reproducible experiments on soil erosion. *Soil Tillage Res.* **2012**, *124*, 131–137.
64. MeteoSwiss. *Monthly Total Precipitation during April, May, and June at Station Arisdorf (47°30'N, 7°46'E) Near Möhlin from 1985 to 2012*; MeteoSwiss, Federal Office of Meteorology and Climatology: Zürich, Switzerland, 2013.
65. Wan, L.; Zhang, X.P.; Ma, Q.; Zhang, J.J.; Ma, T.Y.; Sun, Y.P. Spatiotemporal characteristics of precipitation and extreme events on the Loess Plateau of China between 1957 and 2009. *Hydrol. Process.* **2014**, *28*, 4971–4983.
66. Torri, D.; Regüés, D.; Pellegrini, S.; Bazzoffi, P. Within-storm soil surface dynamics and erosive effects of rainstorms. *Catena* **1999**, *38*, 131–150.
67. Flanagan, D.C.; Livingston, S.J. (Eds.) Water Erosion Prediction Project (WEPP) Version 95.7, User Summary. In *WEPP User Summary*, Report No. 11; NSERL: West Lafayette, IN, USA, 1995.

Chapter 6

Summary and Conclusions

6.1. Summary of primary results from each experiment

Improving our understanding of soil erosion and its impact on carbon (C) cycling requires a better understanding of the redistribution of eroded sediment and associated soil organic carbon (SOC) across agricultural landscapes (Kuhn, 2013). Recent studies conducted in the laboratory have illustrated that aggregation can profoundly increase the settling velocities of individual mineral particles, and thus skew the redistribution and subsequent fate of eroded SOC (Hu and Kuhn, 2014; Hu and Kuhn, 2016). However, the erodibility of soils in the field is more temporally and spatially variable due to the impacts of tillage, rainfall, wetting-drying cycles, freezing, and biological processes (Fox et al., 1998). It is not entirely clear whether changes in natural surface conditions, such as the development of a surface crust, could impact on the characteristics of eroded sediment and thereby diminishes the effect of aggregation on the fate of eroded SOC. The first aim of this study therefore was to investigate the potential effect of aggregation of a natural crusted soil surface on the redistribution and mineralization of sediment associated SOC during erosion events. Based on measurements of the first experiment, the second aim of this study was to develop a proxy means of more accurately capturing the effect of aggregation on sediment transport and to effectively provide actual settling information for erosion models. In order to address those two aims, four objectives were identified: 1) to quantitatively identify the potential fate of SOC eroded from natural crusted soil surface and further compare the observations with that based on dry-sieved aggregates in the laboratory; 2) to examine the effect of aggregation on the quality of sediment associated SOC and investigate the sensitivity of the sediment settling behavior to increased kinetic energy in a series of rainfall events; 3) to develop a simple but efficient proxy method to generate natural or quasi-natural sediment; and 4) to evaluate the feasibility and sensitivity of such a proxy method. A series of experiments was conducted in both field and laboratory settings to address each of those research objectives. The experimental design, results, discussion and conclusions of each experiment have been described in previous chapters. Primary results from all experiments are concluded here as a summary of this study.

Chapter 2 mainly examined the effect of aggregation on the potential fate of the SOC eroded from naturally developed soil surface. Short-term wind driven storms, simulated with a portable wind and rainfall simulator (PWRS), were conducted on a crusted soil in the field. A settling tube apparatus was applied to predict the potential fate of sediment and associated SOC eroded from the experiment. The results show that: 1) aggregation can potentially increase the deposition of sediment and SOC across landscapes by six times and three times as compared to that implied by mineral grains; 2) the

preferential deposition of SOC-rich fast-settling sediment potentially releases approximately 50% more CO_2 than the same layer of the non-eroded original soil; 3) the SOC associated with fine fraction of EQS < 32 μm was found to have the highest mineralization rate based on the incubation test, indicating the high risk to be mineralized during redistribution. Overall, the data illustrate that aggregation, even for the crusted soil surface, could considerably reduce the potential transport distance of eroded sediment and associated SOC, and thus potentially skew the redistribution of eroded SOC towards landscapes rather than aquatic environments. Such skewed patterns can significantly accelerate C mineralization during redistribution, particularly when repeated erosion and deposition processes along hill-slopes prompt further disintegration of large aggregates during natural erosion events. Therefore, the potential terrestrial SOC redistribution and the mineralization of eroded SOC during redistribution must be taken into account in the investigation of erosion induced C cycling.

Chapter 3 focused on extending work undertaken and reported in Chapter 2 to further investigate the effect of aggregation on SOC quality and examined the sensitivity of the sediment settling behavior to increased kinetic energy in four rainfall runs. The results show: 1) if applying mineral grain specific SOC distribution, the potential deposition of MOC across landscapes would be completely overlooked. Further exposure of deposited MOC, due to aggregate breakdown over the proceeding erosion events, can potentially lead to additional CO_2 emission; 2) the settling velocity distributions of eroded sediment as well as the SOC concentration and cumulative mineralization of each fraction did not change during a series of rainfall events, suggesting that the properties of eroded sediment are very stable as cumulative rainfall increased. The results illustrate that settling velocity distribution of eroded sediment, as well as the SOC concentration of each fraction, could now be regarded as stable parameters in erosion models. It therefore offers the opportunity to develop a simple proxy indicator to generate similar sediment as that eroded from the natural surface for the purpose of optimizing current erosion models.

Chapter 4 described the use of a proxy method of generating quasi-natural sediment, termed Raindrop Aggregate Destruction Device-Settling Tube (RADD-ST), to further identify the effect of aggregation on the settling velocity of sediment and the associated SOC. Two agricultural soils with different sandy and silty loam textures were subjected to rainfall using a raindrop aggregate destruction device (RADD). Aggregates sustained after raindrop impact were thereafter fractionated by a settling tube (ST) into six different size classes. The SOC content was measured for each settled and dispersed class. The results demonstrate that: 1) for an aggregated soil, applying dispersed mineral grain size distribution, rather than its actual aggregate distribution, to soil erosion models would lead to an underestimation of the deposition of eroded sediment and SOC across landscapes; 2) the settling velocity distribution of the well aggregated soil generated with the RADD is comparable with that from material eroded under the field conditions (Chapter 2) and that from a previous flume experiment

(Hu and Kuhn, 2014). This indicates that the RADD developed in this study represents an effective proxy for generating quasi-natural sediment from well-aggregated soil.

In Chapter 5, the feasibility and sensitivity of the RADD-ST approach was further examined by applying the technique to four soil-types with similar texture, but different degrees of aggregation. Through comparing the Mean Weight Settling Velocity (MWSV) of raindrop-dispersed aggregates with dispersed mineral grains, the results show that the settling velocity of the four soils and their SOC deposited across landscapes would have been underestimated by at least six times, if not considering the actual aggregate settling velocity distribution. This demonstrates the feasibility of the RADD-ST approach to capture the effect of aggregation onto sediment size and subsequent re-distribution. The feasibility of the approach was also illustrated by the comparable settling velocity distributions between aggregates collected from the RADD-ST in this study and that of the same soil collected from a previous flume experiment and a field experiment. Furthermore, the settling velocities gradually declined as raindrop kinetic energy increased, and the declining patterns differed between the four soils. This clearly illustrates the sensitivity of this RADD-ST approach to detect the minor differences in soil erodibility properties.

6.2. General conclusions

This study aimed to investigate the potential effect of aggregation of a natural crusted soil surface on the redistribution and mineralization of sediment associated SOC, and to develop a proxy method to effectively capture the effect of aggregation on sediment settling behavior. A series of experiments conducted in both the laboratory and under field conditions were conducted to address these aims. Results obtained in this study have contributed to improving our current understanding of slope-scale C dynamics. The spatial variations during SOC re-deposition observed in the field experiments verify previous studies conducted on a simulated seedbed in laboratory-based setting. Aggregation, even on a crusted soil surface, considerably reduced the likely transport distance of eroded sediment and associated SOC, and hence potentially skewed the deposition of SOC-rich fast-settling fractions towards the terrestrial system. The increased SOC stock at depositional sites may consequently result in a substantially higher mineralization and considerably strengthen C-source effects at depositional sites. Furthermore, the accelerated respiration rates of the fractionated size-classes, as compared to the original bulk soil, suggest that erosion was prone to accelerate the mineralization of eroded SOC immediately after erosion. It is highly likely that this effect could be contributing additional CO_2 to the atmosphere. The results therefore highlight the critical impacts of redistribution processes on C dynamics during erosion events. This includes preferential deposition of SOC-rich fast-settling fractions caused by aggregation, C mineralization change caused by aggregate breakdown, and effective time that eroded SOC is exposed to atmosphere. This study also demonstrates that C fluxes drawn only from the SOC inventories based on the site of erosion and deposition may not adequately reflect C dynamics at slope scales. This is because the C-inventory approach can neither properly

distinguish the SOC likely re-deposited in terrestrial systems from the portion potentially transported to aquatic systems, nor fairly capture the effect of differentiation and mineralization of eroded SOC during redistribution. Overall, this study illustrates that unless the impacts of the redistribution of sediment and sediment associated SOC on C dynamics is adequately addressed, erosion-induced carbon sink or source effects are still far from being fully understood.

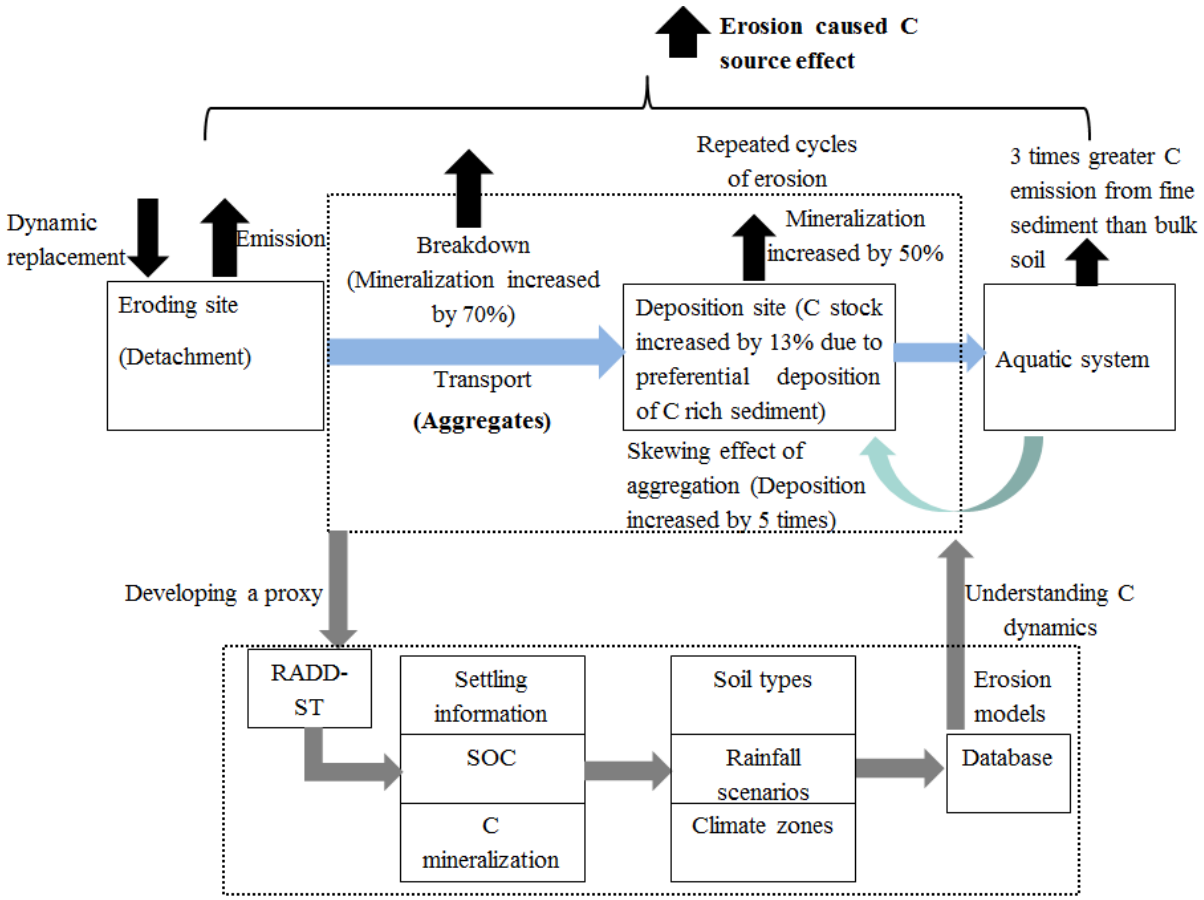

Figure 6.1 A schematic concluding the effect of aggregation on C dynamics and the further application of the RADD-ST in C dynamics research. The blue arrows represent water flow; the black arrows represent C fluxes; the green arrow represents the skewing effect of aggregation; the grey arrows represent the application procedures in C dynamics research.

The settling velocity distributions of eroded sediment across the cumulative rainfalls, as well as the SOC concentration of each fraction, did not change during the series of rainfall events. This suggests that the properties of eroded sediment can be regarded as a stable parameter during redistribution. It is thus promising to develop a computable parameter integrating aggregated-sediment settling velocity and the associated SOC distribution to optimize current erosion models, such as the Multi-Class Sediment Transport model (MCST) (van Oost et al., 2004). The RADD-ST approach developed in this study could generate comparable sediment as that eroded from the field and that from a flume experiment. It therefore has the potential to provide actual settling information under relatively simple simulated rainfall conditions to optimize the parametrization of sediment behavior and quality in

erosion models. If further extrapolated appropriately to a specific erosion scenario, the RADD-ST derived sediment quality parameters can also help improve our understanding of sediment movement through watersheds and the environmental impacts of the spatial distribution of eroded substances. The RADD-ST approach therefore could become a useful tool to help improve the understanding the impacts of erosion induced SOC redistribution across landscapes on global C cycling.

6.3. Potential research in the future

Field Experiments 1&2 were based on plot experiments under certain patterns of simulated rainfalls. Despite undertaking attempts to simulate the effects of natural rainfall by combining the impact of wind, the raindrop kinetic energy is still weaker when compared to natural rainfall. In addition, the transport distances of eroded sediment were relatively short due to the limited plot size, so the possible breakdown and disintegration that eroded sediment might undergo during transport under natural erosion conditions was, by necessity, overlooked. ***Laboratory Experiments 1&2*** were based on limited soil types under a single rainfall scenario, and thus restrains the application of these results to other erosion scenarios. Therefore, several open questions still merit further attention, and these could be addressed during research in the future. They are:

1) Field surveys of eroded and/or deposited sediment in natural erosion events are essential to determine the effect of aggregation on the redistribution of sediment associated SOC and the mineralization potential of SOC under more complex natural conditions. Systematic field experiments and monitoring of a range of soils with different textures, aggregation degrees, and various soil management regimes are necessary to more fully investigate the potential effect of aggregation onto the potential transport fate of eroded SOC.
2) The aerobic decomposition rate of the SOC associated with the slow-settling fraction may decline after being transported to aquatic systems, whereas the prevalence of anaerobic conditions may accentuate methanogenesis and lead to efflux of CH_4, which has a much higher global warming potential than CO_2. Therefore, the potential fate of the slow-settling fraction after being transported to aquatic systems deserves further investigation.
3) A wider range of soils with various aggregation characteristics should be investigated under more varied rainfall conditions. This will help optimize the RADD apparatus and further construct a settling information database of aggregated soils for spatially distributed erosion models.
4) The RADD apparatus designed in this study basically provides settling information of quasi-natural sediment by simulating natural aggregate breakdown processes under raindrop impact. The effect of shear stress on aggregate breakdown caused by turbulent flow during transport is also important in determining the settling velocity distribution of the eroded sediment, as well as further redistribution across landscapes. It is therefore necessary to take into account the possible evolution of settling velocity distribution during long-distance transport across landscapes.

References

- Angima, S.D., Stott, D.E., O'Neill, M.K., Ong, C.K., Weesies, G.A., 2003. Soil erosion prediction using RUSLE for central Kenyan highland conditions, Agriculture, Ecosystems & Environment 97, 295– 308.
- Baker, L.A., 1992. Introduction to nonpoint source pollution in the United States and prospects for wetland use, Ecological Engineering 1, 1–26.
- Belsky, J.A., Matzke, A., Uselman, S., 1999. Survey of livestock influences on stream and riparian ecosystems in the western United States, Journal of Soil and Water Conservation 54, 419–431.
- Berhe, A.A., Harte, J., Harden, J.W. and Torn, M.S., 2007. The significance of the erosion-373 induced terrestrial carbon sink, BioScience 57, 337–346.
- Beuselinck, L., Govers, G., Steegen, A., Hairsine, P.B., Poesen, J., 1999. Evaluation of the simple settling theory for predicting sediment deposition by overland flow, Earth Surface Processes and Landforms 24, 993–1007.
- Billings, S.A., Buddemeier, R.W., deB. Richter, D., Van Oost, K., Bohling, G., 2010. A simple method for estimating the influence of eroding soil profiles on atmospheric CO_2: ATMOSPHERIC C POOL AND SOIL EROSION, Global Biogeochemical Cycles 24, GB2001. doi:10.1029/2009GB003560
- Borselli, L., Torri, D., Poesen, J., and Sanchis, P., 2001. Effects of water quality on infiltration, runoff and interrill erosion processes during simulated rainfall, Earth Surface Processes and Landforms 26, 329–342.
- Cerdà, A., Giménez-Morera, A., Bodí, M.B, 2009a. Soil and water losses from new citrus orchards growing on sloped soils in the western Mediterranean basin, Earth Surface Processes and Landforms 34, 1822–1830.
- Cerdà, A., Flanagan, D.C., Le Bissonnais, Y., Boardman, J., 2009b. Soil erosion and agriculture, Soil & Tillage Research 106, 107–108.
- Cheng, N.S., 1997. Simplified settling velocity formula for sediment particle, Journal of Hydrological Research 123, 149–152.
- Climate-Data.org. Climate data for cities worldwide, Witterswil. Available online: http:// http://zh.climate-data.org/location/160889/ (accessed on 8 December 2014).
- Colazo, J.C., Buschiazzo, D., 2015. The impact of agriculture on soil texture due to wind erosion, Land Degradation & Development 26, 62–70.
- Cornelis, W.M., Oltenfreiter, G., Gabriels, D., Hartmann, R., 2004. Splash-saltation of sand due to wind-driven rain: vertical deposition flux and sediment transport rate, Soil Science Society of America Journal 68, 32-40.
- Croft, H., Kuhn, N. J., and Anderson, K., 2012a. On the use of remote sensing techniques for monitoring spatio-temporal soil organic carbon dynamics in agricultural systems, Catena 94, 64–74.
- Croft, H., Anderson, K., Kuhn, N.J., 2012b. Reflectance anisotropy for measuring soil surface roughness of multiple soil types, Catena 93, 87-96.

- De Baets, D., Torri, D., Poesen, J., and Meersmans, J., 2008. Modelling increased soil cohesion due to roots with EUROSEM, Earth Surface Processes and Landforms 33, 1948–1963.
- De Lima, J.L.M.P., van Dijk, P.M., Spaan, W.P., 1992. Splash-saltation transport under wind-driven rain, Soil Technology 5, 151-166.
- Dietrich, W.E., 1982. Settling velocity of natural particles, Water Resource Research 18, 1615–1626.
- Elliott, E.T., 1986. Aggregate structure and carbon, nitrogen, and phosphorus in native and cultivated soils, Soil Science Society of America Journal 50, 627–633.
- FAO/ISRIC/ISSS.: World Reference Base for Soil Resources, FAO: Rome, 1998.
- Fentie, B., Rose, C.W., Coughlan, K.J., 1999. GUEST 3.0: A program for calculating a soil erodibility parameter in a physically-based erosion model. Faculty of Environmental Sciences, Griffith University, Queensland, Australia, Brisbane. ISBN 0 86857 944 0.
- Ferguson, R.I., Church, M., 2004. A simple universal equation for grain settling velocity, Journal of Sediment Research 74, 933–937.
- Fiener, G., Govers, G., van Oost, K., 2008. Evaluation of a dynamic multi-class sediment transport model in a catchment under soil-conservation agriculture, Earth Surface Processes and Landforms 33, 1639–1660.
- Fiener, P., Dlugoß, V., Van Oost, K., 2015. Erosion-induced carbon redistribution, burial and mineralisation — Is the episodic nature of erosion processes important? Catena 133, 282–292.
- Fister, W., Iserloh, T., Ries, J.B., Schmidt, R.G., 2012. A portable combined wind andrainfall simulator for in situ soil erosion measurements, Catena 91, 72-84.
- Flanagan, D.C., 1995. Livingston, S.J. (Eds.) Water Erosion Prediction Project (WEPP) Version 95.7, User Summary. In WEPP User Summary, Report No. 11; NSERL: West Lafayette, IN, USA.
- Foster, G.R., Young, R.A., Neibling, W.H., 1985. Sediment composition for nonpoint source pollution analyses, Trans. ASAE 28, 133–139, 146.
- Gibbs, R.J., Matthews, M.D. and Link, D.A., 1971. The relationship between sphere size and settling velocity, Journal of Sedimentary Research 41, 7–18.
- Greenwood, P., Kuhn, N.J., 2014. Does the invasive plant, Impatiens glandulifera, promote soil erosion along the riparian zone? An investigation on a small watercourse in northwest Switzerland, Journal of Soils and Sediments, 14, 637–650.
- Hallermeier, R.J., 1981. Terminal settling velocity of commonly occurring sand grains, Sedimentology 28, 859–865.
- Hairsine, P.B., McTainsh, G.H., 1986. The Griffith tube: a simple settling tube for the measurement of settling velocity of soil aggregates, AES working paper 3/86, Griffith University, Brisbane.
- Hairsine, P.B., Rose, C.W., 1991. Rainfall detachment and deposition: Sediment transport in the absence of flow-driven processes, Soil Science Society of American Journal 55, 320–324.
- Hairsine, P.B., Rose, C.W., 1992a. Modelling water erosion due to overland flow using physical principles: I. Uniform flow, Water Resource Research 28, 237–243.
- Hairsine, P.B., Rose, C.W., 1992b. Modelling water erosion due to overland flow using physical principles: II. Rill flow. Water Resource Research 28, 245–250.

- Harden, J.W., Sharpe, J.M., Parton, W.J., Ojima, S., Fries, T.L., Huntington, T.G. and Dabney, S.M.: Dynamic replacement and loss of soil carbon on eroding cropland, Global Biogeochemical Cycles 13, 885–901.
- Hardy, N., Shainberg, I., Gal, M., Keren, R., 1983. The effect of water quality and storm sequence upon infiltration rate and crust formation, Journal of Soil Science 34, 665-676.
- Hoffmann, T., Mudd, S.M., van Oost, K., Verstraeten, G., Erkens, G., Lang, A., Middelkoop, H., Boyle, J., Kaplan, J.O., Willenbring, J. Aalto, R., 2013. Short Communication: Humans and the missing C-sink: erosion and burial of soil carbon through time, Earth Surface Dynamics 1, 45–52.
- Hu, Y., Fister, W., Kuhn, N.J., 2013a. Temporal variation of SOC enrichment from interrill erosion over prolonged rainfall simulations, Agriculture 3, 726–740.
- Hu, Y., Fister, W., Rüegg, H.-R., Kinnell, P.A., Kuhn, N.J., 2013b. The Use of Equivalent Quartz Size and Settling Tube Apparatus to Fractionate Soil Aggregates by Settling Velocity. Geomorphology Techniques (Online Edition), British Society for Geomorphology Section–1.
- Hu, Y., Kuhn, N.J., 2014. Aggregates reduce transport distance of soil organic carbon: are our balances correct? Biogeosciences 11, 6209–6219.
- Hu, Y., Kuhn, N.J., 2016. Erosion-induced exposure of SOC to mineralization in aggregated sediment, Catena 137, 517-525.
- IPCC, 2014: Climate Change 2014: Synthesis Report. Contribution of Working Groups I, II and III to the Fifth Assessment Report of the Intergovernmental Panel on Climate Change [Core Writing Team, R.K. Pachauri and L.A. Meyer (eds.)]. IPCC, Geneva, Switzerland,
- Iserloh, T., Fister, W., Seeger, M., Willger, H., Ries, J.B., 2012. A small portable rainfall simulator for reproducible experiments on soil erosion. Soil & Tillage Research 124, 131–137.
- Iserloh, T., Fister, W., Marzen, M., Seeger, M., Kuhn, N.J., Ries, J.B., 2013a. The role of wind-driven rain for soil erosion – an experimental approach, Zeitschrift für Geomorphologie 57, 193-201.
- Iserloh, T., Ries, J.B., Arnaez, J., Boix Fayos, C., Butzen, V., Cerdá, A., Echeverría, M., Fernández-Gálvez, J., Fister, W., Gómez, J.A., 2013b. European small portable rainfall simulators: A comparison of rainfall characteristics, Catena 110, 100–112.
- Jacinthe, P. A. and Lal, R., 2001. A mass balance approach to assess carbon dioxide evolution during erosional events, Land Degradation & Development 12, 329–339.
- Jacinthe, P.A., Lal, R., Kimble, J.M., 2002. Carbon dioxide evolution in runoff from simulated rainfall on long-term no-till and plowed soils in southwestern Ohio, Soil & Tillage Research 66, 23–33.
- Jacinthe, P.A., Lal, R., Owens, L.B., Hothem, D.L., 2004. Transport of labile carbon in runoff as affected by land use and rainfall characteristics, Soil & Tillage Research 77, 111–123.
- Jordan, C., McGuckin, S.O., Smith, R.V., 2000. Increased predicted losses of phosphorus to surface waters from soils with high Olsen-P concentrations, Soil Use and Management 16, 27–35.
- Kaiser, M., Berhe, A.A., Sommer, M., Kleber, M., 2012. Application of ultrasound to disperse soil aggregates of high mechanical stability, Journal of Plant Nutrition and Soil Science 175, 521–526.
- Kinnell, P.I.A., 2001. Particle travel distance and bed and sediment compositions associated with rain-impacted flows, Earth Surface Processes and Landforms 26, 749–758.

- Kinnell, P.I.A., 2005. Raindrop-impact-induced erosion processes and prediction: a review, Hydrological Processes 19, 2815–2844.
- Kirkels, F.M.S.A., Cammeraat, L.H., Kuhn, N.J., 2014. The fate of soil organic carbon upon erosion, transport and deposition in agricultural landscapes — A review of different concepts. Geomorphology 226, 94-105.
- Knisel, W.G., 1980. CREAMS: a field-scale model for Chemicals, Runoff, and Erosion from Agricultural Management Systems. US Department Agriculture, Conservation Research Report No. 26.
- Kuhn, N., Bryan, R. and Navar, J., 2003. Seal formation and interrill erosion on a smectite-rich Kastanozem from NE-Mexico, Catena 52, 149–169.
- Kuhn, N.J., Bryan, R.B., 2004. Drying, soil surface condition and interrill erosion on two Ontario soils, Catena 57, 113–133.
- Kuhn, N. J., 2007. Erodibility of soil and organic matter: independence of organic matter resistance to interrill erosion, Earth Surface Processes and Landforms 32, 794-802.
- Kuhn, N.J., Hoffmann, T., Schwanghart, W. and Dotterweich, M., 2009. Agricultural soil erosion and global carbon cycle: controversy over? Earth Surface Processes and Landforms 34, 1033–1038.
- Kuhn, N.J., Armstrong, E.K., 2012. Erosion of organic matter from sandy soils: Solving the mass balance, Catena 98, 87–95.
- Kuhn, N.J., 2013. Assessing lateral organic Carbon movement in small agricultural catchments. Publikation zur Jahrestagung der Schweizerischen Geomorphologischen Gesellschaft. Ed: 413 Graf C. 29, 151–164.
- Lal, R., 2003. Soil erosion and the global carbon budget, Environment International 29, 437–450.
- Lal, R., 2004. Soil carbon sequestration impacts on global climate change and food security, Science 304, 1623-1627.
- Lal, R., 2005. Soil erosion and carbon dynamics, Soil & Tillage Research 81, 137–142.
- Lal, R., Pimentel, D., 2008. Letter on “Soil Erosion: A carbon sink or source?”, Science 319, 1040–1041.
- Larson, W.E., Lindstrom, M.J., Schumacher, T.E., 1997. The role of severe stormes in soil erosion: a problem needing consideration, Journal of Soil and Water Conservation 52, 90-95.
- Le Bissonnais, Y., Renaux, B., Delouche, H., 1995. Interactions between soil properties and moisture content in crust formation, runoff and interrill erosion from tilled loess soils, Catena 25, 33-46.
- Le Bissonnais, Y., 1996. Aggregate stability and assessment of soil crustability and erodibility: I. Theory and methodology, European Journal of Soil Science 47, 425–437.
- Legout, C., Leguedois, S. and Le Bissonnais, Y., 2005. Aggregate breakdown dynamics under rainfall compared with aggregate stability measurements, European Journal of Soil Science 56, 225–237.
- Levy, G.J., Warrington, D.N., Bhardwaj, A.K., Mamedov, A.I., 2007. Changes in eroded material and runoff as affected by rain depth and aggregate slaking in three semiarid region soils. Geophysical Research Abstracts 9, 05380.
- Li, Y., Quine, T.A., Yu H.Q., Govers, G., Six, J., Gong, D.Z., Wang, Z., Zhang, Y.Z., VanOost, K., 2015. Sustained high magnitude erosional forcing generates an organic carbon sink: Test and implications in the Loess Plateau, China. Earth and Planetary Science Letters 411, 281-289.

- Lieskovský, J., Kenderessy, P, 2014. Modelling the effect of vegetation cover and different tillage practi-ces on soil erosion in vineyards: A case study en Vráble (Slovakia) using Watem/Sedem, Land Degradation & Development, 25, 288–296.
- Liu, S., Bliss, N., Sundquist, E., Huntington, T.G., 2003. Modeling carbon dynamics in vegetation and soil under the impact of soil erosion and deposition, Global Biogeochemical Cycles 17, 1074.
- Loch, R.J., 2001. Settling velocity–a new approach to assessing soil and sediment properties, Computers and Electronics in Agriculture 31, 305–316.
- Lovell, C.J., Rose, C.W., 1991a. Wake capture effects observed in a comparison of methods to measure particle settling velocity beyond Stokes' range, Journal of Sedimentary Petrology, 61, 575–582.
- Lovell, C.J., Rose, C.W., 1991b.The effects of sediment concentration and tube-diameter on particle settling velocity measured beyond Stokes' range: Experiment and theory, Journal of Sedimentary Petrology 61, 583–589.
- Lu, H., Moran, C.J., Prosser, I.P., 2006. Modelling sediment delivery ratio over the Murray Darling Basin, Environmental Modelling & Software 21, 1297–1308.
- MeteoSwiss, 2013. Monthly total precipitation during April, May, and June at Station Arisdorf near Möhlin from 1985 to 2012.
- Nadeu, E., De Vente, J., Martínez-Mena, M., Boix-Fayos, C., 2011. Exploring particle size distribution and organic carbon pools mobilized by different erosion processes at the catchment scale, Journal of Soils and Sediments 11, 667–678.
- Navara, A., Armstrong, A., Gristina, L., Semple, K.T, Quinton, J.N., 2012. Effects of soil compaction, rain exposure and their interaction on soil carbon dioxide emission, Earth Surface Processes and Landforms 37, 994-999.
- Nearing, M.A., Foster, G.R., Lane, L.J., Finkner, S.C., 1989. A process-based soil erosion model for USDA-water erosion prediction project technology, Trans. ASAE 32, 1587–1593.
- Olsen, P. and Kristensen, P. R., 1998. Using a GIS system in mapping risks of nitrate leaching and erosion on the basis of SOIL/SOIL-N and USLE simulations, Nutrient Cycling in Agroecosystems 50, 307–311.
- Parmesan, C., Yohe, G., 2003. A globally coherent fingerprint of climate change impacts across natural systems, Nature 421, 37–42.
- Pert, M.R., Walling, D.E., 1982. Particle size characteristics of fluvial suspended sediment. In Recent Developments in the Explanation and Prediction of Erosion and Sediment Yield; International Association of Hydrological Sciences (IAHS): Exeter, UK, pp. 397–407.
- Pieri, L., Bittelli, M., Wu, J.Q., Dun, S., Flanagan, D.C., Pisa, P.R., Ventura, F., Salvatorelli, F., 2007. Using the Water Erosion Prediction Project (WEPP) model to simulate field-observed runoff and erosion in the Apennines Mountain Range, Italy, Journal of Hydrology 336, 84–97.
- Pimentel, D., Harver, C., Resosudarmo, P., Sinclair, K., Kurz, D., McNair, M., Crist, S., Shpritz, L., Fitton, L., Saffouri, R., et al., 1995. Environmental and economic costs of soil erosion and conservation benefits, Science 267, 1117–1123.
- Polyakov, V.O., Lal, R., 2004. Soil erosion and carbon dynamics under simulated rainfall, Soil Science 169, 590-599.

- Polyakov, V.O., Lal, R., 2008. Soil organic matter and CO_2 emission as affected by water erosion on 442 field runoff plots, Geoderma 143, 216–222.
- Proffitt, A.P.B., Rose, C.W., 1991. Soil erosion processes II. Settling velocity characteristics of eroded sediment, Australian Journal of Soil Research 29, 685–695.
- Proffitt, A.P.B., Rose, C.W., Lovell, C.J., 1993. Settling velocity characteristics of sediment detached from a soil surface by raindrop impact, Catena 20, 27–40.
- Quinton, J.N., Catt, J.A., Hess, T.M., 2001. The selective removal of phosphorus from soil: is event size important? Journal of Environmental Quality 30, 538–545.
- Quinton J.N., Catt, J.A., 2004. The effects of minimal tillage and contour cultivation on surface runoff, soil loss and crop yield in the long-term Woburn Erosion Reference Experiment on sandy soil at Woburn, England, Soil Use and Management 20, 343-349.
- Quinton, J.N., Govers, G., Van Oost, K., Bardgett, R.D., 2010. The impact of agricultural soil erosion on biogeochemical cycling, Nature Geoscience 3, 311–314.
- Renard, K.G., Foster, G.R., Weesies, G.A., Porter, J.P., 1991. Rusle: Revised universal soil loss equation. Journal of Soil and Water Conservation 46, 30–33.
- Robertson, G.P., Wedin, D., Groffmann, P.M., Blair, J.M., Holland, E.A., Nadelhoffer, K.J., Harris, D., 1999. Soil carbon and nitrogen availability - Nitrogen mineralization, nitrification, and soil respiration potentials, in: Standard Soil Method for Long-Term Ecological Research. Ed: G.Philip Robertson, David C. Coleman, Caroline S. Bledsoe, Phillip Sollins. Oxford University Press, Oxford.
- Robinson, D.A., Phillips C.P., 2001. Crust development in relation to vegetation and agricultural practice on erosion susceptible, dispersive clay soil from central and southern Italy, Soil & Tillage Research 60, 1-9.
- Ries, J.B., Iserloh, T., Seeger, M., Gabriels, D., 2013. Rainfall simulations—Constraints, needs and challenges for a future use in soil erosion research, Zeitschrift für Geomorphologie 57, 1–10.
- Ritter, W.F., Shirmohammadi, A., 2001. Agricultural Nonpoint Source Pollution, Watershed Management and Hydrology; Lewis Publishers: New York, NY, USA, p. 342.
- Robertson, G.P., Wedin, D., Groffmann, P.M., Blair, J.M., Holland, E.A., Nadelhoffer, K.J., Harris, D., 1999. Soil carbon and nitrogen availability - Nitrogen mineralization, nitrification, and soil respiration potentials, in: Standard Soil Method for Long-Term Ecological Research. Ed: G.Philip Robertson, David C. Coleman, Caroline S. Bledsoe, Phillip Sollins. Oxford University Press, Oxford.
- Ries, J.B., Marzen, M., Iserlo, T., Fister, W., 2014. Soil erosion in mediterranean landscapes experimental investigation on crusted surfaces by means of the Portable Wind and Rainfall Simulator, Journal of Arid Environments 100, 42-51.
- Saleh, A., 1993. Soil roughness measurement: Chain method. Journal of Soil and Water Conservation 48, 527-529.
- Salles, C., Poesen, J., Govers, G., 2000. Statistical and physical analysis of soil detachment by raindrop impact: rain erosivity indices and threshold energy, Water Resource Research 36, 2721– 2729.
- Schiettecatte, W., Gabriels, D., Cornelis, W.M., Hofman, G., 2008. Enrichment of organic carbon in sediment transport by interrill and rill erosion processes, Soil Science Society of America Journal 72, 50–55.

- Savat, J., DePloey, J., 1982. Sheetwash and rill development by surface flow. In: Bryan, R.; Yair, A. (eds) Badland Geomorphology and Piping. Geo Books, Norwich. 113–126.
- Schlesinger, W.H. et al., 1990. Biological feedbacks in global desertification, Science 247, 1043–1048.
- Schiettecatte, W., Gabriels, D., Cornelis, W.M., Hofman, G., 2008. Enrichment of organic carbon in sediment transport by interrill and rill erosion processes, Soil Science Society of America Journal 72, 50–55.
- Stallard, R.F., 1998. Terrestrial sedimentation and the carbon cycling: coupling weathering and erosion to carbon burial, Global Biogeochemical Cycles 12, 231–257.
- Starr, G.C., Lal, R., Malone, R., Hothem, D., Owens, L. and Kimble, J., 2000. Modeling soil carbon transported by water erosion process, Land Degradation & Development 11, 83–91.
- Stokes, G.G., 1985. On the effect of the internal friction of fluids on the motion of pendulums, Trans. Camb. Phil. Soc., 9, 8–106.
- Six, J., Conant, R. T., Paul, E. A. and Paustian, K., 2002. Stabilization mechanisms of soil organic matter: Implications for C-saturation of soils, Plant Soil 241, 155–176.
- Six, J., Bossuyt, H., Degryze, S., Denef, K., 2004. A history of research on the link between (micro)aggregates, soil biota, and soil organic matter dynamics, Soil & Tillage Research 79, 7–31.
- Smith, R.E., Quinton, J., Goodrich, D.C., Nearing, M., 2010. Soil-erosion models: Where do we really stand? Earth Surface Processes and Landforms 35, 1344–1348.
- Tisdall, J.M. and Oades, J.M., 1982. Organic matter and water-stable aggregates in soils, Journal of Soil Science 33, 141–163.
- Torri ,D., Regüés, D., Pellegrini, S., and Bazzoffi, P., 1999. Within-storm soil surface dynamics and erosive effects of rainstorms, Catena 38, 131–150.
- Van Hemelryck, H., Fiener,P., Van Oost, K., Govers, g., Merckx, R., 2010a. The effect of soil redistribution on soil organic carbon: an experimental study, Biogeosciences 7, 3971-3986.
- Van Hemelryck, H., Govers, G., Van Oost, K., Merckx, R., 2010b. Evaluating the impact of soil redistribution on the in situ mineralization of soil organic carbon, Earth Surface Processes and Landforms. doi:10.1002/esp. 2055.
- Van Oost, K., Beuselinck, L., Hairsine, P.B. and Govers, G., 2004. Spatial evaluation of a multi-class sediment transport and deposition model, Earth Surface Processes and Landforms 29, 1027–1044.
- Van Oost, K., Govers, G., Quine, T.A., Heckrath, G., Olesen, J.E., de Gryze, S., Merckx, R., 2005. Landscape-scale modeling of carbon cycling under the impact of soil redistribution: The role of tillage erosion, Global Biogeochemical Cycles 19, 1733–1739.
- Van Oost, K., Quine, T.A., Govers, G., De Gryze, S., Six, J., Harden, J.W., Ritchie, J.C., McCarty, G.W., Heckrath, G., Kosmas, C., Giraldez, J.V., Marques da Silva, J.R. and Merckx, R., 2007. The impact of agricultural soil erosion on the global carbon cycle, Science 318, 626–629.
- Walling, D.E., 1988. Erosion and sediment yield research – some recent perspectives, Journal of Hydrology, 113-141.
- Wan, L., Zhang, X.P., Ma, Q., Zhang, J.J., Ma, T.Y., Sun, Y.P., 2014. Spatiotemporal characteristics of precipitation and extreme events on the Loess Plateau of China between 1957 and 2009, Hydrological Processes 28, 4971–4983.

- Wang, J.G., Li, Z.X., Cai, C.F., Ma R.M, 2014. Particle size and shape variation of Ultisol aggregates affected by abrasion under different transport distances in overland flow, Catena 123, 153-162.
- Wang, X., Cammeraat, E.L.H., Romeijin, P, Kalbitz, K., 2014. Soil organic carbon redistribution by water erosion –the role of CO_2 emissions for the carbon budget, PLoS ONE 9: e96299.
- Wang, Z., Govers, G., Steegen, A., Clymans,W., Van den Putte, A., Langhans, C., Merckx, R., and Van Oost, K., 2010. Catchment-scale carbon redistribution and delivery by water erosion in an intensively cultivated area, Geomorphology 124, 65–74.
- Wang, Z., Govers, G., Van Oost, K., Clymans, W., Van den Putte, A., Merckx, R., 2013. Soil organic carbon mobilization by interrill erosion: Insights from size fractions, Journal of Geophysical Research: Earth Surface 118, 348–360.
- Wang, Z., Van Oost, K., Lang, A., Quine, T., Clymans, W., Merckx, R., Notebaert, B., Govers, G., 2014. The fate of buried organic carbon in colluvial soils: a long-term perspective, Biogeosciences 11, 873–883.
- Walling, D.E., 1988. Erosion and sediment yield research – some recent perspectives, Journal of Hydrology 100, 113-141.
- Xiao, L., Hu, Y., Greenwood, P., Kuhn, N.J., 2015a. The use of a raindrop aggregate destruction device to evaluate sediment and soil organic carbon transport, Geographica Helvetica 70, 167-174.
- Xiao, L., Hu, Y., Greenwood, P., Kuhn, N.J., 2015b. A Combined Raindrop Aggregate Destruction Test-Settling Tube (RADT-ST) Approach to Identify the Settling Velocity of Sediment, Hydrology 2, 176-192.
- Zhao, G., Mu, X., Wen, Z., Wang, F., Gao, P., 2013. Soil erosion, conservation, and Eco-environment changes in the Loess Plateau of China, Land Degradation & Development 24, 499–510.
- Zibilske, L.M., 1994. Carbon mineralization., in: Soil Science Society of America, Part 2. Microbiological and Biochemical Properties. Madison, Wisconsin, USA, pp. 835–863.